Jonas Ingves

GEOLOGICAL, PETROGRAPHIC AND GEOCHEMICAL EVALUATION OF TWO SVECOFENNIAN ULTRAMAFIC SERPENTINIZED BODIES IN PERNAJA, SE FINLAND

Master's thesis
Department of Geography and Geology
Turku 2018

University of Turku
Faculty of Science and Engineering
Department of Geography and Geology

INGVES, JONAS: Geological, petrographic and geochemical evaluation of two Svecofennian serpentinized ultramafic bodies in Pernaja, SE Finland

Master's thesis, 66 pages, 1 appendix
40 ECTS, Geology
Supervisor: professor Krister Sundblad
December 2018

When mafic-ultramafic rocks get encountered with fluids in conditions of low temperature and pressure, they are subject to an alteration form known as serpentinization. It is a process which causes several changes in the physical properties of the affected lithologies, including an increase in volume, a decrease in density, a strengthening of magnetism and an increase in the water content. Serpentinites make up a considerable volume of the upper oceanic crust, and as they inherently bear influence on e.g. the geodynamics in subduction zones and the geochemical cycle in subduction-related volcanism, a significant amount of research has focused on them during the last few decades.

This thesis presents the results of a new discovery of two serpentinite bodies at Tjusterby in the southern part of the Svecofennian domain in Finland. The study object is composed of two separate bodies, both limited in size, and located completely under sea water. As such, they have been investigated through magnetometry and data gathered from till and boulder samples in neighbouring land areas. Ultramafic and amphibolitic reference samples have also been investigated from Pukkila in Päijät-Häme and Mallusjärvi in Uusimaa, both within 50 km from the Tjusterby area, as a comparison with the geological conditions recognized at Tjusterby

Based on comparisons of geochemical data of the serpentinites in Tjusterby to data from serpentinites in other publications, the environment in which the ultramafic protolith in Tjusterby was serpentinized has been linked to a subduction zone, as opposed to abyssal (mid-ocean ridge) or mantle wedge environments. As a result of petrographic studies in thin sections, the Tjusterby serpentinites contain serpentine, phlogopite, opaque minerals, plagioclase and in some occasions brucite, chlorite and garnet. From the presence of brucite, and absence of talc, the protolith of the Tjusterby serpentinites is likely to have been rich in Mg, implying an olivine-rich source rock. High magnetic susceptibility in all serpentinite samples also suggests magnetite to be common among the opaque minerals. The serpentinized ultramafic bodies presented in this study are the only known of their kind in the Pernaja region, but as the Svecofennian bedrock is typically fragmented into rather small units, it is likely that similar bodies can be found in other areas in southern Finland.

Tags: serpentinite, ultramafic, boulder tracing, magnetometry, Pernaja

Table of contents

1. Introduction

Mafic-ultramafic rock associations of various sizes are fairly common in the Finnish bedrock. They occur in Archaean and early Paleoproterozoic units in the northern and eastern parts of the country (Makkonen et al. 2017) and by late Paleoproterozoic Svecofennian lithologies in the center and the south. When mafic-ultramafic lithologies react with water under low to moderate temperature/pressure conditions, they can be subject to an alteration form known as serpentinization. It is a process that mainly affects olivine and orthopyroxene through hydration, turning them into the serpentine group minerals chrysotile, lizardite and antigorite (Guillot & Hattori 2013). Serpentinization causes major changes in the physical properties of the affected rock, as the addition of water in the system increases its volume, decreases its density and seismic velocity and often strengthens its magnetism by the formation of magnetite (Iyer 2007, Schmitt et al. 2007). Chemically the most notable differences are the addition of water and the reduction of calcium (Mével 2003) as well as the enrichment of several incompatible and Rare Earth elements (Deschamps et al. 2013). The most common environments for serpentinization are slowly moving mid ocean ridges and subduction along convergent plate boundaries (Mével 2003, Reynard 2012). Being a notable part of the oceanic plates, serpentinites also play a major part in the global geochemical and geotectonic cycles. This is due to their large water content, which makes serpentinites rheologically weaker, affecting movements at plate boundaries in subduction zones (Hirth & Guillot 2013) and releases several fluid mobile elements (e.g. Li, As, Sr, Pb) back into the geochemical cycle when fluids are released from the subducting plate (Guillot & Hattori 2013). The same fluids also affect volcanic units as they move upwards in the crust and decrease its solidus temperature. Although serpentinites make up a major part of the surface of the oceanic crust, they are less common within the continents, where they are mostly found as parts of ophiolite sequences associated with paleo-oceans (Guillot & Hattori 2013).

Most serpentinite bodies in Finland are associated with greenstone belts in the northern and eastern parts of the country (Sotka 1983), while descriptions of corresponding units in the Svecofennian of Finland are missing. This study presents a new discovery of two serpentinite bodies at Tjusterby in the Loviisa region of southern Finland. Two reference areas (Mallusjärvi and Pukkila), with similar geological properties as Tjusterby, were chosen for comparisons with Tjusterby. Locations for all three areas are shown in Fig. 1. Since the Tjusterby bodies are located under water, all investigations have been dependent on indirect methods like magnetometry, boulder tracing and soil geochemistry, the latter reported by Ingves (2016). Although the Tjusterby discovery can be considered unique, it is suggested that similar bodies must exist elsewhere in the southern parts of the Svecofennian region, particularly in the Häme Belt.

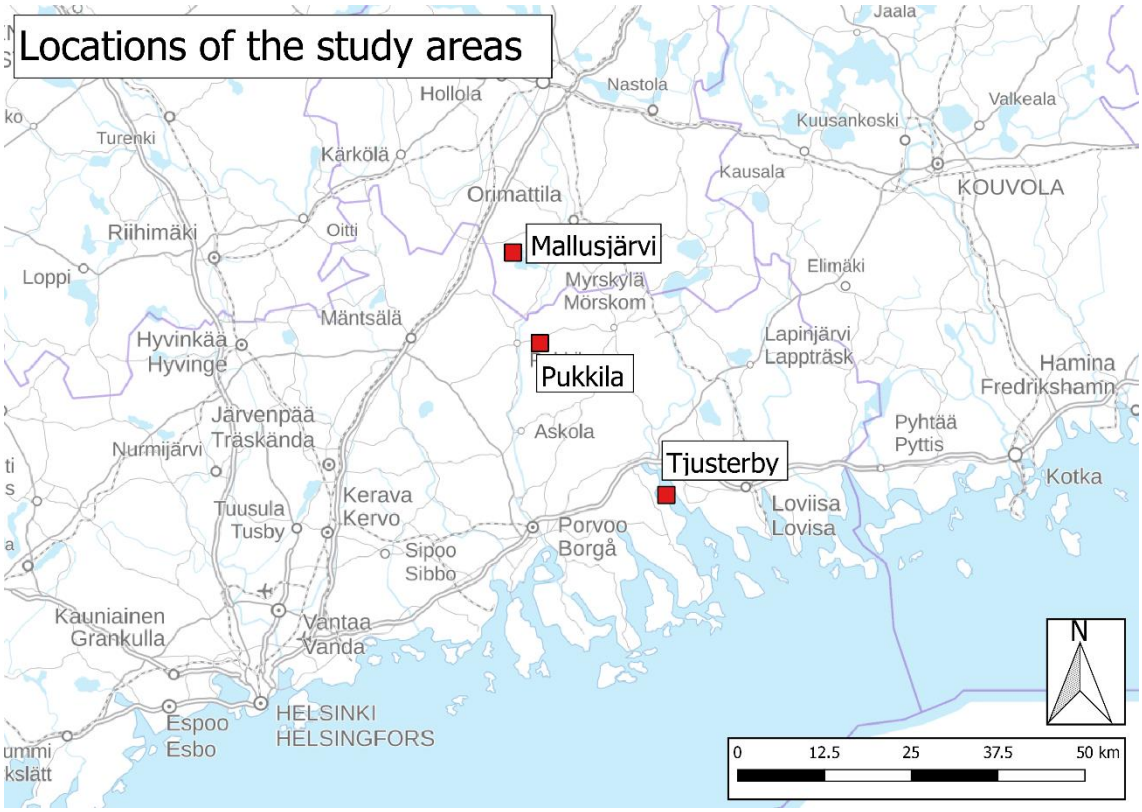

Figure 1: Locations of the three study areas in southern Finland. Original map acquired from the open data file download service of the National Land Survey of Finland (background map 1:320 000).

2. Study areas, material and methods

2.1. Study areas and material

The main study object for this thesis is a previously unknown occurrence of ultramafic rocks identified in two separate bodies in Tjusterby, near the village of Pernaja in the Uusimaa region in SE Finland. For comparison, two other known occurrences with similar properties were chosen as reference localities for geochemical and mineralogical investigations. These objects are located in Mallusjärvi, Päijät-Häme and Pukkila, Uusimaa, both within 50 km of the main study object in Tjusterby.

The study target in Tjusterby is situated entirely under water, and thus direct sampling of it is impossible without a large scale drilling operation. Therefore, most information about it has been dependent on boulder findings onshore, a few hundred meters S-SE from the target itself. In addition, a few bedrock samples were also taken on the southern side of the object, in order to gain knowledge about the lithologies surrounding the underwater feature. In Mallusjärvi and Pukkila, all samples were taken directly from available outcrops. When collected, all samples were given names with running numbers, with boulders and outcrop samples having separate codes. In total, altogether 42 boulder samples and 51 bedrock samples were gathered during the field work for this study.

2.1.1. Tjusterby

The area referred to here as Tjusterby is located approximately 1–2 kilometers west of the village of Pernaja (figure 2), between the towns of Loviisa and Porvoo in SE Finland. The studied ultramafic object, with its two separate bodies, is situated in the Pernajanlahti bay, closely surrounded by a small island to the north and mainland to the south. According to an old bedrock map produced by the Geological Survey of Finland (GTK) (Laitala 1964, figure 3), the immediate surroundings of the study area are dominantly composed of granites, with a minor patch of mica schist identified just south of the Pernajanlahti bay. Further to ne north, the main rock type turns into granodiorites, with smaller units of gabbro and amphibolites to the west and east, respectively. As Tjusterby is located close to the western margin of the Wiborg batholith, rapakivi granites are the dominant rock type a few kilometers east of the study area.

After some ground work had been conducted in the Tjusterby area, it was realized that the existing bedrock map by GTK was inaccurate in the areas south of the Pernajanlahti bay. The areas marked to be composed of granites and mica-schists were then identified to actually form an amphibolite-gabbro association (figure 4). Later discussion in this thesis will thus refer to the lithologies shown in figure 4, rather than the locally erroneous model in figure 3.

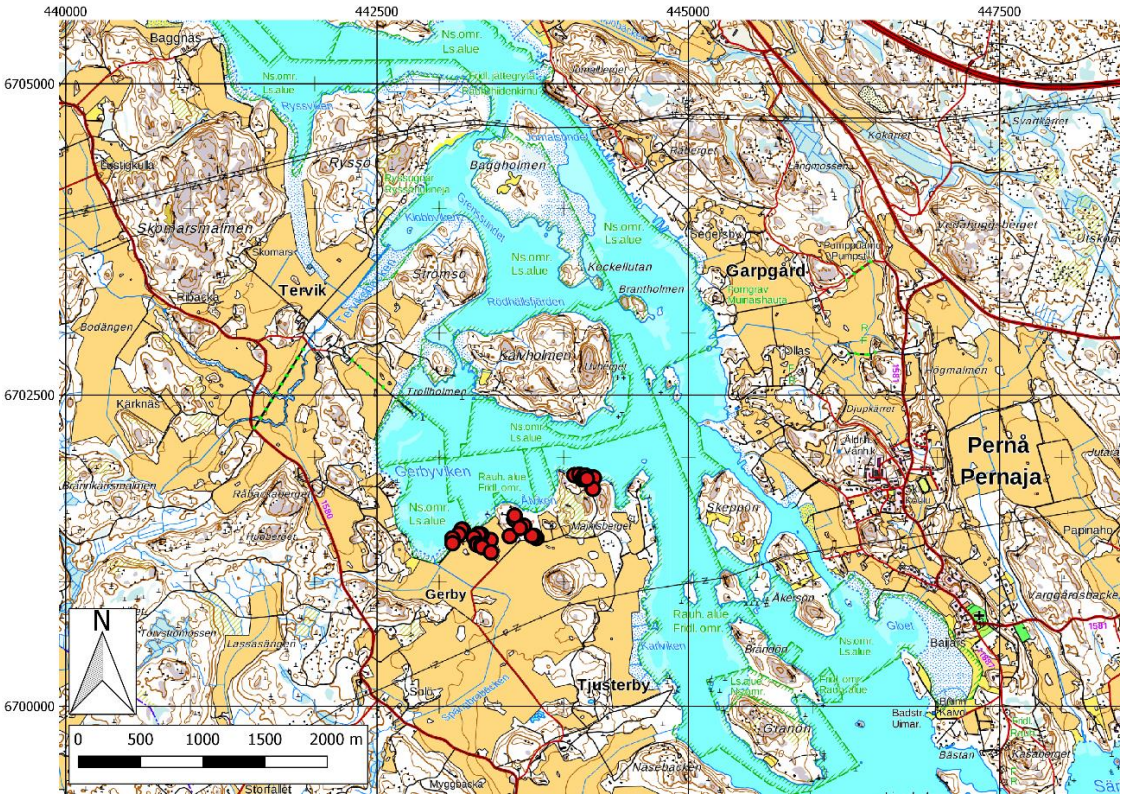

Figure 2: The study area referred to as Tjusterby, west of the village of Pernaja. The red dots mark the locations of collected boulder samples. Original map acquired from the open data file download service of the National Land Survey of Finland (topographic map raster 1:50 000).

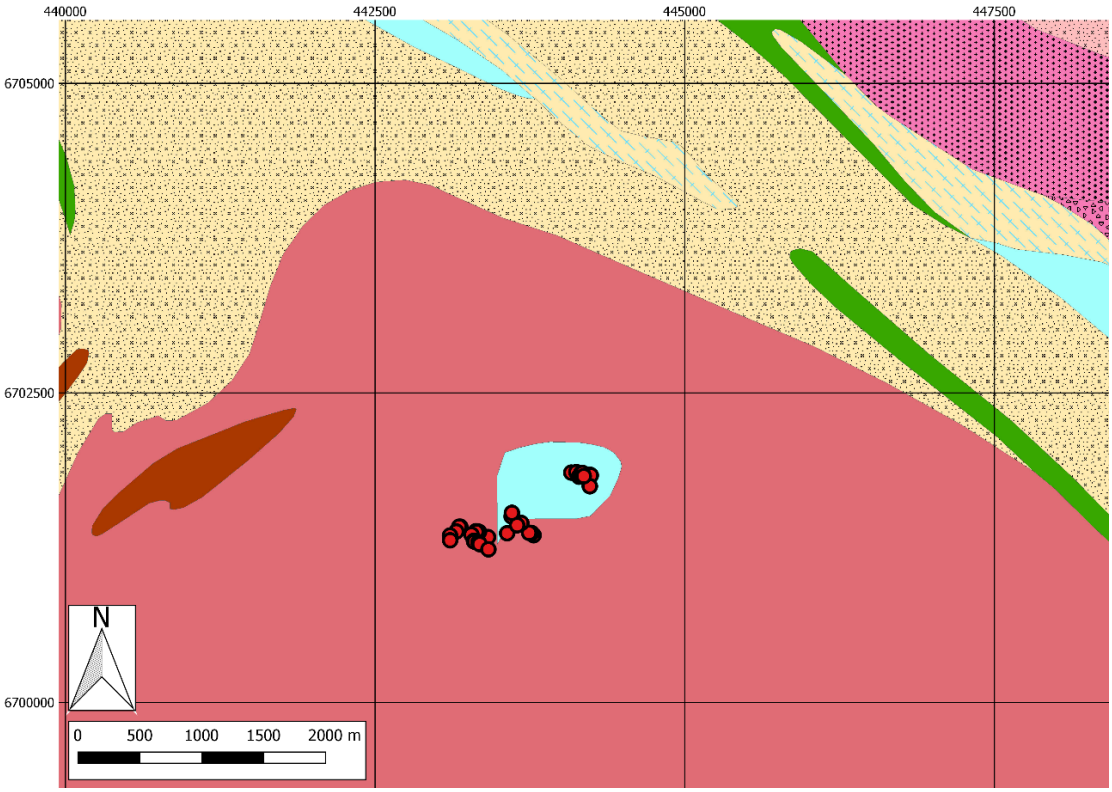

Figure 3: Bedrock map showing the locations of the sampling points in Tjusterby and the surrounding lithologies. Reddish pink = microcline granite, light blue = mica schist, dotted light brown = granodiorite, brown = gabbro, green = amphibolite, light yellow with blue lines = quartz-feldspar gneiss, dotted pink = porphyritic rapakivi granite, dotted light red = aplitic rapakivi granite. Original map from DigiKP 200, digital bedrock map database (Geological Survey of Finland). The map covers the same area as was shown in figure 2.

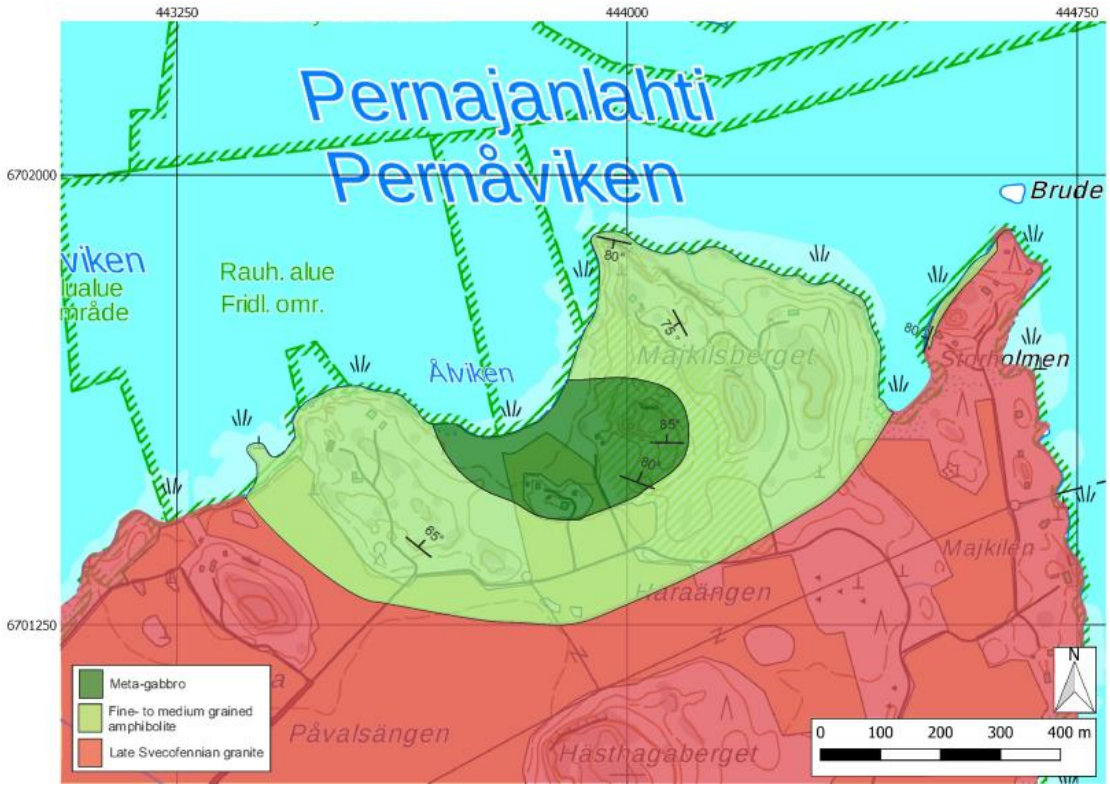

Figure 4: A customized bedrock map showing the lithological units at the study area in Tjusterby. Map redrawn for this thesis based on an unpublished (2015) original version by prof. Krister Sundblad. Terrain map underneath acquired from the open data file download service of the National Land Survey of Finland (basic map raster).

The interest for the study object in Tjusterby was initially generated in connection with a field course in ore prospecting which was arranged in the area in April and May 2015 by the University of Turku. Students attending the course took till samples, which were later analyzed for their geochemistry with a portable XRF-analyzer and for magnetic properties with a susceptibility meter. Based on the geochemical results, some of the samples were found to be enriched in Ni and Cr (Ingves 2016). The bedrock source for these enrichments was believed to be linked to two magnetic anomalies in the Pernajanlahti bay on the northern side on the sampling site, which were visible in an aeromagnetic anomaly map produced by the GTK (Geological Survey of Finland 2001). In October 2016, the same field course was again arranged in the region, including a short visit to the present study area in Tjusterby. During this half-day visit a few new till samples, along with altogether nine boulder samples were gathered. Parts of these boulder samples were sent for geochemical analysis to Actlabs in Ontario, Canada, where three of them were confirmed to be of ultramafic composition, with Ni contents ranging from 0.12 to 0.20 %. With no known exposed ultramafic outcrops within tens of kilometers distance, the source for these boulders, along with the Ni and Cr enriched till, was believed to originate from the magnetic anomalies under the Pernajanlahti bay.

During the same field courses in 2015 and 2016, ground magnetometry surveys were conducted on mainland by walking and over the bay from a rowing boat, with the aim of getting a more accurate determination of the magnetic features compared with the aeromagnetic map produced by GTK. The results from these surveys confirmed the existence of the magnetically anomalous bodies. Additional ground magnetometry measurements were conducted again in October 2017 to further improve the accuracy of the results. A magnetometry map with the combined results from all three years is shown in figure 5.

Further field work was conducted in the Tjusterby area on five separate days in September 2017, with the main emphasis on boulder tracing. The target areas were planned on the SE side of the previously identified magnetic bodies, including and extending the areas where the three ultramafic boulders were found in October 2016. Samples of altogether 51 new boulders were gathered during these five days. The bulk of the samples were classified as ultramafic, the rest being identified as amphibolites and gabbros. In the field, some variations in grain size and weathering were observed in the ultramafic boulders. Most of the samples had a high magnetic susceptibility, in accordance with the aeromagnetic (GTK) and ground magnetometry surveys done above the presumed source area for the boulders. Altogether 22 boulder samples were chosen for proper chemical analysis at Actlabs, of which 12 samples also were cut into thin sections for mineralogical evaluation. All four bedrock samples collected from outcrop in Tjusterby were also sent for chemical analysis and cut into thin sections.

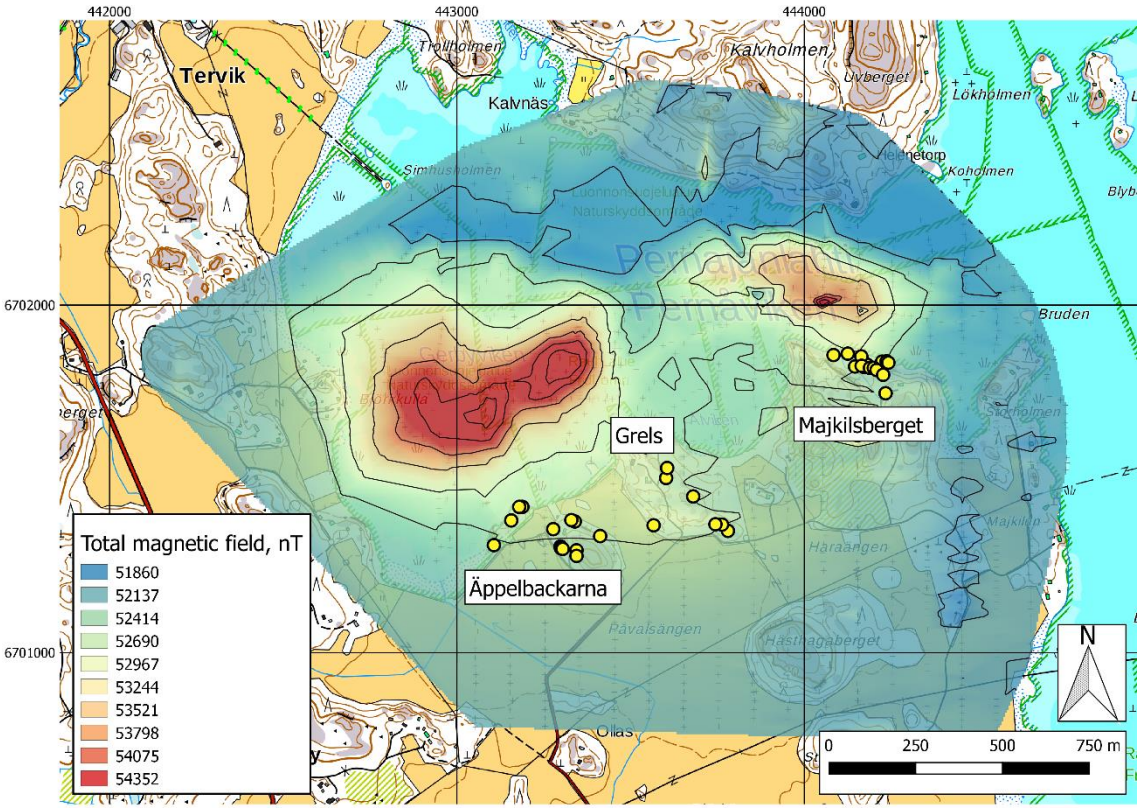

Figure 5: A magnetic anomaly map showing the extent of the magnetic bodies, marking the presumed ultramafic intrusions in Tjusterby. Map produced from 1733 ground magnetometry points, interpolated in QGIS version 2.18 with the TIN-method. Yellow dots show the locations of boulders with measured magnetic susceptibility higher than 10^{-3} Si units. The three names on the map mark the sub-localities within the Tjusterby area. Map underneath acquired from the open data file download service of the National Land Survey of Finland (basic map raster).

In this thesis, Tjusterby is used as a general name for this study area. As shown in figure 5, it includes three more specific location names. From west to east, these are Äppelbackarna, Grels and Majkilsberget. These names were used when collecting boulder samples to more easily keep track on to which area they belonged, and to try to spot spatial variations within and between the intrusions from which they originated. The three localities can be seen as three different populations in figure 5. The boulder samples collected in the Äppelbackarna and Grels areas are considered to have been transported from the larger magnetic body seen in figure 5, whereas the samples from Majklisberget are considered to originate from the smaller anomaly.

2.1.2. Mallusjärvi

Mallusjärvi, located some 40 km NNW from Tjusterby and 12 km SW from the town of Orimattila (figure 6), was chosen as a reference area due to a highly magnetic ultramafic intrusion marked on bedrock and aeromagnetic maps produced by the GTK (figures 7 and 8). The magnetic properties and sizes of the units in Tjusterby and Mallusjärvi bear resemblance to each other, although the surrounding lithologies are different. Whereas the ultramafics in Tjusterby are surrounded by gabbro and amphibolite embedded in granites, the intrusion in Mallusjärvi is completely surrounded by Svecofennian biotitic

gneisses, with granodiorites and granites constituting the other major rock types in the area. However, according to the bedrock map by the GTK (DigiKP 200, digital bedrock map database, figure 7) there are gabbroic and amphibolitic rocks about 1.5 km to the south of the ultramafic intrusion in Mallusjärvi.

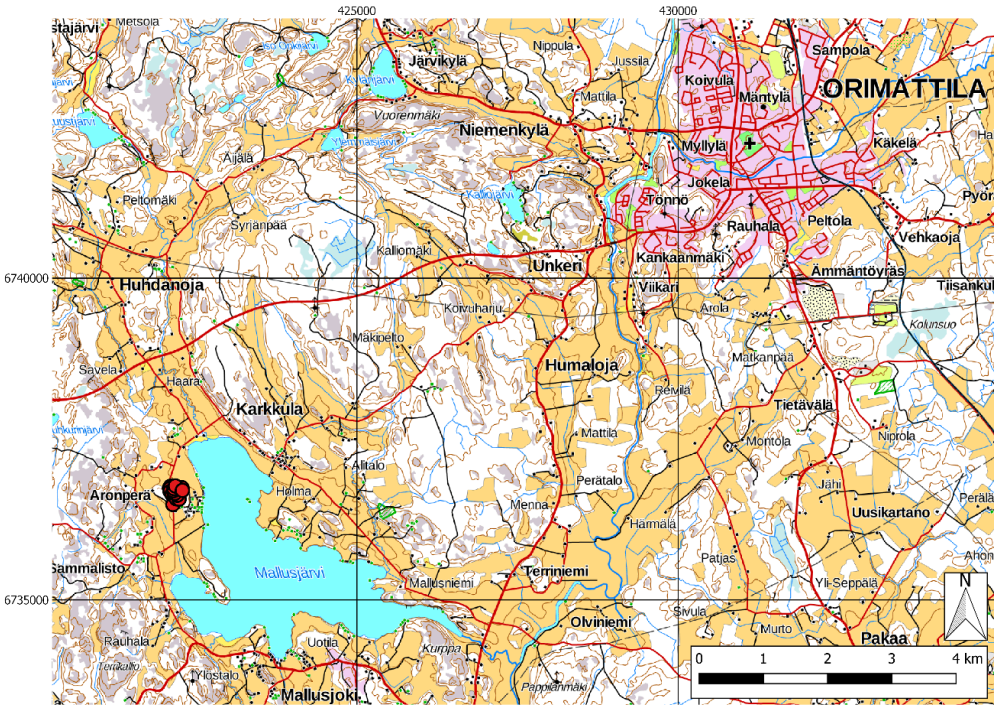

Figure 6: Map showing the location of the study area in Mallusjärvi (red dots), about 12 km SW from the town of Orimattila. Original map acquired from the open data file download service of the National Land Survey of Finland (topographic map raster 1:100 000).

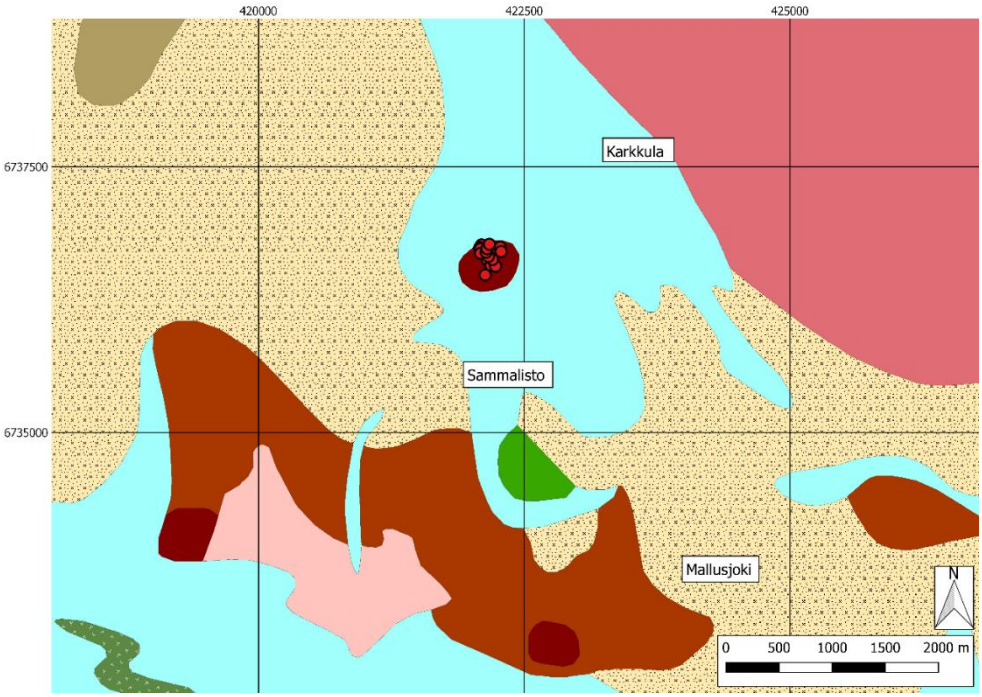

Figure 7: Bedrock map showing the locations of the sampling points in Mallusjärvi and its surrounding lithologies. Dark brown = peridotite, brown = gabbro, green = amphibolite, pink = pegmatite granite, light blue = mica schist, dotted light brown = granodiorite, reddish pink = granite, dotted green = plagioclase porphyrite, beige = hornblende gabbro. Original map from DigiKP 200, digital bedrock map database (Geological Survey of Finland).

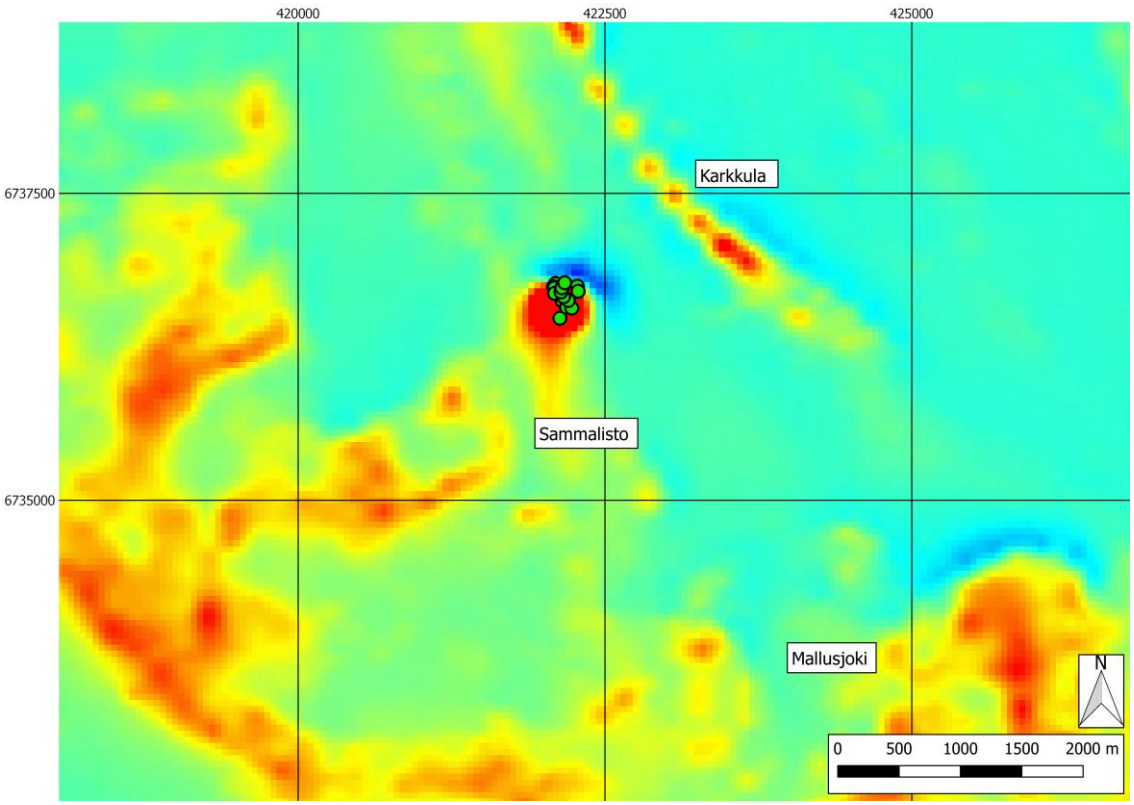

Figure 8: Aeromagnetic anomaly map showing the differences in the strength of the Earth's magnetic field caused by variations in the bedrock. Blue color implies a weaker magnetic field, red a stronger one. The map covers the same area as the one in figure 7, with green dots showing the locations of the collected bedrock samples. Original anomaly map acquired from GTKWMS Interface Service (Geological Survey of Finland).

The Mallusjärvi intrusion is well exposed and forms a significant topographic high, clearly differing from the surrounding landscape. Due to the easy access and limited size, the field work could be done on a single day. Altogether 16 bedrock samples were collected in a pattern covering most of the exposed outcrop. Textural variations between the samples were found to be limited, the bulk of the samples being even-grained, dark and without signs of significant weathering**.** Values for magnetic susceptibility were high and relatively even when measured in outcrop. In the initial pXRF analyses, the Ni values were found to be about one order of magnitude lower compared with the ultramafic boulders sampled in Tjusterby. The Cr contents were more similar between the two sampling sites. Altogether five of the bedrock samples collected in Mallusjärvi were sent for chemical analysis to Actlabs, three of which were cut into thin sections for mineralogical identification.

2.1.3. Pukkila

Pukkila was the third area to be investigated for the purposes of this thesis. It is located about 29 km NE of Tjusterby and 13 km S of Mallusjärvi, between the towns of Pukkila and Myrskylä (figure 9). Pukkila was chosen as a reference for Tjusterby due to its relatively close location and resembling lithology. According to the bedrock map of Finland (DigiKP 200, digital bedrock map database, figure 10) the study area is

composed of peridotitic bodies, gabbros, amphibolites and granites embedded in a larger unit of mica schist and mica gneiss. The ultramafic rocks in Pukkila do not show any significant magnetic properties in the aeromagnetic anomaly maps of GTK (figure 11), and magnetic susceptibilities measured on samples in the field were correspondingly low. The amount of exposed outcrops in the area is limited, but some deviations from the bedrock map were recognized during the two field work days in the area. In reality, the areas covered by amphibolites seem to be larger, with ultramafics and gabbros being either absent or less profound than shown in bedrock maps from the area.

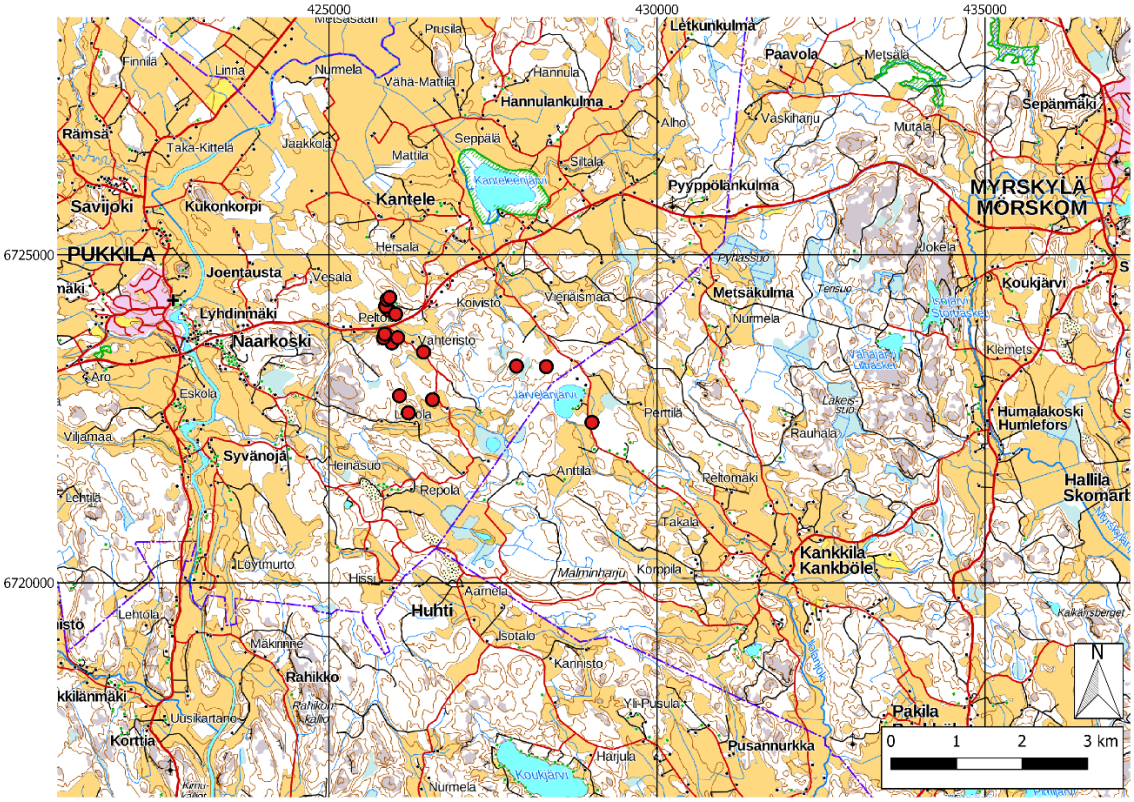

Figure 9: Map showing the location of the sample points in Pukkila (red dots), between the towns of Pukkila and Myrskylä. Original map acquired from the open data file download service of the National Land Survey of Finland (topographic map raster 1:100 000).

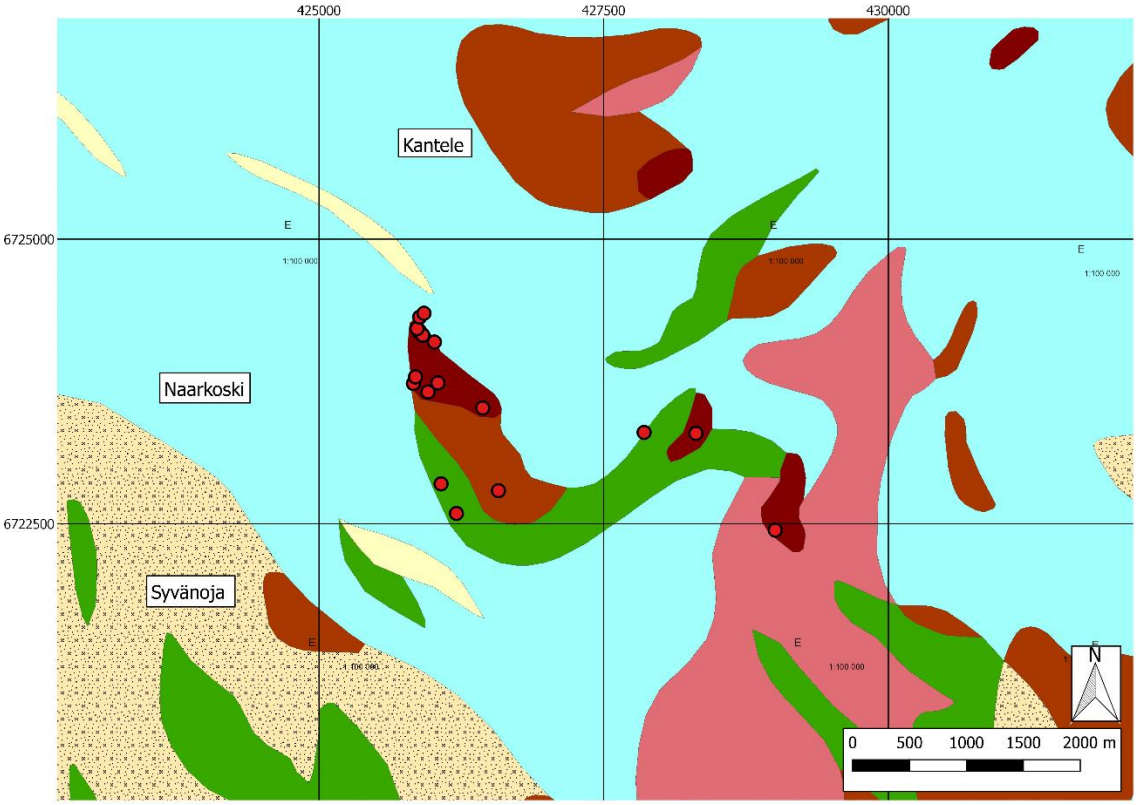

Figure 10: Bedrock map showing the locations of the sampling points in Pukkila and the surrounding lithologies. Dark brown = peridotite, brown = gabbro, green = amphibolite, light blue = mica schist, dotted light brown = granodiorite, reddish pink = granite. Original map from DigiKP 200, digital bedrock map database (Geological Survey of Finland).

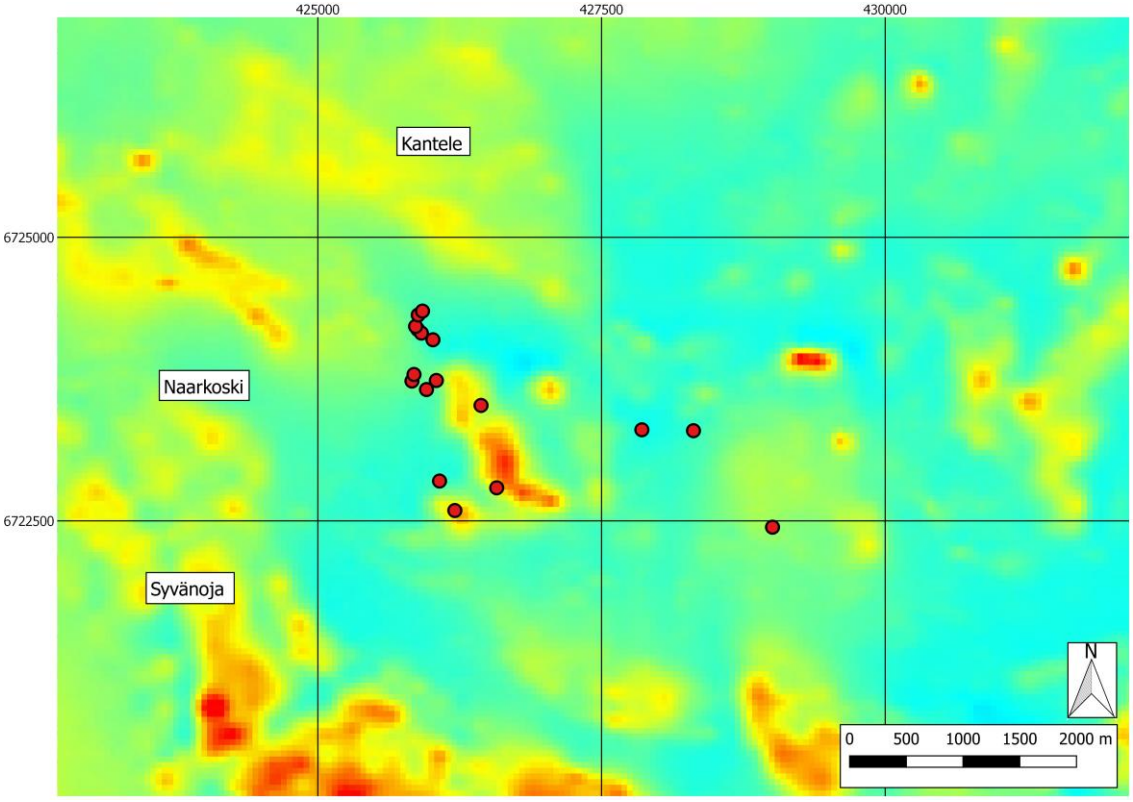

Figure 11: Aeromagnetic anomaly map showing the differences in the strength of the Earth's magnetic field caused by variations in the bedrock. Blue color implies a weaker magnetic field, red is stronger. The map covers the same area as the one in figure 10, with red dots showing the locations of the collected bedrock samples. Original anomaly map acquired from GTKWMS Interface Service (Geological Survey of Finland).

Altogether 17 bedrock samples were collected in the Pukkila area, representing units identified as amphibolites and mica schists. Of these samples, seven were sent for proper chemical analysis to Actlabs, and of them, five were cut into thin sections for mineral identification with a polarizing microscope. Values of magnetic susceptibility were also measured in the field, but are not further discussed in this study, as they were constantly low and as magnetism was initially not a point of interest in the case of Pukkila.

2.2. Methods

Sampling in all areas was systematic and covered the areas effectively where boulders or outcrops of interest were expected to be found. The field work conditions were, however, significantly different when comparing Tjusterby with the two reference areas Mallusjärvi and Pukkila. In Tjusterby, the field courses (2015 and 2016) had provided some information about where ultramafic boulders were most likely to be found, and as the terrain in the area also was quite well known, suitable sampling sites could be planned in detail beforehand. Field work in Tjusterby mostly focused on finding boulders, considered to represent both the ultramafic unit under the Pernajanlahti bay and other lithologies surrounding it. Minor focus was put on outcrop sampling in on-shore areas (Majkilsberget) south of the strong magnetic anomalies. Mallusjärvi and Pukkila were initially unknown areas, and as such planning for the field work in these localities was more dependent on pre-existing information on bedrock, aeromagnetics and terrain maps. All samples in Mallusjärvi and Pukkila were taken from outcrops that had been identified in terrain maps before the field work began. As boulder tracing is different from bedrock sampling in the way that some boulders may be soil covered and thus more difficult to discover, a systematic approach was particularly important in Tjusterby. More time was thus required for the work in Tjusterby (altogether five days of field work), compared to Mallusjärvi (one day) and Pukkila (two days).

For both boulder and bedrock samples, about fist sized pieces were knocked off with a hammer, marked with tape and put in plastic bags marked with their individual sample names. Remaining pieces of boulders were left in their original positions. Coordinates for the locations of all boulders and sampled outcrops were marked with a handheld Garmin GPS-instrument in the national Finnish KKJ Zone 3 system and written down in a notebook. Notes about e.g. weathering, roundness and burial depth of boulders and texture and petrology of outcrops were taken in the field. Data for magnetic susceptibility of all samples were also measured with a Terraplus KT-10 Magnetic Susceptibility Meter directly at the sampling sites. Afterwards, all 78 samples were analyzed with a handheld XRF-device (pXRF) to get preliminary results about the elemental composition of the samples. The XRF-instrument used was an Innov-X Systems Olympus Delta DP-6500 portable X-Ray fluorescence spectrometer, manufactured in 2011 and acquired by the

University of Turku in 2015. The analyses were performed with the Mining Plus setting, using a measuring time of 20+20+20 seconds. All samples were analyzed on three different spots, and average results were then calculated for each sample based on the three readings. The average results were then treated as the final result for the pXRF-analysis.

Based on the pXRF results and on the spatial distribution of the collected samples, altogether 38 of them were chosen to be sent for geochemical assaying to Activation Laboratories Ltd. (Actlabs) in Ontario, Canada to be analyzed with the FUS-ICP and FUS-MS methods. Of this material, 22 were boulder samples collected from the Tjusterby area and 16 were bedrock samples, of which 4 were from Tjusterby, 5 from Mallusjärvi and 7 from the Pukkila area. Before sending them to the laboratory, the samples were prepared for analysis at the University of Turku. The fist sized samples were first cut into smaller pieces with a diamond saw, then crushed into a fine powder in a mortar. The powdered samples were then poured into individual plastic containers, each labeled with their specific sample names. To avoid contamination, all tools used in the powdering process were cleaned with water between the preparation of each sample.

When cutting the samples for laboratory analysis, suitable pieces for the preparing of thin sections were also simultaneously made. After consideration, 26 out of the 38 samples that were sent for laboratory analysis were chosen to also be cut into thin sections. Of these, 14 were boulder samples from the Tjusterby area and 12 were bedrock samples, of which 4 were from Tjusterby, 3 from Mallusjärvi and 5 from Pukkila. The thin sections were non-polished with a standard 30 µm thickness, made at the University of Turku.

3. Results

3.1. Generally

The results acquired in this study are composed of geochemical analytical data (tables 1–10), magnetic susceptibility measurements (table 11) and descriptions based on a petrographic evaluation with a polarizing microscope (figures 14–18). As the geochemical data reported by Actlabs also included elements without main interest for this study, only selected elements are shown and discussed, with a complete list presented in appendix A. Measurements of the magnetic susceptibility are shown in tables for samples collected from the Tjusterby and Mallusjärvi areas, while the Pukkila data were left out due to consistently low values. Petrographic observations consist of written notes together with representative photographs of selected thin sections.

3.2. Geochemistry

The geochemical data presented below consist of whole rock FUS-ICP (for all major elements shown in the tables) and FUS-MS (for all trace elements) analysis data. The preliminary pXRF results are not shown here, since their accuracy is not regarded to be as precise as the results received from the laboratory and as such they would not yield any useful additional information. In order to facilitate comparison, the geochemical data have been divided into four separate groups. These are: serpentinized rocks from Tjusterby (only boulder samples), non-serpentinized rocks from Tjusterby (both bedrock and boulder samples), bedrock samples from Mallusjärvi and bedrock samples from Pukkila. In addition to data in numeric form, chondrite-normalized REE-diagrams are shown for all laboratory-analyzed serpentinitic rocks from Tjusterby, as a comparison to non-serpentinized mafic-ultramafic bedrock samples from Mallusjärvi (figures 12 and 13). As the serpentinitic samples from Tjusterby are of major focus in this work, a specific table with trace element data is shown for them, with the idea of using these data to identify signs from the initial protolith of the serpentinite.

Table 1: Geochemical data (%) of major elements in serpentinized rock samples from Tjusterby (FUS-ICP).

Sample	SiO2	Al2O3	Fe2O3(T)	MnO	MgO	CaO	Na2O	K2O	TiO2	LOI
T17 01	34.04	2.93	12.28	0.215	34.22	0.17	0.04	0.49	0.087	12.9
T17 07	32.89	1.62	14.92	0.123	35.19	0.05	0.05	0.39	0.035	12.16
T17 09	31.9	3.71	14.27	0.101	32.49	0.04	0.07	0.67	0.093	11.69
T17 10	37.98	2.62	11.64	0.118	32.81	0.11	0.03	0.69	0.053	12.48
T17 13	33.2	1.97	15.63	0.13	34.33	0.08	0.02	0.01	0.066	13.13
T17 14	32	2.49	13.08	0.114	35.63	0.06	0.04	0.02	0.095	13.42
T17 17	33.54	1.96	12.44	0.118	37.4	0.04	0.01	< 0.01	0.084	12.99
T17 22	34.55	1.71	12.36	0.11	36.16	0.06	0.05	0.59	0.075	12.09
T17 26	35.09	1.63	12.78	0.114	35.12	0.05	0.04	0.52	0.037	12.92
T17 27	35.34	1.2	8.22	0.118	38.67	0.06	0.05	0.28	0.042	13.84

T17 30	34.95	3.67	13.86	0.138	33.2	0.71	0.14	0.26	0.107	12.35
T17 32	40.22	6.55	11.64	0.166	26.8	5.88	0.69	0.06	0.449	6.41
T17 33	34.96	2.44	10.77	0.138	34.92	0.04	0.04	0.79	0.063	13.61
T17 36	33.14	2.35	12.42	0.119	35.87	0.04	0.02	< 0.01	0.098	13.83
T17 39	33.87	1.82	10.94	0.14	36.69	0.03	0.04	0.02	0.053	14.51
T17 42	34.68	2.34	12.52	0.109	36.04	0.06	0.05	0.03	0.084	13.15

Table 2: Geochemical data of selected minor elements in serpentinized rock samples from Tjusterby (FUS-MS, Cr for sample T1709 analyzed with FUS-XRF). With the exception of S, all values shown are in ppm.

Sample	Ni	Cr	Zn	Cu	Pb	As	V	Co	S (%)
T17 01	2480	3810	1340	550	834	813	56	191	0.44
T17 07	1790	6590	210	190	10	189	66	149	0.11
T17 09	4290	> 10000	200	500	26	46	199	185	0.38
T17 10	1710	2360	750	110	308	138	79	146	0.13
T17 13	2010	2900	50	880	30	47	87	146	0.14
T17 14	2330	4960	490	350	104	12	56	155	0.15
T17 17	1650	4720	70	130	7	55	57	138	0.02
T17 22	2280	5700	180	< 10	8	934	62	126	0.02
T17 26	1960	4420	2830	280	749	17	41	141	0.21
T17 27	2190	4230	970	110	56	14	50	142	0.14
T17 30	1120	2680	1300	220	836	< 5	68	132	0.35
T17 32	720	2050	50	220	< 5	< 5	164	101	0.32
T17 33	1810	3360	1350	10	15	284	48	117	0.29
T17 36	1770	2250	1740	240	1460	43	48	131	0.2
T17 39	1780	2880	550	110	31	8	47	141	0.1
T17 42	1630	2810	150	90	5	284	43	144	< 0.01

Table 3: Geochemical data (ppm) of selected trace elements in serpentinized rock samples from Tjusterby (FUS-MS).

Sample	U	Cs	Sr	Rb	Th	La	Ce	Pr	Nd	Sm	Eu
T17 01	< 0.1	107	10	287	< 0.1	0.9	2.4	0.28	1.1	0.3	0.09
T17 07	2.2	13.8	4	142	0.2	0.6	1.9	0.24	0.8	0.2	< 0.05
T17 09	0.1	41.7	4	302	0.3	1.2	2.8	0.4	1.4	0.5	0.06
T17 10	0.1	57.5	5	265	0.4	0.8	2.7	0.39	1.7	0.5	0.08
T17 13	0.2	0.6	3	3	< 0.1	0.5	1.2	0.13	0.5	0.2	< 0.05
T17 14	< 0.1	0.9	< 2	< 2	< 0.1	1.6	2.7	0.23	0.8	0.1	0.1
T17 17	1.3	< 0.5	2	< 2	0.1	1.6	2.4	0.24	1	0.3	0.07
T17 22	< 0.1	41.2	4	155	< 0.1	0.9	3.6	0.52	2.3	0.7	0.08
T17 26	03	50.3	6	131	0.4	1.7	4.9	0.65	2.7	0.9	0.08
T17 27	8,2	20.2	4	48	< 0.1	2.6	7.5	0.9	3.4	1.3	0.06
T17 30	0,1	34.8	12	63	0.2	3.6	9.2	1.06	3.9	0.7	0.19
T17 32	0,2	0.9	13	< 2	0.2	1.3	3.4	0.56	2.8	1.1	0.28
T17 33	< 0.1	20.1	4	155	< 0.1	1.8	6.1	0.89	3.9	1.3	0.1
T17 36	0.5	< 0.5	< 2	< 2	< 0.1	1.7	3.8	0.4	1.5	0.3	0.07
T17 39	2.3	0.6	< 2	< 2	< 0.1	2.2	7.4	0.9	3.7	0.8	0.11
T17 42	1.6	< 0.5	2	< 2	< 0.1	2.5	4.1	0.4	1.8	0.3	0.09

Table 4: Geochemical data (%) of selected major elements in non-serpentinized rock samples of various types from Tjusterby (FUS-ICP).

Sample	SiO2	Al2O3	Fe2O3(T)	MnO	MgO	CaO	Na2O	K2O	TiO2	LOI
T17 03	52.61	14.87	11.3	0.172	6.17	5.74	3.67	2.68	1.372	1.83
T17 11	50.36	4.74	7.9	0.154	16.93	16.2	0.65	0.23	0.585	1.94
T17 20	41.14	11.61	14.96	0.234	11.77	15.02	1.15	0.88	2.335	1.14
T17 21	37.75	10.67	41.59	1.407	3.87	2.09	0.02	0.14	0.626	1.96
T17 28	43.67	8.61	12.71	0.217	18.16	9.8	0.66	0.73	0.666	3.38
T17 41	33.99	11.26	43.51	1.553	3.95	2.4	0.02	0.37	0.56	2.28
JI17 01	54.66	16.09	10.64	0.156	4.28	7.11	3.31	1.71	1.275	1
JI17 02	62.63	13.9	10.22	0.144	1.19	4.25	2.94	1.98	1.02	0.52
JI17 03	57.58	17.39	7.29	0.115	2.78	6.23	3.59	2.3	0.878	1.4
JI17 04	50.75	14.21	16.37	0.281	4.12	9.83	2.27	0.52	1.838	0.26

Table 5: Geochemical data (ppm) of selected minor elements in non-serpentinized rock samples of various types from Tjusterby (FUS-MS).

Sample	Ni	Cr	Zn	Cu	Pb	As	V	Co
T17 03	< 20	60	90	< 10	< 5	6	283	32
T17 11	200	1570	50	40	5	6	231	50
T17 20	700	1420	170	< 10	8	8	337	84
T17 21	40	80	170	220	7	< 5	137	48
T17 28	540	1600	220	< 10	< 5	40	240	67
T17 41	50	80	160	330	9	< 5	141	55
JI17 01	< 20	30	90	< 10	7	< 5	216	23
JI17 02	< 20	< 20	120	< 10	12	14	20	11
JI17 03	< 20	40	100	30	19	39	103	10
JI17 04	< 20	< 20	140	< 10	7	26	358	34

Table 6: Geochemical data (%) of selected major elements in bedrock samples from Mallusjärvi (FUS-ICP).

Sample	SiO2	Al2O3	Fe2O3(T)	MnO	MgO	CaO	Na2O	K2O	TiO2	LOI
JI17 05A	42.92	5.21	16.93	0.202	15.33	14.48	0.63	0.19	1.153	1.62
JI17 06	43.21	3.43	13.39	0.213	19.35	14.42	0.45	0.16	0.394	3.61
JI17 07	45.31	3.95	12.73	0.2	18.45	14.85	0.67	0.16	0.512	1.49
JI17 15	44.19	4.82	10.94	0.183	18.93	14.51	0.68	0.32	0.544	3
JI17 17	45.06	3.56	12.33	0.178	20.51	12.42	0.52	0.18	0.41	3.12

Table 7: Geochemical data (ppm) of selected minor elements in bedrock samples from Mallusjärvi (FUS-MS).

Sample	Ni	Cr	Zn	Cu	Pb	As	V	Co
JI17 05A	200	740	100	< 10	< 5	< 5	609	77
JI17 06	270	1370	70	10	< 5	< 5	197	84
JI17 07	240	1480	80	10	< 5	< 5	236	78
JI17 15	260	1540	60	10	< 5	< 5	207	72
JI17 17	280	1630	60	< 10	< 5	< 5	192	74

Table 8: Geochemical data (%) of selected major elements in bedrock samples from Pukkila (FUS-ICP).

Sample	SiO2	Al2O3	Fe2O3(T)	MnO	MgO	CaO	Na2O	K2O	TiO2	LOI
JI17 35	48.78	10.05	11.11	0.207	12.43	11.45	1.13	0.86	0.829	1.97
JI17 36	74.43	11.42	4.73	0.036	1.52	1.51	2.27	2.22	0.479	0.82
JI17 37	53.51	10.33	10.93	0.18	10.68	9.55	1	0.94	0.569	1.48
JI17 40	51.92	12.89	11.34	0.172	9.6	9.75	1	1.05	0.664	1.73
JI17 41	49.59	16.72	14.23	0.137	6.17	6.74	0.99	2.51	0.921	2.29
JI17 48	53.38	11.49	10.39	0.166	9.74	10.49	0.8	0.7	0.596	1.93
JI17 49	66.85	14.21	6.2	0.05	2.15	2.17	2.92	2.6	0.634	1.17

Table 9: Geochemical data (ppm) of selected minor elements in bedrock samples from Pukkila (FUS-MS).

Sample	Ni	Cr	Zn	Cu	Pb	As	V	Co
JI17 35	210	1140	180	60	< 5	< 5	327	55
JI17 36	30	100	50	30	14	< 5	56	8
JI17 37	60	140	70	80	< 5	< 5	261	49
JI17 40	60	500	80	40	7	< 5	271	42
JI17 41	< 20	20	100	60	6	< 5	606	46
JI17 48	130	700	80	20	8	< 5	239	43
JI17 49	30	110	70	20	15	< 5	90	12

Two chondrite-normalized REE-spider plots were constructed based on the data in table 10 (figures 12 and 13). These were created with the freeware software GCDkit (version 4.1), after the model of Boynton (1984). Figure 12 shows The REE patterns for the serpentinized rocks from Tjusterby, whereas figure 13 shows the REE patterns for the bedrock samples from Mallusjärvi.

Table 10: Geochemical data (ppm) of REE in serpentinized rock samples from Tjusterby (T1701–T1742) and bedrock samples from Mallusjärvi (JI1705A–JI1717).

	La	Ce	Pr	Nd	Sm	Eu	Gd	Tb	Dy	Ho	Er	Tm	Yb	Lu
T17 01	0.9	2.4	0.28	1.1	0.3	0.09	0.4	< 0.1	0.3	< 0.1	0.2	< 0.05	0.2	< 0.01
T17 07	0.6	1.9	0.24	0.8	0.2	< 0.05	0.2	< 0.1	0.2	< 0.1	< 0.1	0.06	< 0.1	< 0.01
T17 09	1.2	2.8	0.4	1.4	0.5	0.06	0.5	< 0.1	0.3	< 0.1	0.2	< 0.05	0.2	< 0.01
T17 10	0.8	2.7	0.39	1.7	0.5	0.08	0.4	< 0.1	0.3	< 0.1	0.2	< 0.05	0.2	< 0.01
T17 13	0.5	1.2	0.13	0.5	0.2	< 0.05	0.2	< 0.1	0.2	< 0.1	0.1	< 0.05	0.1	< 0.01
T17 14	1.6	2.7	0.23	0.8	0.1	0.1	0.2	< 0.1	0.2	< 0.1	0.1	< 0.05	0.1	< 0.01
T17 17	1.6	2.4	0.24	1	0.3	0.07	0.3	< 0.1	0.4	< 0.1	0.2	< 0.05	0.2	< 0.01
T17 22	0.9	3.6	0.52	2.3	0.7	0.08	0.8	0.1	0.9	0.2	0.5	0.06	0.3	< 0.01
T17 26	1.7	4.9	0.65	2.7	0.9	0.08	1.1	< 0.1	0.4	< 0.1	0.1	< 0.05	0.1	< 0.01
T17 27	2.6	7.5	0.9	3.4	1.3	0.06	1.7	0.3	1.7	0.3	0.8	0.09	0.5	0.06
T17 30	3.6	9.2	1.06	3.9	0.7	0.19	0.8	0.1	0.6	0.1	0.4	0.05	0.4	0.06
T17 32	1.3	3.4	0.56	2.8	1.1	0.28	1.5	0.3	1.7	0.4	1.1	0.15	0.9	0.13
T17 33	1.8	6.1	0.89	3.9	1.3	0.1	1.7	0.2	1.1	0.2	0.4	< 0.05	0.2	< 0.01
T17 36	1.7	3.8	0.4	1.5	0.3	0.07	0.4	< 0.1	0.3	< 0.1	0.1	< 0.05	0.2	< 0.01
T17 39	2.2	7.4	0.9	3.7	0.8	0.11	0.8	< 0.1	0.3	< 0.1	0.1	< 0.05	< 0.1	< 0.01
T17 42	2.5	4.1	0.4	1.8	0.3	0.09	0.4	< 0.1	0.5	< 0.1	0.3	< 0.05	0.3	< 0.01

JI17 05A	3.8	10.2	1.56	8	2.4	0.7	2.8	0.4	2.5	0.5	1.3	0.17	1.1	0.16
JI17 06	2.6	6.4	0.94	4.5	1.3	0.39	1.6	0.2	1.4	0.2	0.7	0.09	0.6	0.09
JI17 07	3.7	9.2	1.35	6.9	2	0.58	2.2	0.3	2	0.4	1	0.14	0.8	0.12
JI17 15	3.7	9.1	1.35	6.4	2	0.59	2.1	0.3	1.8	0.3	0.9	0.12	0.8	0.13
JI17 17	2.8	6.7	1.02	4.9	1.4	0.45	1.7	0.3	1.5	0.3	0.8	0.1	0.6	0.1

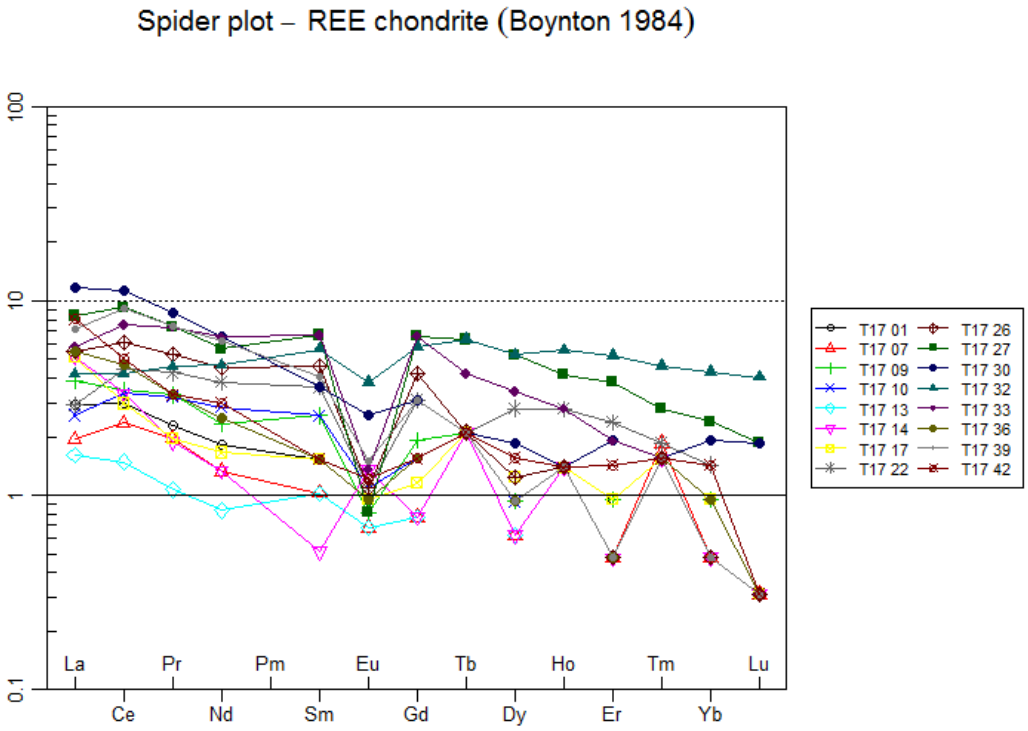

Figure 12: Chondrite-normalized REE-diagram for serpentinized rock samples from Tjusterby. Calculated with GCDkit, version 4.1.

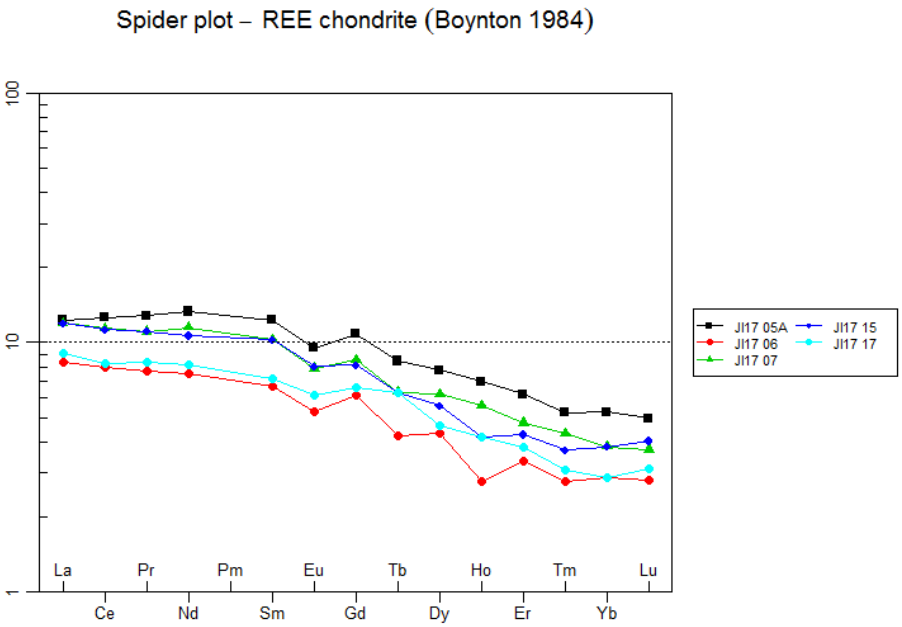

Figure 13: Chondrite-normalized REE-diagram for bedrock samples from Mallusjärvi. Calculated with GCDkit, version 4.1.

3.3 Magnetic susceptibility

Values for magnetic susceptibility were calculated as averages of three to eight separate readings from different points of each sample. All boulder and bedrock samples from Tjusterby and Mallusjärvi were measured directly at the sampling site. Results from the Pukkila area were excluded as the values were constantly very low, expressing no magnetic properties.

Table 11: Average values of magnetic susceptibility for all measured samples, calculated from three to eight individual readings. Areas Majkilsberget, Grels and Äppelbackarna are all parts of the Tjusterby area.

Sample	Area	Susceptibility (10^{-3} Si)	Rock type
T1701	Majkilsberget	14.600	Serpentinite
T1702	Majkilsberget	0.145	Amphibolite
T1703	Majkilsberget	0.454	Amphibolite
T1704	Majkilsberget	0.474	Amphibolite
T1705	Majkilsberget	73.388	Serpentinite
T1706	Majkilsberget	18.750	Serpentinite
T1707	Majkilsberget	70.088	Serpentinite
T1708	Majkilsberget	19.738	Serpentinite
T1709	Majkilsberget	45.163	Serpentinite
T1710	Majkilsberget	32.638	Serpentinite
T1711	Majkilsberget	7.443	Gabbro
T1712	Majkilsberget	20.850	Serpentinite
T1713	Majkilsberget	34.463	Serpentinite
T1714	Majkilsberget	41.775	Serpentinite
T1715	Majkilsberget	3.377	Amphibolite
T1716	Majkilsberget	12.670	Serpentinite
T1717	Majkilsberget	62.063	Serpentinite
T1718	Grels	4.295	Amphibolite
T1719	Grels	4.411	Amphibolite
T1720	Grels	4.148	Gabbro
T1721	Grels	275.100	Magnetite-rich biotite schist
T1722	Grels	82.200	Serpentinite
T1723	Grels	10.035	Amphibolite
T1724	Äppelbackarna	7.351	Gabbro
T1725	Äppelbackarna	6.648	Serpentinite
T1726	Äppelbackarna	32.400	Serpentinite
T1727	Äppelbackarna	1.666	Serpentinite
T1728	Äppelbackarna	0.925	Gabbro
T1729	Äppelbackarna	0.537	Amphibolite
T1730	Äppelbackarna	12.173	Serpentinite
T1731	Äppelbackarna	15.974	Serpentinite
T1732	Äppelbackarna	13.513	Serpentinite
T1733	Äppelbackarna	0.705	Serpentinite
T1734	Äppelbackarna	37.275	Serpentinite

T1735	Äppelbackarna	12.830	Gabbro
T1736	Äppelbackarna	48.150	Serpentinite
T1737	Äppelbackarna	18.276	Amphibolite
T1738	Äppelbackarna	2.206	Serpentinite
T1739	Äppelbackarna	31.888	Serpentinite
T1740	Äppelbackarna	11.870	Serpentinite
T1741	Grels	67.660	Magnetite-rich biotite schist
T1742	Majkilsberget	80.000	Serpentinite
JI1701	Majkilsberget	0.409	Biotite-hornblende schist
JI1702	Majkilsberget	0.463	Biotite-hornblende schist
JI1703	Majkilsberget	0.116	Gabbro
JI1704	Majkilsberget	0.181	Amphibolite
JI1705a	Mallusjärvi	129.800	Peridotite
JI1706	Mallusjärvi	44.388	Peridotite
JI1707	Mallusjärvi	67.283	Peridotite
JI1709	Mallusjärvi	86.775	Peridotite
JI1710	Mallusjärvi	59.438	Peridotite
JI1711	Mallusjärvi	52.188	Peridotite
JI1713	Mallusjärvi	48.388	Peridotite
JI1714	Mallusjärvi	27.138	Peridotite
JI1715	Mallusjärvi	22.675	Peridotite
JI1716	Mallusjärvi	19.850	Peridotite
JI1717	Mallusjärvi	40.850	Peridotite
JI1718	Mallusjärvi	63.913	Peridotite
JI1719	Mallusjärvi	43.675	Peridotite
JI1720	Mallusjärvi	75.038	Peridotite
JI1721	Mallusjärvi	45.025	Peridotite

3.4. Petrography

Of the 78 samples initially collected for this study, 26 were cut into thin sections for petrographical investigations. The samples are divided in similar groups as for the geochemical data. These groups are presented in two ways: for the internally more similar serpentinites and the Mallusjärvi samples the description begins with an evaluation of minerals seen in the thin sections and continues with textural descriptions of each individual sample. For the other groups, with more internal variations, each thin section is described fully individually. Along with a written evaluation, photographs of some of the most representative parts are shown below (figures 14–18).

3.4.1. Serpentinites

The serpentinite group contains the largest amount of thin sections in this study. Because the samples in their nature are quite similar to each other, the main minerals and the basis of their identification are collectively described first, with differences in abundance and texture of individual samples shown below. Sample T1732 is an exception, because

the serpentinization process is here more incomplete compared to the other samples. The serpentine group is composed of antigorite, lizardite and crysotile, but as they are optically indistinguishable, they will here be treated collectively under the name serpentine.

Serpentine: Dominant mineral in all serpentinized thin sections. Minor textural variations between the samples, but generally serpentines are fine grained and have irregular chaotic patterns. Occurs often as networks around other mineral grains. Mostly light green and pleochroic in PPL, although internal variations within the thin sections occur, with some clustered grains showing very little pleochroism. Interference colors are of low order grey, green and yellow, with greyish colors being the most common. Grains show high relief, but are too fine to allow for extinction angles or interference figures to be determined.

Phlogopite: Occurs typically as small to medium coarse grain sheets typical of mica. More often present individually than in clusters. Sometimes with minor inclusions of serpentine minerals and brucite. Appears to be colorless in PPL, although many grains are in places pleochroic in a bluish green color, especially along the grain boundaries and along narrow fractures. Grains show high relief. Phlogopite is often present in two forms: some grains show a clear parallel extinction to one cleavage direction, others have no visible cleavage. Grains with profound cleavage have often bright third order interference colors and a more angular shape, while grains lacking cleavage show low first order interference colors and are more rounded. The general shape and bluish pleochroic colors are similar between the two grain types, as is the zoned extinction visible in XPL. Measured interference figures are biaxial with 2V 0 degrees.

Plagioclase: Typically small grains with shapes reminding of mica, sheet like, sometimes wedge like shapes. Sub- and anhedral. Sometimes intergrown with phlogopite. Good cleavage along the length oriented direction, parallel to extinction. The cleavage has often a slightly bent appearance. Faint albite twinning often visible close to extinction. Alteration is very rare. Some grains lack cleavage and twinning and are more irregularly shaped. Both grain types are colorless in PPL, without clear pleochroism. Interference colors are of low 1st order, typically whitish grey. Grains have often relatively well developed shapes, suggesting a possible later stage growth.

Brucite: Typically fine anhedral rounded and roundish grains, often occurring individually in the serpentine matrix. Some grains are more elongated, but rounded and irregular. No visible cleavage. Extinction is gradational or undulating. Always colorless in PPL, with no clear pleochroism. Interference colors are of low 1st order, typically whitish grey. Interference figure is uniaxial positive, relief higher than for phlogopite. No alteration.

Chlorite: Sometimes seen as an alteration product of phlogopite, rarely also present along fractures filled with fine opaque minerals. Fine grained with irregular boundaries, often overriding primary minerals. Green in PPL, pleochroic. High order interference colors, anomalous Berlin blue colors are sometimes present.

Garnet: Rarely present as fine to medium coarse subhedral grains. Brown in PPL, black in XPL. High relief. No cleavage, has often irregular cracks.

Opaque minerals: Ranging from very fine to medium coarse. Irregular shapes, no pattern.

T1701

Serpentine (68%): two grain types; most grains are greenish both in PPL and XPL, weak pleochroism. Two bigger clusters with serpentine grains are colorless in PPL, dark grey in XPL. Texture for both is fine grained and network like. Opaque minerals are present as inclusions in both varieties, but are more common in the colorless serpentine minerals.

Phlogopite (12%): grains are sub and anhedral with sheety mica like shapes. Occurs more often as individual grains than in clusters. Dispersed grain size from finer to relatively coarse (0.5 to 2 mm). Bluish pleochroism. Some grains lack cleavage and have lower order interference colors.

Plagioclase (8%): 0.2 to 0.5 mm, sheet like grains resembling of mica. Subhedral and with straight grain boundaries. Weak albite twinning, visible close to extinction. One good cleavage parallel to twinning. Colorless in PPL, white/grey in XPL. Scattered, also as inclusions in phlogopite.

Brucite (4%): anhedral, roundish, no specific shape. Fine grains, sizes from 0.2 to 0.6 mm. Individual scattered grains. Colorless in PPL, dark grey in XPL. Interference figure uniaxial positive. No cleavage, undulating extinction.

Opaque minerals (8 %): variable grain sizes from very fine to medium coarse. No specific shapes, although some more rounded grains remind of pseudomorphic olivine. Highest concentration of opaque minerals is along the darker grey serpentine clusters.

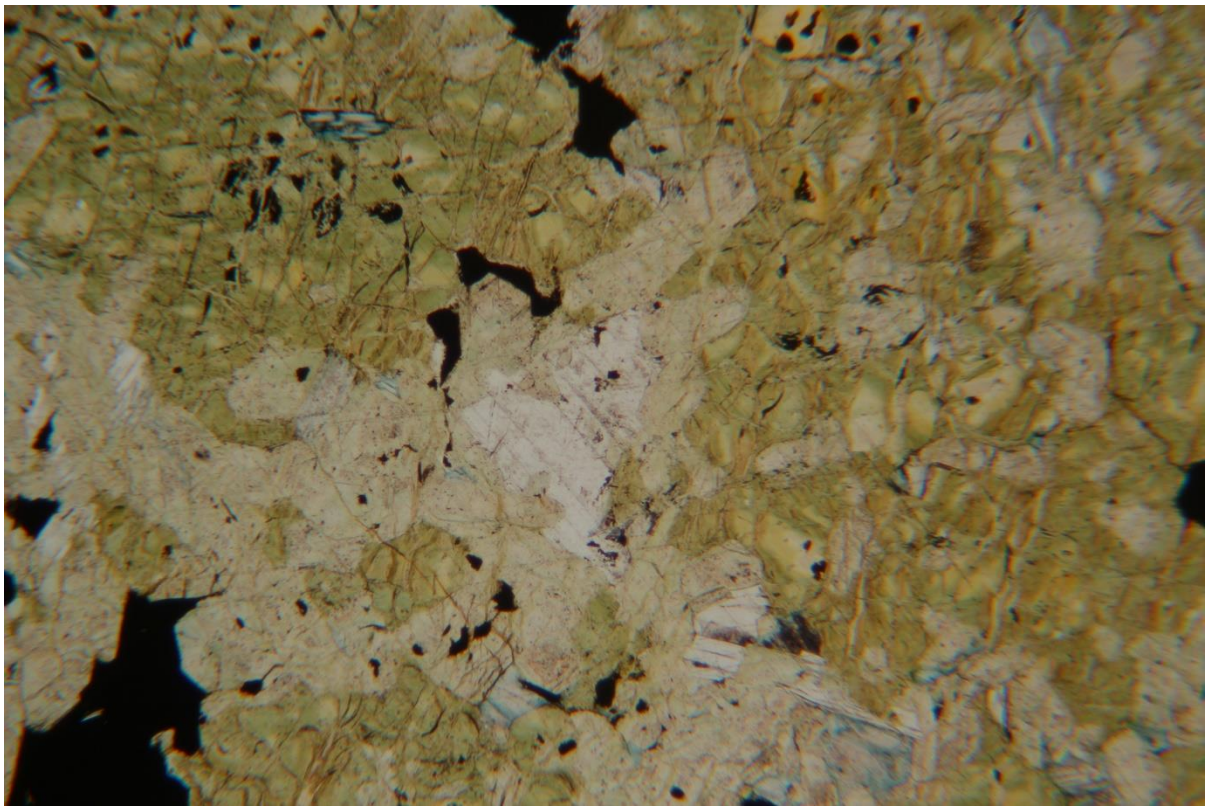

Figure 14: Microphotograph of sample T1701. Fine grained serpentine is the dominant mineral, with an irregular, network like texture. Colors are typical light green and light yellow. In the center of view is a grain of brucite (white, surrounded by light yellow serpentine). On the upper right side is a grain of phlogopite, partly white, partly bluish green. Field of view is about 2 mm.

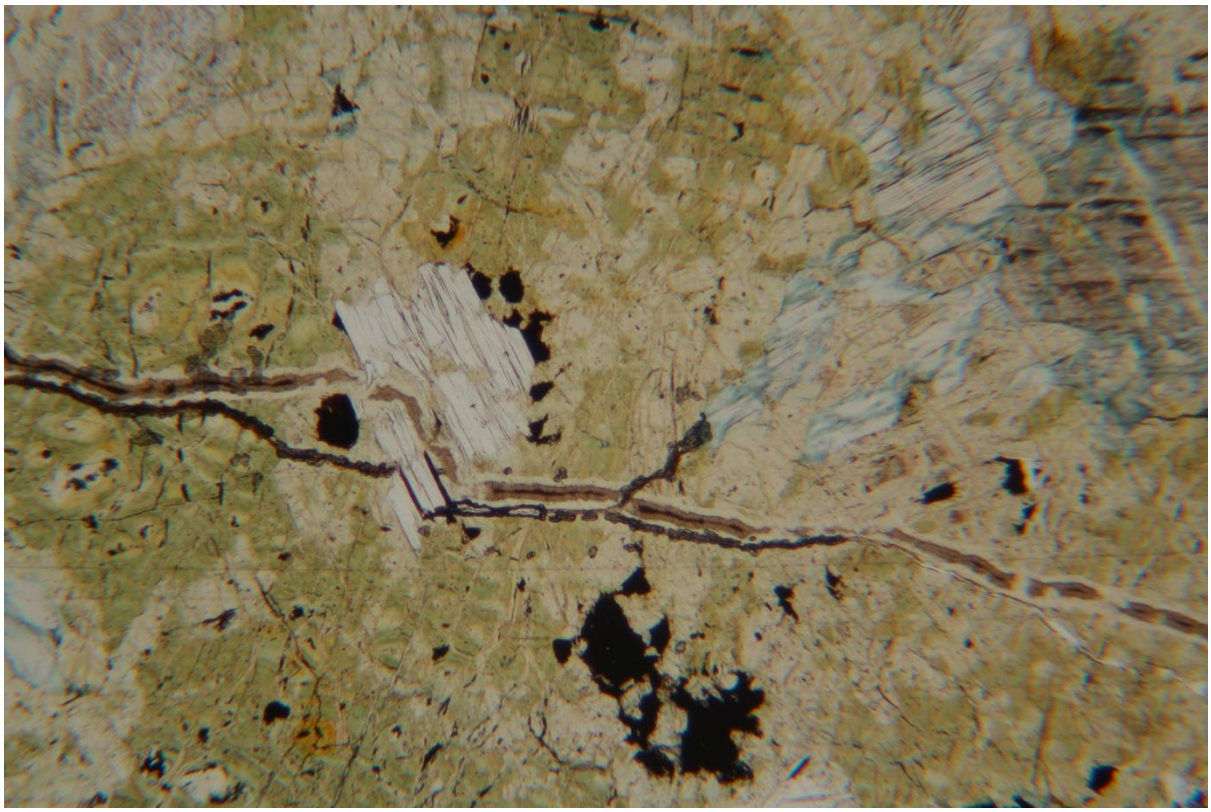

Figure 15: Microphotograph of sample T1701. Typical appearances of plagioclase (center left, pure white, mica like, angular) and phlogopite (center right, white with bluish green colors, more broken look) grains in a dominant serpentine matrix. The width of the plagioclase grain is about 0.5 mm.

T1707:

Serpentine (71%): homogenous mass of fine and very fine grains, no textural pattern. Weak green color in PPL, grey and dark toned in XPL, sometimes white. Lots of fine grained opaque minerals as inclusions.

Phlogopite (14%): irregular, anhedral grain shapes with almost no straight grain boundaries. Some variation in grain size, from fine to medium coarse (0.3-1.2 mm). Elongated opaque inclusions along well developed cleavage. Parallel extinction.

Brucite (3%): small 0.1-0.2 mm round isolated grains, with an exception of one elongated 1.0 mm elongated rounded grain. Inclusions of opaque minerals and serpentine.

Plagioclase (2%): rare, fine (0.1-0.2 mm) tabular, mica like grains. Occasionally more elongated. Sub- and anhedral, albite twinning.

Opaque minerals: (10%) fine to medium grained, relatively small variations in grain size. More often roundish than elongated, although dominantly angular and anhedral.

T1709

Serpentine (64%): fine to very fine grained with one cluster of slightly coarser grains, otherwise no visible pattern. Snake skin texture typical of serpentine minerals. Weak pleochroism in PPL, white to dark gray in XPL.

Phlogopite (20%): sub- to anhedral platy grains, ranging from fine grained to relatively coarse (up to 2-3 mm). Some grains are more intact, others cracked and disturbed, with elongated opaque inclusions along cleavage planes.

Plagioclase (5%): platy, sub- to anhedral, occurs individually or as clusters of a few grains. Mica like appearance. Often in contact with larger opaque grains. Size up to 1.0 mm, usually finer. Albite twinning.

Opaque minerals (11%): fine to medium coarse, highly irregular shapes. Most grains are dark brown with black rims in PPL, black in XPL.

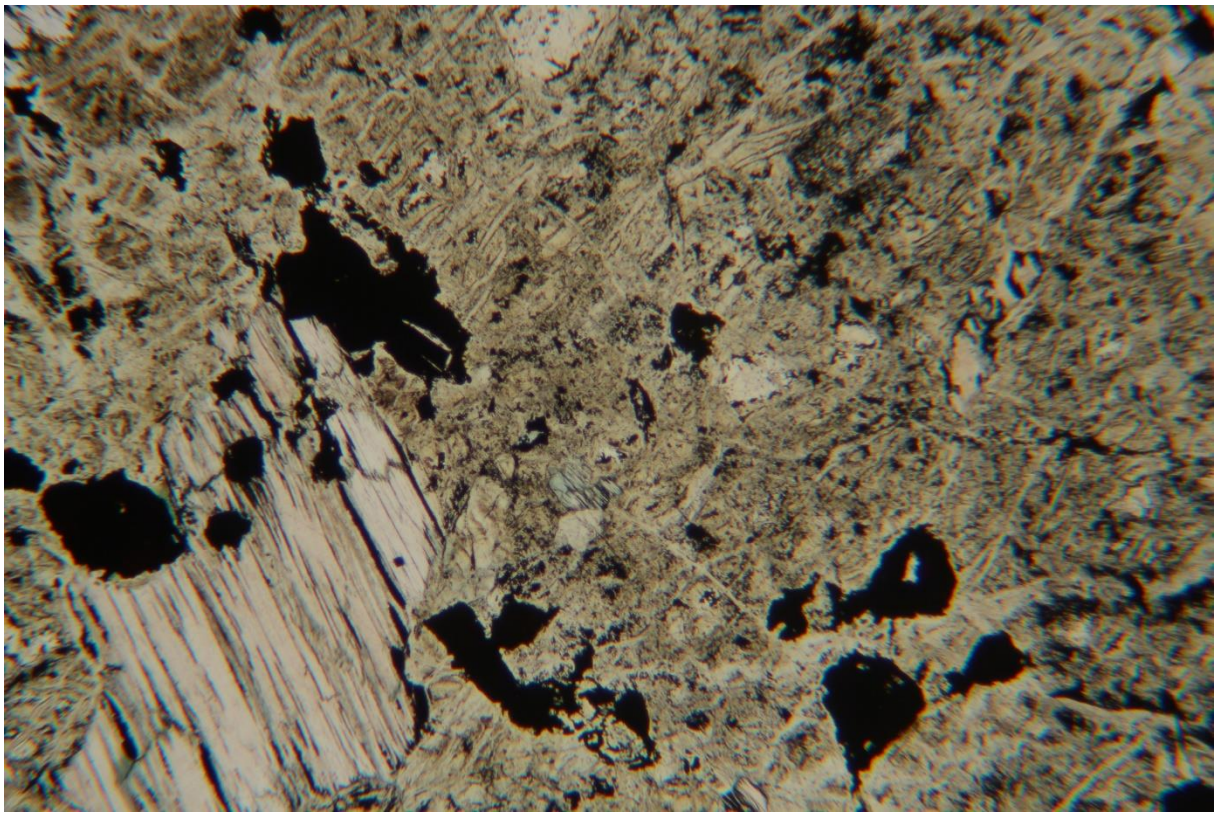

Figure 16: Microphotograph of sample T1709. Coarse 1mm phlogopite grain in a serpentine matrix. Faint green alteration visible along grain boundaries.

T1717

Serpentine (81%): forms a network of very fine to fine grains, with an exception of a few elongated, cracked and irregular grains of medium coarse size.

Plagioclase: (5%) fine mica-like grains, individual and as clusters with a few grains. Size 0.1 to 0.8 mm. Sometimes grown around larger opaque grains. Opaque phases also as inclusions along cleavage planes in plagioclase grains. Albite twinning.

Garnet (3%): few fine (0.4 mm), angular, individual grains in contact with serpentine and opaque minerals. Fractured, no cleavage. Dark brown in PPL, black in XPL.

Opaque minerals (10%): fine to medium coarse. Irregular shapes; sometimes angular and elongated, sometimes more rounded. Dark brown or black in PPl, black in XPL.

T1722

Serpentine (81%): grain size generally very fine to fine, slightly coarser close to two larger sub-parallel fractures penetrating the thin section. Light pleochroism in PPL, white to dark grey colors in XPL.

Phlogopite (10%): variable grain sizes (from fine to medium coarse, 0.2 to 1.5 mm). Subhedral to anhedral grains, often clear with a mica like form. Individual grains, no

clusters. Occasional opaque minerals as inclusions along cleavage plains. Some grains lack cleavage, and have lower interference colors. Bluish pleochroism.

Plagioclase (2%): quite rare, present as fine (0.1-0.5 mm) scattered individual grains. Mostly with a mica-like appearance, sometimes more rounded with no visible cleavage. Occasional opaque minerals as inclusions.

Opaque minerals (7%): fine, relatively even grain sizes. Mostly rounded grains, more elongated as inclusions in phlogopite or plagioclase.

T1726

Serpentine (82%): Heavily serpentinized, grains can be divided into three types: mostly as a similar fine grained mass as in other thin sections, but partly also as more homogenous, vein like infill material. Sometimes also as narrow wedge shaped crystals with fine grained interiors occurring in random orientations, length up to 2.5 mm

Phlogopite (7%): mostly as fine platy grains scattered throughout the thin section, some grains are slightly coarser. Strong greenish alteration in PPL, pleochroic. Disturbed, anhedral shapes.

Plagioclase (2%): rare and fine grained (<0.5 mm). Mica-like texture with straight edges and an elongated shape. Faint albite twinning.

Opaque minerals (9%): rounded, narrow, elongated. Sizes from <0.1 to 0.5 mm. Partly as filling in very narrow fractures. No specific textural pattern.

T1727

Serpentine (80%): fine grained and homogenous, snake skin texture. Very little variation in grain size or appearance. Very faint greenish pleochroism in PPL, grey 1st order interference colors in XPL.

Phlogopite (10%): anhedral, 0.2 to 1.0 mm coarse sheety mica-like grains. Good cleavage with slight bending, almost parallel extinction. Some grains appear to be disturbed with irregular grain boundaries and lack of cleavage. Others have one or two straight edges and profound cleavage. Light green pleochroism with a bluish tint along all grain boundaries.

Plagioclase (1%): very rare, grains 0.1 to 0.5 mm. Subhedral with straight edges. Texture reminding of mica.

Opaque minerals (9%): roundish grains, size <0.5 mm. Some grains are not completely black, more dark brown and surrounded by a pale orange rim that overlaps the surrounding serpentine minerals.

T1732

Orthopyroxene (35%): Anhedral grains, partly large (up to 3-5 mm) roundish and irregularly shaped and partly smaller, equally anhedral elongated. Two cleavage directions are locally visible, intersecting at 90 degrees. Extinction parallel to the longitudinal axis of the elongated grains. Colorless in PPL, with interference colors from 1st order grey to 2nd order blue in XPL. 2V 90 degrees. Inclusions of serpentine and olivine in the largest grains.

Serpentine (30%): abundant, but not as dominant as in other serpentinitic samples. Present as fine grained patches of variable sizes, often with inclusions of fine remnants of unserpentinized minerals. Chaotic texture. Surrounds olivine in places where the serpentinization process is incomplete. Also surrounding and included in grains of pyroxene. Strong green color in PPL, pleochroic to other shades. Dark green in XPL.

Olivine (15%): rather fine, 0.1 to 0.5 mm rounded grains. No cleavage, but often irregularly fractured. Alteration to serpentine along fractures and at grain margins. Colorless in PPL, no pleochroism. Very high relief. 2nd or 3rd order interference colors in XPL. Present both as clusters of several grains and individually.

Clinopyroxene: (10%) Anhedral, sub rounded, grain sizes <1 mm. Two slightly oblique cleavage planes. Extinction oblique to cleavage at about 37/53 degrees. Colorless in PPL with very weak yellowish pleochroism. Interference colors in XPL 1st order yellow. Also present as more elongated anhedral grains with 2nd order blue colors in XPL. These grains identified as orthopyroxene through similar cleavage and extinction.

Phlogopite (2%): rare, with 0.3 mm subhedral elongated mica-like grains. Yellowish pleochroism in PPL, also spotty green pleochroism as in most other thin sections. 2nd/3rd order blue interference colors in XPL. Extinction parallel to cleavage. In contact with serpentine and pyroxene.

Plagioclase (1%): very rare. Subhedral with undisturbed edges, size up to 0.3 mm. In contact with pyroxene and the opaque minerals. Mica like texture. Colorless in PPL, 1st order white in XPL. Parallel extinction to cleavage. Also present as small clusters of narrow elongated, slightly bent grains collectively creating a fibrous looking texture.

Opaque minerals (7%): two forms: as more rounded, 0.5 mm grains present in the entire thin section and as material reminding of fracture filling in serpentine.

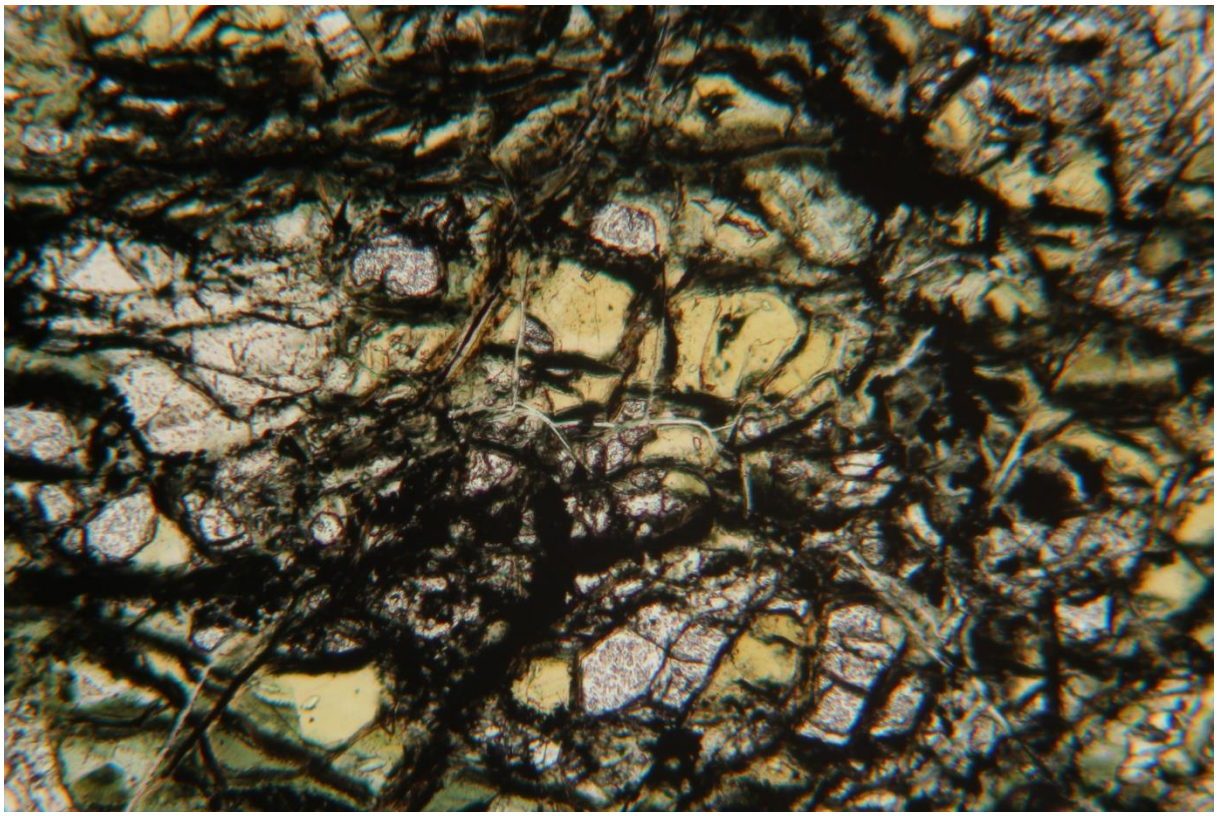

Figure 17: Microphotograph of sample T1732. Olivine (white) partly altered to serpentine (light yellow). Olivine grain c. 1 mm in diameter.

T1733

Serpentine (67%): fine grained and homogenous, snake skin texture with slightly coarser grains between a very fine mass. Yellowish green in PPL, very weak pleochroism. Dark grey in XPL.

Phlogopite (13%): sub and anhedral grains, 0.2 to 1.0 mm. Some grains with straight boundaries, others more disturbed. Good cleavage. 2nd/3rd order interference colors. Weak greenish pleochroism, possible chlorite alteration on some grains. Also as cleavage-lacking grains with 1st order interference colors. Same greenish pleochroism in all grain types.

Chlorite (8%): Present along two narrow fractures and as fine individual grains, possibly as alteration of phlogopite. Pleochroic in PPL from colorless to strongly green, anomalous Berlin blue colors in XPL. Good cleavage in one direction, parallel extinction to it.

Plagioclase (4%): Mica-like grains. Subhedral. Often with good cleavage, sometimes without. Albite twinning. Mostly as individual 0.1 to 0.6 mm grains in serpentine.

Opaque minerals (8%): rounded and irregularly shaped, sometimes in serpentine, otherwise surrounded by phlogopite or as inclusions within it.

T1736

Serpentine (83%): very heavily serpentinized. Fine grained mass with snake skin texture. Homogenous, no specific patterns. Colorless in PPL, dark grey in XPL.

Plagioclase (4%): rare, fine (<0.3 mm) mica-like grains. Individual. Subhedral, good cleavage. Also some elongated and narrow, almost fibrous grains. Weak albite twinning in most grains.

Opaque minerals (13%): highly variable shapes, from roundish to very irregular. Sometimes dark brown cores in PPL, grains mostly pure black.

T1742

Serpentine (80%): fine grained, chaotic texture. Present as fine and really fine grains that follow a relict fracture in serpentine. These finest grains are darker in both PPL and XPL than the slightly coarser grains, which have a lighter grey color in XPL.

Plagioclase (6%): present as narrow, elongated grains in serpentine. Coorless in PPL, white and light grey in XPL. Mostly individual, excluding some small clusters with 5-10 fine grains. Sometimes with opaque inclusions parallel to cleavage direction. Albite twinning.

Opaque minerals (14%): highly irregular shapes, mostly concentrated along the darker and finer serpentine grains, following some relict fractures. Also as inclusions in plagioclase. Size up to 0.6 mm.

3.4.2. Unserpentinized boulder samples from Tjusterby

T1703

Hornblende (58%): subhedral grains, rounded to semi-angular. Grain size 0.1-0.5 mm. Grains have almost a parallel orientation, creating a layered texture. Pleochroic green in PPL, with various second order colors in XPL. 56/124 degree cleavage angles visible in some grains. Rare augite law twinning.

Plagioclase (25%): grains roundish but semi-angular, relatively even grain size (0.3-0.5 mm). Weak elongation towards direction of layering. Often heavy mica alteration, “dirty” appearance. Unaltered grains rare, but when present, with visible lamellae twinning.

Biotite (10%): rather small platy grains, narrow and elongated, typically 0.3 mm in length. Angular, subhedral. Often altered to chlorite. Pleochroic green in PPL, often bluish colors in XPL. Length oriented in direction of layering.

Quartz (3%): small (0.1-0.3 mm) rounded, anhedral grains. Colorless in PPL, white in XPL. No twinning, interference figure uniaxial positive.

Apatite (1%) very rare, as fine (less than 0.1 mm) roundish inclusions in hornblende. Colorless in PPL, dark colors in XPL. Very high relief.

Opaque minerals (3%): fine grained (0.1-0.3 mm), roundish shapes. Evenly scattered throughout the thin section.

T1721

Biotite (30%): most commonly tabular mica-like grains, sometimes also more irregularly formed. Size 0.2-0.8 mm. Somewhat clustered in layers, although all grains are not parallel. Pleochroic from yellow to greenish in PPL, light yellow and light blue in XPL. Often chloritized, which could explain low interference colors. Good cleavage in one direction, parallel extinction. Without them it could be mistaken for hornblende. Inclusions of zircon are common.

Garnet (25%): forms anhedral roundish but angular grains with numerous inclusions of quartz and opaque minerals. Size 0.3-0.8 mm. Weak brown color in PPL, black in XPL. High relief. Dirty appearance, often fractured causing an unusually broken appearance.

Quartz (18%): grains are typically anhedral, often clustered in a layered texture. Variable sizes (0.2-1.0 mm). Colorless in PPL, low 1st order colors in XPL. Interference figure uniaxial positive.

Epidote (2%): very fine grained (0.1 mm), grains in small clusters. Often as inclusions in biotite. Colorless and with a high relief in PPL, very colorful in XPL.

Opaque minerals (25%): grains are roundish and relatively evenly sized (0.1-0.6 mm). Abundant throughout the entire thin section. Similar layered texture as for most minerals.

T1741

Biotite (27%): fine (0.2-0.4 mm), elongated grains forming layered clusters. Subhedral, angular, semi parallel. Grains are pleochroic from light yellow to greenish in PPL, in XPL they are light blue or brown. Parallel extinction to cleavage.

Garnet (23%): roundish grains together making up a layered texture. Subhedral, size 0.3-0.5 mm. High relief in PPL, black in XPL. Numerous inclusions of very fine grained opaque minerals.

Quartz (20%): common, forming typical anhedral roundish grains. Sizes 0.2-1.0 mm. Layered, as the other minerals. Colorless, uniaxial positive.

Epidote (5%): forms variously sized aggregates of fine (<0.1 mm) grains. Colorless with marginal pleochroism in PPL, high relief. Colorful, high interference colors in XPL. Often associated with biotite.

Opaque minerals (25%): Semi-rounded, fine to medium grained (0.1-1.0 mm), layered. Sometimes with a more angular shape.

3.4.3. Bedrock samples from Tjusterby

JI1701

Quartz (33%): typical rounded anhedral grains, size 0.2-0.5 mm. Colorless, uniaxial positive. Grains slightly elongated in the layering direction. Possible apatite inclusions.

Biotite (27%) has narrow elongated sheeted grains with a clear layered texture. Subhedral, angular. Identifiable through parallel extinction and typical interference colors. Pleochroism is very strong, from light to very dark brown.

Hornblende (20%) forms shorter (0.1-0.4 mm) subhedral grains with weak orientation in the direction of layering. There is also one larger aggregate of mostly hornblende crystals, with the rest of the mineral matrix diverting around the aggregate cluster, as for some prekinematic porphyroblasts. Clear cleavages, intersecting at 124/56 degrees.

Plagioclase (15%): grain shapes very similar to quartz. Moderate to strong mica alteration. Rare albite twinning. Dirty appearance.

Opaque minerals (5%): sub-rounded, sizes <0.5 mm.

JI1702

Quartz (40%): rounded anhedral grains, minor size variations (0.2-0.8 mm). Some of the more elongated grains are oriented in the direction of layering. No twinning or alteration.

Plagioclase (25%): texturally similar to quartz, identifiable by albite law twinning. Anhedral grains, only minor mica alteration that sometimes creates a dirty appearance. 2V 75-80 degrees.

Biotite (22%): grains are elongate and sheet like, forming a clearly layered texture. Angular, subhedral. Size 0.2-0.6 mm. Some grains have zircon inclusions. Light to dark brown in PPL, greenish brown in XPL.

Hornblende (10%): generally short roundish grains, locally more elongated and angular. Subhedral, sizes <0.7 mm. Strong green pleochroism, low colors in XPL. 124/56 degree cleavage angles.

Opaque minerals (3%): roundish, fine grained, no specific textural pattern.

JI1703

Plagioclase (49%): grains both rounded and subhedral rectangular. Sizes 0.3-0.8 mm. Some grains almost completely seritized, others not at all. 40% anorthite with the Michel Levy method (albite twinning). No specific textural pattern.

Biotite (20%): forms elongated and rather small (0.2-0.6 mm) grains, with no layering or other textural pattern. Heavy pleochroism, typical appearance in XPL. Good cleavage, albeit for one abnormally large dark brown, half-rectangular grain without cleavage. Some chloritization. Inclusions of very fine zircon grains are relatively common.

Quartz (15%): forms round fine (0.3-0.6 mm) anhedral grains. Minor undulating extinction. No alteration or twinning, colorless.

Pyroxene (15%): variously sized (0.4-1.5 mm), irregular shape, grains often partly broken. Mostly clinopyroxene, judging by the inclined extinction angle and second order interference colors. Some grains have lower order interference colors and show parallel extinction to cleavage (orthopyroxene). Colorless in PPL, no pleochroism,

Opaque minerals (1%): rare, roundish, fine grained.

JI1704

Hornblende (60%): forms mostly roundish or slightly elongated grains parallel to the direction of layering. Size 0.05-0.5 mm. Pleochroic green in PPL, various second order interference colors in XPL. 124/56 degree cleavage angles in some samples. Minor inclusions of some very fine grained minerals with pleochroic halos.

Quartz (25%): has mostly fine (0.05-0.3 mm) round, anhedral grains. Partly clustered in a layered orientation, following the general texture in the sample. Colorless. Rare undulating extinction.

Plagioclase (10%): often with coarser grains than quartz (0.1-0.5 mm, rarely up to 1.0 mm) Anhedral and roundish, often altered to sericite. Twinning is rare.

Opaque minerals (5%) size up to 0.5 mm, irregular shapes. Layered (as all other minerals).

3.4.4. Mallusjärvi

JI1705a

Pyroxene (55%): coarse grains, up to several mm in size. Often hard to see boundaries between separate grains, intergrown and messy. Disturbed. Cleavage rarely visible, but sometimes weak with oblique extinction (clinopyroxene). Colorless grains in PPL, no pleochroism. First and second order colors in XPL, with brighter colors more common.

Olivine (5%): fine (0.2-0.4 mm) roundish grains. Often clustered in groups of several grains. Colorless with high relief in PPL, $2^{nd}/3^{rd}$ order interference colors in XPL. No cleavage, but often fractured.

Iddingsite (10%): highly irregularly shaped grains, partly intergrown into a network. 0.1-0.5 mm. In contact with olivine and pyroxene. Sometimes surrounding small olivine grains. Yellow, brownish yellow or greenish in PPL, dark green/brown in XPL. Not pleochroic. Fractures resembling olivine. Pseudomorphic olivine texture sometimes quite clear.

Plagioclase (5%): Sheet like form, resembling mica. Subhedral, angular, size 0.2-0.5 mm. More often in small clusters than individually. Faint albite twinning close to extinction. Colorless in PPL, white in XPL. Appearance suggests a later growth than for other grains.

Opaque minerals (25%): occur either as very fine (0.1mm) or slightly coarser grains (0.3-0.6 mm). The latter are more angular, but shapes are still irregular.

JI1707

Pyroxene (82%): both anhedral and more rectangular subhedral grains. Often coarse, rare fine grains (general size 0.5-5mm). Neighboring grains have often grown into each other. Sometimes zoned, rare augite twinning. Highly disturbed, cleavage very rarely observable. Grains with 2^{nd} order interference colors (possible clinopyroxene) are more common than grains with lower colors (orthopyroxene).

Olivine (8%): roundish and irregular, sometimes elongated grains. Partly broken with truncated pieces of other minerals. Finer than the pyroxenes. Some grains are medium coarse, others broken down into a fine ground mass. Colorless with high relief in PPL, high interference colors in XPL. Fractured, no cleavage. Sometimes altered to iddingsite. Rare minor serpentinization in some fractures.

Iddingsite (6%): associated with olivine. Sometimes surrounding it and in its fractures, sometimes as a complete pseudomorph of it. It has either a shape of the initial olivine or

is more irregular, as most other grains in this thin section. Yellowish brown in PPL, darker shades in XPL. Not really pleochroic.

Opaque minerals (4%): fine grained, no specific textural pattern. Roundish, mostly <0.1 mm in (some 0.2-0.5 mm) grains. As inclusions in pyroxene.

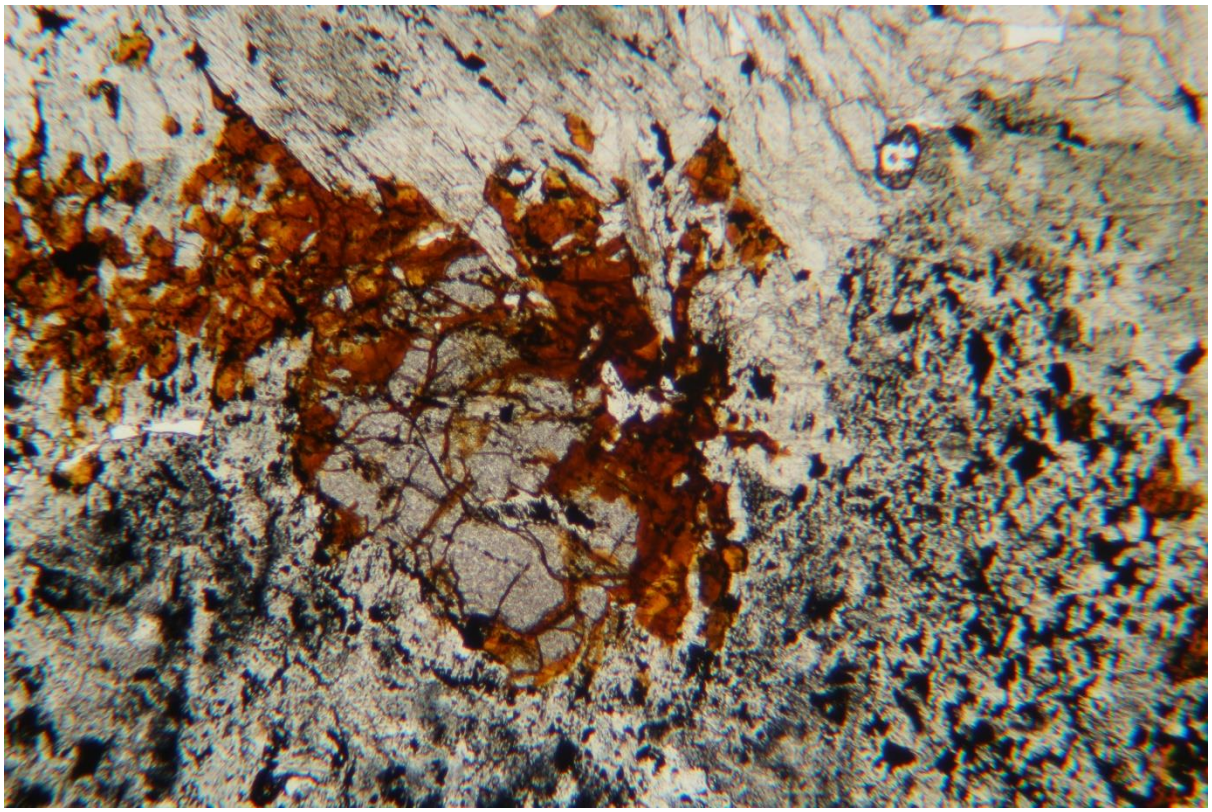

Figure 18: Microphotograph of sample JI1707. Grain of olivine (center, white, high relief) partly altered to iddingsite (orange brown). No alteration to serpentine. Surrounding grains are pyroxene.

JI1715

Pyroxene (64%): mostly coarse grains up to 5 mm in size, both rectangular and irregularly roundish. Grains intergrown and disturbed, messy texture. Rarely more angular, with a subhedral shape. Minor zoning. Interference colors both 1st and 2nd order, extinction both parallel and oblique to cleavage. Roughly equal amounts of ortho- and clinopyroxene.

Olivine (12%) present as clear roundish grains, typical fractured appearance. Size less than 1 mm, anhedral and subhedral. Colorless in PPL, high relief and high interference colors. Minor inclusions of pyroxene. Some grains partly altered to iddingsite, others are completely altered.

Iddingsite (12%): relatively common, sometimes surrounding olivine and its fractures, sometimes as a pure pseudomorph. Partly intergrown from several altered olivine grains, thus grain sizes are up to 2 mm. Strong orange color in PPL, brown in XPL.

Plagioclase (4%): generally less than 0.5 mm (one 0.8 mm grain). Subhedral, tabular, slightly elongated. Angular. Individually and in groups. Occasionally as inclusions in pyroxene. Albite twinning.

Opaque minerals (8%): Grain size from very fine to 0.3 mm. Roundish, no specific textural pattern.

3.4.5. Pukkila

JI1735

Hornblende (71%): diffusive grain boundaries, grains are anhedral and have a broken look. Sizes variable, from 0.2 to >3 mm. Colorless to green in PPL with strong pleochroism, 1st and 2nd order colors in XPL. Sometimes visible cleavage angles of 56/124 degrees, slightly inclined extinction. First and second order interference colors, many grains have inclusions of other minerals.

Plagioclase (10%) forms relatively small anhedral grains, some of which have albite twinning with wide lamellae, others show heavy alteration into mica.

Chlorite (9%): narrow, elongated grains, wedgy shapes. Typical mica shape. Some grains have a bent appearance, extinction is length parallel. Almost colorless, weak pleochroism, Identifiable Berlin blue interference color. Often associated with hornblende.

Biotite (3%): sometimes present in contact with hornblende as small narrow elongated grains. Size 0.4 mm. Strong brown pleochroism, colorful in XPL.

Titanite (3%): as small individual wedge-like fragments. Angular, anhedral and subhedral. Also as inclusions in hornblende. Very high interference colors.

Garnet (1%): anhedral, high relief, black in XPL. Often as inclusions in hornblende. Size typically 0.3 mm.

Opaque minerals (3%) fine grained with a maximum size of 0.5 mm. Angular grains with irregular shapes. No specific textural pattern.

JI1736

Quartz (57%) with anhedral rounded grains, most of which with undulating extinction. Fine and relatively even grain sizes (0.1-0.4 mm). Weak layering observable.

Biotite (25%): grains are elongated and have a parallel orientation, marking a layered texture. Even grain size, slightly smaller than for quartz (0.1-0.3 mm). Strong brown pleochroism.

Plagioclase (15%) often slightly larger than other minerals. Most grains show heavy mica alteration. Rare albite twinning. Rounded shape.

Muscovite (2%): rare, but clearly visible due to neon bright interference colors. Colorless in PPL. Grains are shorter (0.1-0.2 mm) than for biotite, but have similar textural layering.

Opaque minerals (1%): rounded, sizes 0.1-0.2 mm.

JI1737

Hornblende (65%): anhedral, with grain sizes <5 mm. Sometimes forming elongated rectangular grains, sometimes smaller rounded grains. Some grains show augite law twinning. Inclusions of biotite and opaque minerals are common. Strongly pleochroic with greenish colors. 124/56 degree cleavage angles sometimes shown.

Quartz (15%): forms rounded, sometimes elongated grains, some of which show heavily undulating extinction. Some grains have inclusions of hornblende. Sizes variable, from 0.3 to 2.5 mm.

Plagioclase (10%): present as slightly smaller grains (0.3 to 2 mm), some have clear albite twinning, others are heavily altered to fine grained mica.

Biotite (8%): often present as clustered aggregates. Grains are both short and rectangular and elongated. Sometimes as inclusions in hornblende. Grains roughly orientated in the same direction, but no general layered texture can be observed.

Garnet (1%): rare roundish grains, size 0.4 mm. Brown in PPL, black in XPL.

Opaque minerals (1%): rounded, sizes <0.5 mm.

JI1741

Hornblende (30%): grains are anhedral, short, both angular and rounded. Sizes 0.2-0.6 mm. Some have inclusions of quartz. Strong green color in PPL, lower 1st and 2nd order colors in XPL. 124/56 degree cleavage angles in some grains. Elongated grains semi-parallel, indicative of a weak layering.

Biotite (30%): grains are more elongated and sharp, as is typical for mica. Sizes typically 0.2 to 0.6 mm, but can be up to 1.0 mm. Brown in PPL, pleochroic. High green/red colors in XPL. Some grains are partly chloritized and more green in PPL, bluish in XPL. Grains have a semi-parallel orientation.

Plagioclase (25%): forms roundish anhedral, relatively even sized (up to 0.8 mm) grains. Often heavily altered to mica, muscovite can sometimes be identified as an alteration product. Rare albite and Carlsbad law twinning. Grains intergrown, messy texture.

Quartz (10%): present as small (0.2-0.5 mm) rounded grains, many show undulating extinction. Distinguishable from plagioclase by lack of alteration.

Opaque minerals (5%): often anhedral, round shapes. Fine grained.

JI1748

Hornblende (70%): anhedral grains, both sharp and rounded. Variable sizes (0.3–2.5 mm). Rare inclusions of biotite and opaque minerals. Green and pleochroic in PPL, various 1st and 2nd order colors in XPL.

Plagioclase (15%): has smaller (0.3-1.5 mm) and very irregularly shaped grains, more or less altered to fine mica. Some grains are twinned. Colorless in PPL, low 1st order in XPL.

Quartz (8%): grains are mostly small and rounded, coarsest grain is about 1.0 mm. Colorless and low relief, some grains show undulating extinction.

Biotite (5%): has narrow elongated grains, shows sometimes a slightly bent texture. Sizes <0.6 mm. Partly as inclusions in hornblende. Some grains are moderately chloritized. Brown in PPL, high order colors in XPL.

Opaque minerals (2%): rare, shapes range from long and elongated to roundish. No specific textural pattern. Sizes 0.2-0.4 mm.

4. Discussion

4.1. Validity of used ore prospecting methods

As this study presents a previously undefined lithological unit, not exposed in outcrop, the entire work is a combination of the methods used to locate the target, and an evaluation of the results gathered from the collected samples. The main study object itself would not have been localized without the traditional ore prospecting methods of till sampling, boulder tracing and magnetometry. Of these, investigations of aeromagnetic maps by GTK and till samples examined in an earlier study (Ingves 2016) were the first physical evidence of the existence of material differing from known rock units in the area. Especially the enrichments of e.g. Ni and Cr in these samples, together with elevated values of magnetic susceptibility in some of them, raised initial suspicions about an additional unit different to the gabbros, amphibolites and granites identified in outcrop. Till sampling is a widely used method in ore exploration in Finland (Sarala 2015) and useful in indicating potential sources of various metals in the bedrock. But as enough till data already were gathered from 2015 (Ingves 2016), no new samples were seen to be needed for this study. More information was needed from actual rock samples and magnetometry surveys, however, with boulder tracing as a priority during field work in

September 2017. Some knowledge had already been gained from three ultramafic boulder samples discovered during the field course in ore prospecting in 2016. Therefore, it was known that boulders differing from outcrop could be found in the area.

As with till sampling, boulder tracing is a widely used method in ore prospecting, especially in areas influenced by glaciation cycles during the Quaternary. Differing from till, which always is a mixture of various rock units in different fractions, boulders give more direct information about the bedrock source. In ore prospecting, boulder tracing has led to several well-known discoveries in almost every different commodity (McClenaghan & Paulen 2018). Altogether 51 boulder samples from the Tjusterby area were examined in this study, 26 of which had an ultramafic composition. They were all found within the local direction of transportation of the last glaciation (Glückert 1974) when referenced to the magnetic anomalies under the Pernajanlahti bay, but the transportation distances with only a few hundred meters from the original source are clearly shorter than the mean values of the geometric means of 4.6 km calculated for glacial drift for surface boulders in different parts of Finland in one extensive example study (Salonen 1987). However, the sources of the boulders can with high certainty be linked to the underwater magnetic anomalies due to several different reasons. Firstly, there are no known exposures of similar ultramafic rocks within several tens of km from the Tjusterby area (DigiKP 200, digital bedrock map database). Secondly, the examined serpentinized ultramafic boulders show highly enriched values of magnetic susceptibility, which is conclusive with the clear anomaly of several thousands of nanoteslas observed in the magnetometry studies over the Pernajanlahti bay. The amphibolitic boulder and bedrock samples collected in the area, on the other hand, had consistently lower magnetic susceptibility values. And thirdly, several parameters studied in the Tjusterby till samples are consistent with the analytical data of the boulder samples.

The geochemical till sample data are enriched in many of the same elements as the serpentinized boulders, and even though the average transport distance of fine fractions in till have been noted to be shorter than for boulders (Salminen and Hartikainen 1985), similar geochemical information gathered from these differing media from the same locations points to a local source. A map showing the relationships between magnetic susceptibilities measured in till and boulder samples together with the anomalies observed in magnetometry studies is shown in figure 19. The area applicable for boulder tracing was relatively limited in Tjusterby, due the fact that most of the ground consists of clay-rich farm land. At the shoreline, closest to the ultramafic bodies, some of the land was also turned into recreational properties. But even with a search area much smaller than the boulder fan potentially derived from the ultramafic units, the on shore findings can with high certainty be linked to the underwater sources.

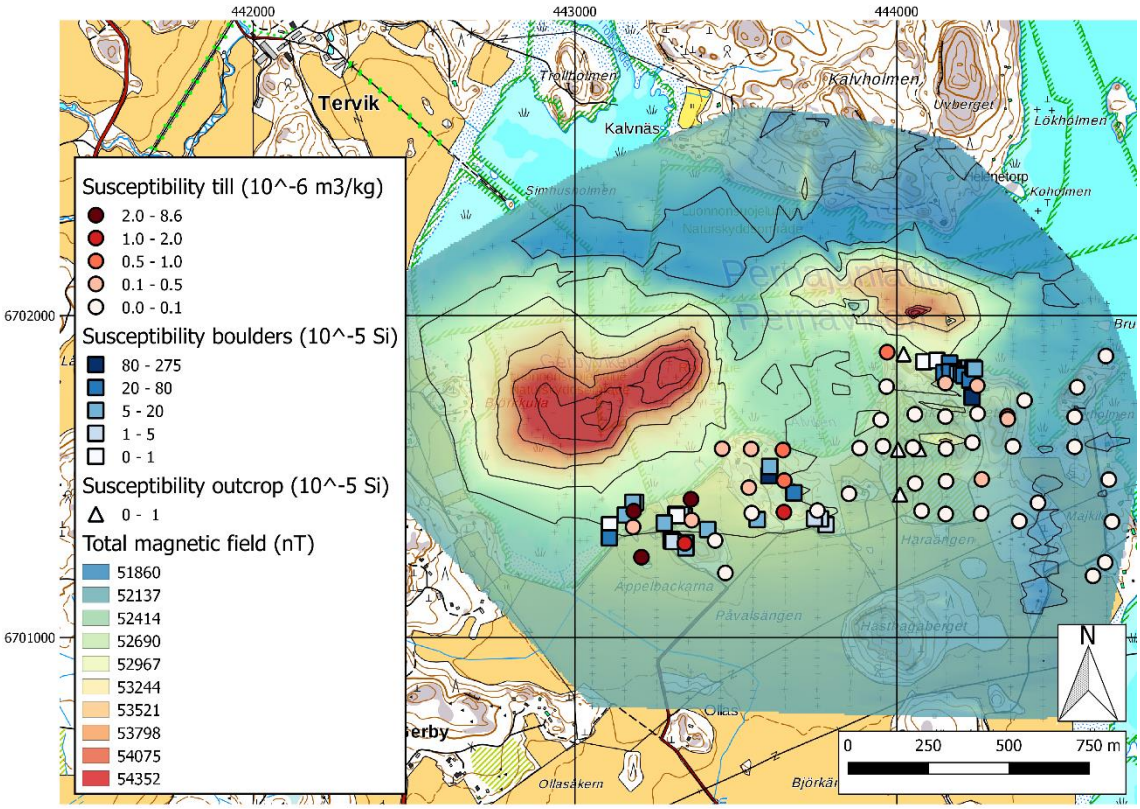

Figure 19: Map showing the relationships between the strength of the magnetic field in bedrock (interpolation based on 1733 magnetometer measurements) and the measured magnetic susceptibilities in boulder, outcrop and till samples in Tjusterby. Map underneath acquired from the open data file download service of the National Land Survey of Finland (basic map raster).

The ground magnetometry map in figure 19 shows quite clear limits for the magnetic anomalies observed in Tjusterby. The contrast between the background values and the most intensely magnetized areas is clear, with a deviation of about 2 500 nT occurring over a few hundred meters. Magnetometry surveys mostly measure the strength of the Earth's magnetic field, in which the variation can range globally from about 23 000 nT to 67 000 nT, depending on latitude (NOAA 2014). But within smaller areas, the change in the strength of the magnetic intensity is practically completely controlled by variations in the bedrock. Cases where a local crustal anomaly causes an increase of 2000-4000 nT compared to the local expected main field value can be regarded as extreme (Lanza & Meloni 2006). Therefore, such a significant and sudden change in the local magnetic intensity in Tjusterby as seen in figure 19 is a clear indication of a major change in local geophysical properties. As such, limits of the magnetically anomalous ultramafic bodies can be quite accurately determined.

4.2. The importance of serpentinization.

When planning for the field work for this thesis, and even after the actual samples had been collected, the role of serpentinization in the Tjusterby bedrock was not recognized at all. Although serpentinites have several characteristic physical and chemical properties, the visual appearance of the dark colored, even grained and homogeneous

boulder samples collected in Tjusterby did not reveal any of them, and the real nature of the sample material was only discovered through geochemical and petrographical investigations. In its nature, serpentinization itself is a process where olivine-rich mafic-ultramafic rocks react with water and get hydrated, which affects their geochemical and mineralogical composition, as well as physical properties, such as density, volume and magnetism (Malpas 1992, Iyer 2007, Guillot & Hattori 2013). Geochemically, the most revealing sign of serpentinization is often a significant rise in the amount of water in the crystal structure, revealed in the geochemical data as a high loss of ignition (LOI). In mineralogical sense, the most noticeable change is the alteration of olivine to the serpentine group minerals antigorite, lizardite and chrysotile.

Although Tjusterby always was the main focal point of this study, serpentinization was not considered as a factor in the planning stage. As the original idea was to acquire as much information as possible about an unknown ultramafic and magnetic rock unit, the two reference areas of Mallusjärvi and Pukkila were chosen due to their partial similarities to the Tjusterby area. Hence, Mallusjärvi and Pukkila do not show mentionable signs of serpentinization. However, these areas are still useful in providing supplementary information. The rock unit studied in Mallusjärvi is homogeneous, mafic-ultramafic and also highly magnetic. As such, it shows some of the features for mafic rocks with potential to be serpentinized, before any significant alteration has taken place. Especially the magnetic properties of the Mallusjärvi unit are interesting, since formation of magnetite is a common, although not unconditional, by-product of serpentinization (Klein et al. 2014). This might raise a question whether the magnetism in Tjusterby was generated pre or post serpentinization. The area studied in Pukkila was initially thought to be more in common with Tjusterby than was later realized. As mentioned earlier, magnetism was never a factor expected to be observed in Pukkila, but the assumed similar ultramafic-gabbroic-amphibolitic lithological association raised a suspicion about potential connection between Tjusterby and Pukkila. But as no ultramafic or gabbroic units were encountered in Pukkila, the discussion regarding the area will be based on the comparison between the amphibolitic samples collected in Tjusterby and Pukkila.

4.3. Geochemisty

The 38 samples that were analyzed in the laboratory were mainly chosen based on their rock type and spatial position. The aim was to get a sufficient amount of examples from each lithology and location in order to compare them to each other. In the cases of the abundant serpentinite boulders in Tjusterby and the homogeneous mafic-ultramafic bedrock unit in Mallusjärvi, this goal was reached, but in the cases of bedrock and unserpentinized boulder samples from Tjusterby the gathered material was not subject of as much interest and is thus not sufficient for a thorough conclusion. The Pukkila

bedrock samples were mostly amphibolites, which are informative of the local bedrock, but do not provide many links to Tjusterby. Attention is put more on the geochemistry of the serpentinitic boulder samples from Tjusterby with a comparison with the Mallusjärvi samples, rather than comparing Tjusterby with Pukkila. Significant attention was also focused on trying to evaluate a possible origin of the Tjusterby serpentinites based on geochemical data bases from literature.

The analytical data shown in the results was in the same form as announced from the laboratory, so this discussion is thus based on these same values. But as Loss of Ignition (LOI) is a considerable constituent in the major component data for serpentinites, but not for unserpentinized samples, it needs some special notice. Since the amounts of other components become proportionally lower with increasing values of LOI, it is easier to compare the compositions of the serpentinized rocks from Tjusterby to other data in this study if LOI is excluded. In the following discussion, elemental data are first shown as announced from the laboratory, followed by a value for the same element that has been calculated by normalizing the remaining elements without the values for LOI to 100%. As can be seen, the elemental amounts for the serpentinized samples become relatively much higher than for the unserpentinized samples, when LOI is excluded from the values. This procedure is only used regarding the major elements, not for minor or trace elements.

4.3.1. Tjusterby serpentinites

The serpentinitic samples from Tjusterby are geochemically relatively homogeneous, although some differences can be found. An exception from the rest of the samples is T1732, which has a composition between an unaltered and a fully serpentinized example. The same is also seen in the amount of the serpentine group minerals in thin section, which are half as abundant as in the more completely serpentinized samples. This sample can therefore provide valuable information about the composition of the protolith prior to serpentinization.

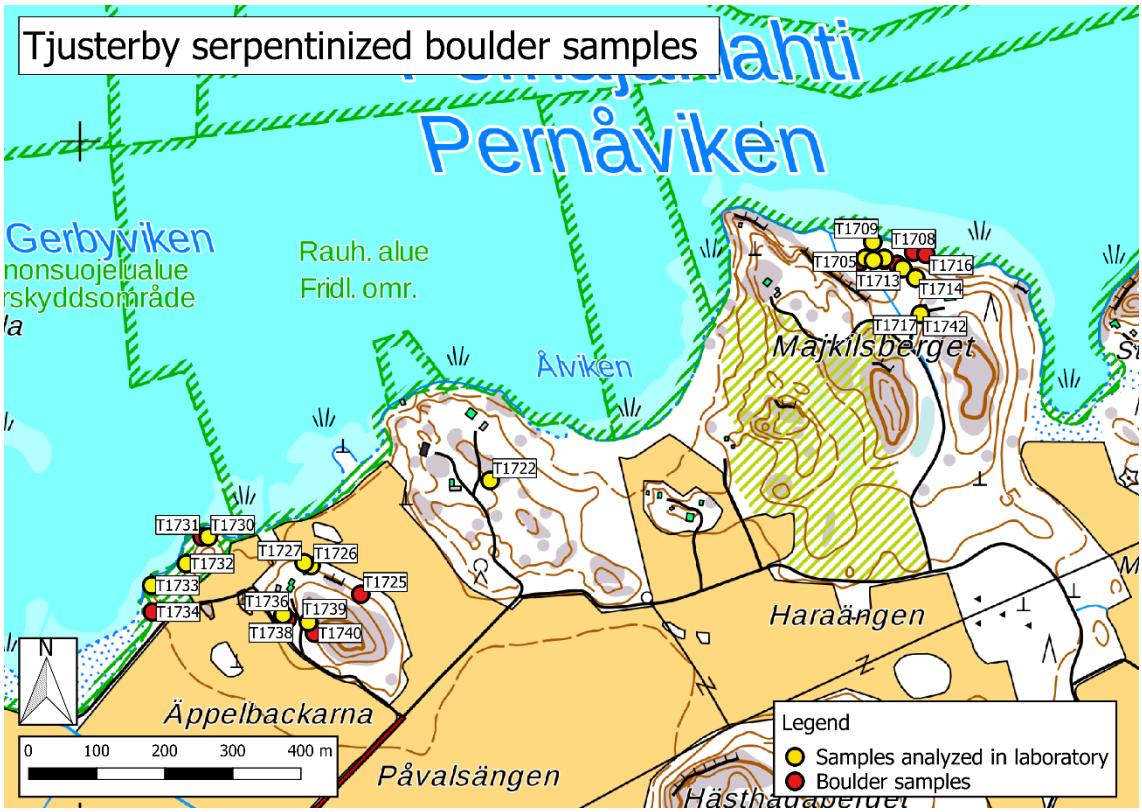

Figure 20: Locations of serpentinitic boulder samples from Tjusterby. Samples marked with a yellow circle have been analyzed for their geochemistry in laboratory, samples marked with a red circle have been determined as serpentinites through their visual appearance and their magnetic properties. Original map acquired from the open data file download service of the National Land Survey of Finland (basic map raster).

When excluding sample T1732, the Tjusterby serpentinites are by their geochemical composition clearly ultramafic, with a maximum SiO_2 content of 37.98% (36.37% with LOI excluded) and with a lowest MgO value of 32.49% (37.05%). The variation of both major components within the sample group is about 6%, with sample T1709 showing the lowest values for both components. For this sample the low SiO_2 and MgO contents are partly compensated by high values of Fe_2O_3 (T) (14.23%, 16.27% without LOI) and Cr (2.03 %). Al_2O_3 shows only small variations with values ranging from 1.62% (1.85%) to 3.71% (4.23%), which is normal for aluminium-poor ultramafic rocks. CaO is very low compared to most rock types, with a range from 0.03% (0.04%) to 0.71% (0.81%). This is quite normal by serpentinitic standards, however, since Ca is readily carried away by fluids during the alteration process, yielding a rock depleted in the element (Palandri & Reed 2004). Na_2O and K_2O are similarly present in only small amounts, with Na_2O showing less variations (range 0.01–0,14%, 0.01–0,016% excluding LOI) than K_2O (<0.01–0.79%, 0.01–0.92%). The amount of K_2O seems to go well together with the appearance of phlogopite, which is logical, since K is a major constituent in the biotite-group minerals. TiO_2 is another element with constantly low amounts (0.35–0.107%, 0.04–0.12%). Ti can substitute Fe and Mg in e.g. pyroxenes and mica and is often enriched in ultramafic rocks with TiO_2 contents of more than 2% (De Vos & Tarvainen 2005). The TiO_2 contents in the Tjusterby serpentinites are consistently considerably

lower than this, reflecting the lack of pyroxene seen in the Tjusterby samples. The values for Loss of ignition (LOI) are quite constant, with a variation from 11.69% to 14.51%, and is mainly caused by the extraction of water from the serpentine group minerals, and to a lesser extent from the brucite. In the Tjusterby serpentinites LOI does not seem to match the degree of serpentinization in thin section. This is not unusual, since LOI values are, together with the variation of the brucite amounts, dependent e.g. on the varying water contents in different serpentine group minerals (Evans 2004). Serpentinization and LOI do still go together generally, since the LOI values for unserpentinized samples are much lower than the consistently high values for serpentinites.

Of the minor elements, nickel and chromium are two metals that were noted to be enriched in the very first pXRF analyses of the Tjusterby till samples (Ingves 2016). Similar enrichments were also noted in the boulder samples, first in the pXRF data, later in the laboratory data. These two elements are enriched compared to most other rock types, but by serpentinitic standards their amounts are quite normal (Deschamps et al. 2013). The internal variations within the sample group is larger for Cr (2050–20900 ppm) than for Ni (1120–4290 ppm) (still excluding sample T1732). The highest amount of both elements is in the same sample, T1709. Zinc was another element that raised interest already in the initial pXRF analysis. In the laboratory data, five samples show >1000 ppm Zn, much higher than the average value of 50 ppm for ultramafic rocks (Mielke 1979). In Tjusterby, a rather large variation in Zn contents can be observed, with the most enriched sample (T1726) having over 50 times more Zn than the sample with the lowest amounts (T1713). However, no correlation could be detected between these Zn variations and minerals in thin section. Copper is moderately enriched compared to most serpentinites (Deschamps et al. 2013) and does not show too much variation between samples, with a maximum of 880 ppm (T1713) and only two samples below 100 ppm (T1722, T1742). Except from occurring in trace amounts in some mafic minerals, Cu can also form copper sulphides, but these were not possible to identify in thin section.

Lead can be divided into two groups in the Tjusterby serpentinites. The first group with lower concentrations (5–56 ppm, 9 samples) and the second one with highly enriched amounts (104–1460 ppm, 6 samples). The enrichment in some samples is considerable, with Pb contents several orders of magnitude higher compared to existing serpentinites from various geotectonic settings (Kodolányi et al. 2011, Deschamps et al. 2013). Pb can be found as trace levels in mica and magnetite (De Vos & Tarvainen 2005), but to reach such levels of enrichment, galena or some other mineral with Pb as a major component is likely to be present. A similar distribution is noted for arsenic, with some samples having clearly elevated values compared to the rest. However, there does not seem to be any correlation between the concentrations of Pb and As. Arsenic is a strongly chalcophile element, and can also to some extent replace Fe^{3+} in some minerals

(De Wos & Tarvainen 2005), but for samples with >100 ppm As, the minor occurrence of arsenopyrite or some other As bearing sulphide is a more probable explanation. As and Pb are both fluid mobile elements (FME), thus their enrichment in these samples might be due to fluid percolation in the serpentinization process, rather than reflecting the composition of the protolith (Deschamps et al. 2013). A simple correlation of the amount of sulphur with the amount of various sulphides is not possible to make, however, since in addition to various minor elements, S can also be tied to Fe-sulphides. In the serpentinites from Tjusterby, the concentration of S varies from <100 ppm to 4400 ppm.

In table 3, the trace element contents in the Tjusterby serpentinites, which includes data for some Light Rare Earth Elements (LREE) (La, Ce, Pr, Nd, Sm, Eu) and FME (U, Cs, Sr, Rb, Th) (divided into groups as by White 2013 and Peters 2017). These two element groups behave differently during serpentinization and can thus be helpful in determining the initial protolith and the geotectonic setting in which the Tjusterby ultramafics were serpentinized. LREE are more incompatible in mantle rocks and are not so strongly affected by fluids, whereas FME are often enriched by fluid transfer in the serpentinization process, depending on the geotectonic environment (Debret et al. 2013, Deschamps et al. 2013). As a reflection of this differing behavior of these two groups, it can be noted that FME vary more in their concentration between samples compared with LREE. Of FME, U and Sr are relatively evenly distributed within the group, with a variation of <0.1–8.2 ppm and <2.0–13.0 ppm, respectively. The same goes for Th, although 9 out of 16 samples had concentrations below the detection limit of 0.1 ppm. Cs and Rb show larger variations, with Cs contents ranging from <0.5 ppm to 107 ppm and amounts of Rb ranging from <2.0 ppm to 302 ppm. For LREE, the largest concentration variation was for Ce, which had a range from 1.2 ppm to 9.2 ppm.

In this discussion about the Tjusterby serpentinites, sample T1732 was excluded. This sample is considered to be a transition between a non serpentinized and a fully serpentinized ultramafic rock, since the concentrations of several elements fall between these two end members. The same is noted for the petrographic composition. Of the major components, SiO_2, Al_2O_3, CaO, and Na_2O are clearly higher for this sample than for the rest of the serpentinites, while the values for MgO and LOI are lower. For minor and trace elements, the values for sample T1732 are consistently on the lower end of the spectrum, with the only exceptions of highest values obtained for Sr and Eu. No major conclusion can be drawn from only one deviating sample, but it still suggests that through a stronger reaction with fluids, the general composition of the affected rock unit has become more ultramafic in composition, CaO has been depleted and several trace/minor elements have been enriched.

As noted earlier, serpentinization involves significant hydration, with a strong increase of water compared to the initial protolith. However, this does not mean a one to one ratio of leached components, since the addition of water is most likely to take place through an increase in the volume of the affected rock unit (Mével 2003). As noted above, Ca is the only major element in Tjusterby for which the amounts are considerably lower than in ultramafic rocks in general. For minor/trace elements, the reactions are more complex. Most of these elements seem to be slightly or moderately enriched compared to unaltered ultramafic rocks, but this does not necessarily have to be connected with the serpentinization process itself. This is often the case with more incompatible elements, such as the REE group. As REE often are accommodated in clinopyroxene, it is the amount of this unreactive mineral group in the protolith that mostly determines the REE content in serpentines (Menzies et al. 1993).

Geochemical data on serpentinized material are available in numerous publications from all parts of the world. Comparison of the geochemical data from this study has mainly been dine with material published by Deschamps et al. (2013), in which geochemical data from >900 serpentinized samples from abyssal (mid-ocean ridge), mantle wedge and subducted and exhumed settings of dunitic and harzburgitic origin are discussed in order to characterize differences between various geochemical environments. Such classifications rely on the fact that different rock types (e.g. dunite and harzburgite) have slightly varying geochemical fingerprints, with enrichments in particular elements. Likewise, each the geochemical environment produces its own mark on geochemistry, mostly through differences in the affecting fluids. By comparing the data from Tjusterby to the data compiled by Deschamps et al. (2013), an attempt is made to recognize a protolith for the Tjusterby serpentinites. These interpretations are of course limited because the data of Deschamps et al. (2013) do not cover every possible rock type/geotectonic environment, and the elemental distributions in all individual serpentinitic units do necessarily follow the theoretical models. Different analytical methods also yield slightly varying results, which should be kept in mind when comparing elemental contents from different data sets. As the results compiled in Deschamps et al. (2013) come from various databases, they contain analytical data obtained by different methods. Therefore, it is not possible to estimate a general variance when comparing these data to the FUS-ICP and FUS-MS data on the Tjusterby serpentinites. The comparisons between the data for the Tjusterby samples and those of Deschamps et al. (2013) are based on their original data, without normalizing values for LOI.

The easiest way to compare the data for the Tjusterby serpentinites with the data from Deschamps et al. (2013) is to create two diagrams (figures 21 and 22), both with average compositions for serpentinites from different geological backgrounds from Deschamps et al. (2013) normalized with the average values from the Tjusterby samples. The first

diagram (figure 21) is for major elements and the second diagram (figure 22) for trace elements. Data for refertilized dunites and harzburgites from Deschamps et al. (2013) were excluded from the calculations to make the graphs easier to interpret, since these petrological units deviated most from the Tjusterby samples. That information is valuable in itself, since as no unit in the diagrams directly matches the normalized values, i.e. has a flat line in the diagram, non-matching compositions help to rule out unlikely sources.

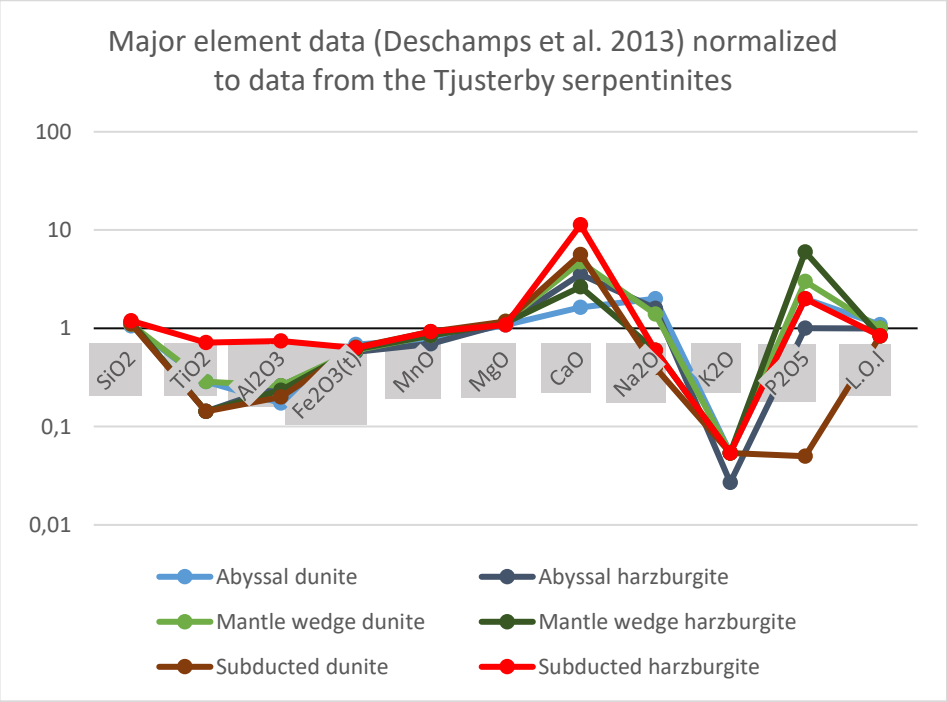

Figure 21. Data for major elements for serpentinized rocks from different geochemical environments from Deschamps et al. (2013) normalized with data for the Tjusterby serpentinites.

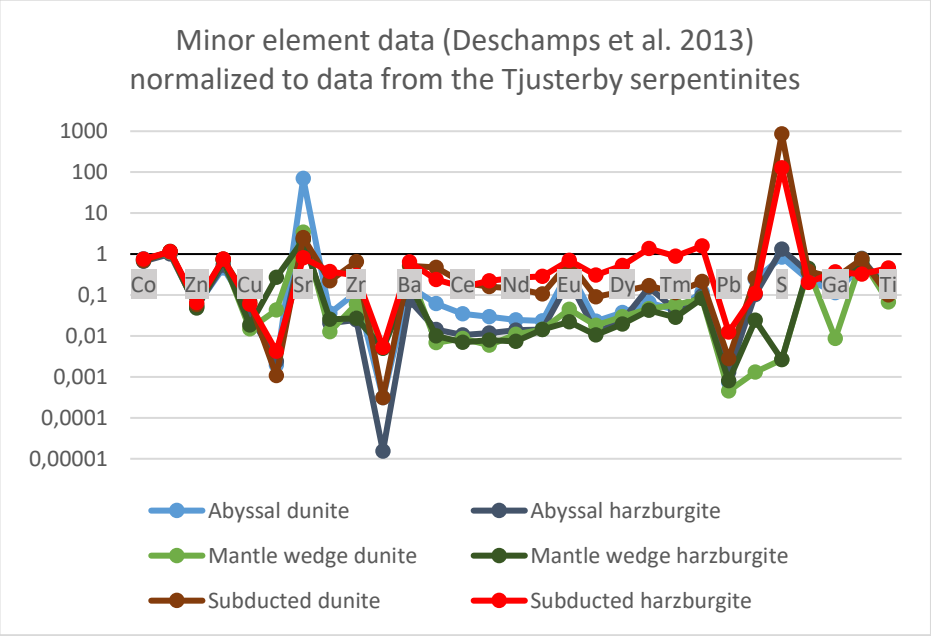

Figure 22: Data for trace elements for serpentinized rocks from different geochemical environments from Deschamps et al. (2013) normalized with data for the Tjusterby serpentinites.

Several reflections can be made when looking at the diagrams in figures 21 and 22. Firstly, the variation in contents of the major elements is much smaller than for the trace elements. For the major elements, the only one in which the Tjusterby samples are constantly depleted, when comparing to the data from Deschamps et al. (2013), is CaO, for which there is a one magnitude difference to subducted harzburgites. Most other components are slightly enriched in the Tjusterby samples, with the extreme case of a 37-fold difference when comparing K_2O in Tjusterby and abyssal harzburgites. For trace elements, the variations in elemental contents for different geochemical settings are much larger. For most elements, the Tjusterby samples are slightly to moderately enriched when compared with data from other environments. Of the elements where the Tjusterby data are depleted, S is most dramatic, with a roughly 1000-fold difference between the Tjusterby samples and the data from subducted dunites. It should be noted, however, that the variations in the amounts of S are significant between geotectonic settings, since samples from mantle wedge environments are strongly depleted in S compared to other samples in the examined database. Of the elements for which the Tjusterby samples are enriched, when compared to other serpentinite data, As and Pb stand out the most, as does Cs, which shows a maximum variation of any element in the diagram, with a difference of roughly 70 000 times between the Tjusterby serpentinites and serpentinites with a harzburgite protolith in an abyssal setting.

Extreme values set aside, the trace element diagram effectively shows that the Tjusterby samples are dominantly enriched in most elements, compared with the data in Deschamps et al. (2013). The enrichments do not show any clear pattern, but some rough variations can be seen with a division into groups of compatible and incompatible elements and FME. Of the elements shown in the diagrams, mantle-compatible elements include metals that can substitute for Fe and Mg in olivine and pyroxenes (such as Ni, Cr and Co), whereas incompatible elements are more likely to be part of, or replace, elements in felsic minerals, and hence escape from the mantle into the melt (such as K, Y, Cs, Zr, Eu, Ba, U and most REEs) (Best 2003, White 2013). In the graph in figure 22, it seems that the compatible elements are only lightly enriched, or even slightly depleted, in the Tjusterby samples, whereas the incompatible elements are generally moderately to strongly enriched. The incompatible and FME groups are partially overlapping, since elements such as Cs, U and Ba are included in both of them. Thus their behavior can be quite complex. Most FME (e.g. Cs, U, Ba, Pb, As, Sr, Rb) are generally strongly enriched in the Tjusterby samples when compared to the data from Deschamps et al. (2013), which might be due to strong fluid percolation in the protolith during the serpentinization process. As is understandable, the effect of fluid action is strongest on FME, but with a clear enrichment of most elements shown in figure 22, fluids probably affect other components as well. The difference of several magnitudes for many elements between

the Tjusterby samples and the other data suggests this. Peters et al. (2017) explained a similar situation with both differences in the initial elemental composition prior to serpentinization, and with variations in the permeability of the lithological unit once the serpentinization process had begun. It is logical that a more permeable unit allows for stronger fluid action to take place and to modify the elemental composition, but it is difficult to estimate whether the enrichments observed in this study are due to fluid action in a permeable rock unit, or if the initial protolith itself was unusually enriched in some elements.

Taking into account the factors of differing analytical methods and uncertainties in the role of fluids vs. initial elemental contents in the graphs in figures 21 and 22, picking a most probable protolith for the Tjusterby serpentinites is uncertain. The closest match in both graphs, i.e. the line being closest to the normalized average of the Tjusterby samples, seems to be the harzburgites serpentinized in a subduction zone. These lines are not exclusively closest to the Tjusterby samples, since in the major elements there is a clear variation in the amounts of CaO and K_2O, and in the minor/trace element graph in the amounts of As and S. But in both the compatible (Ni, Co, Cr) and incompatible (e.g. REEs) groups most elements are relatively close to the Tjusterby samples. On the other hand, both dunites and harzburgites from mantle wedge environments seem often to have elemental contents relatively different from the Tjusterby serpentinites. As serpentinites formed in subduction zones are by their nature quite heterogeneous (Deschamps et al. 2013) no final conclusion should be drawn for the Tjusterby samples to have been formed in this geotectonic environment, but in this view a subductional origin seems more likely compared with abyssal and mantle wedge environments.

4.3.2. Mallusjärvi

As the material collected in Mallusjärvi was quite homogeneous, both in visual characteristics and in the initial pXRF analyses, only five samples were sent for FUS-ICP and FUS-MS analyses. Looking at the final laboratory results, this interpretation was justified. In this study the aim of Mallusjärvi was to serve as a reference point for the serpentinitic samples from Tjusterby, helping in evaluating some differences between serpentinized and unserpentinized lithologies. This is more of a general comparison, since the origin of the unit in Mallusjärvi is not evaluated, and it is not regarded as being a direct representative of a protolith for the Tjusterby serpentinites. As was done for the serpentinites, normalized values, with LOI excluded, have also been calculated for the Mallusjärvi samples, again shown in parentheses. As can be seen when comparing these values, the relative difference with and without normalizing LOI is clearly smaller than in the case of the serpentinite samples.

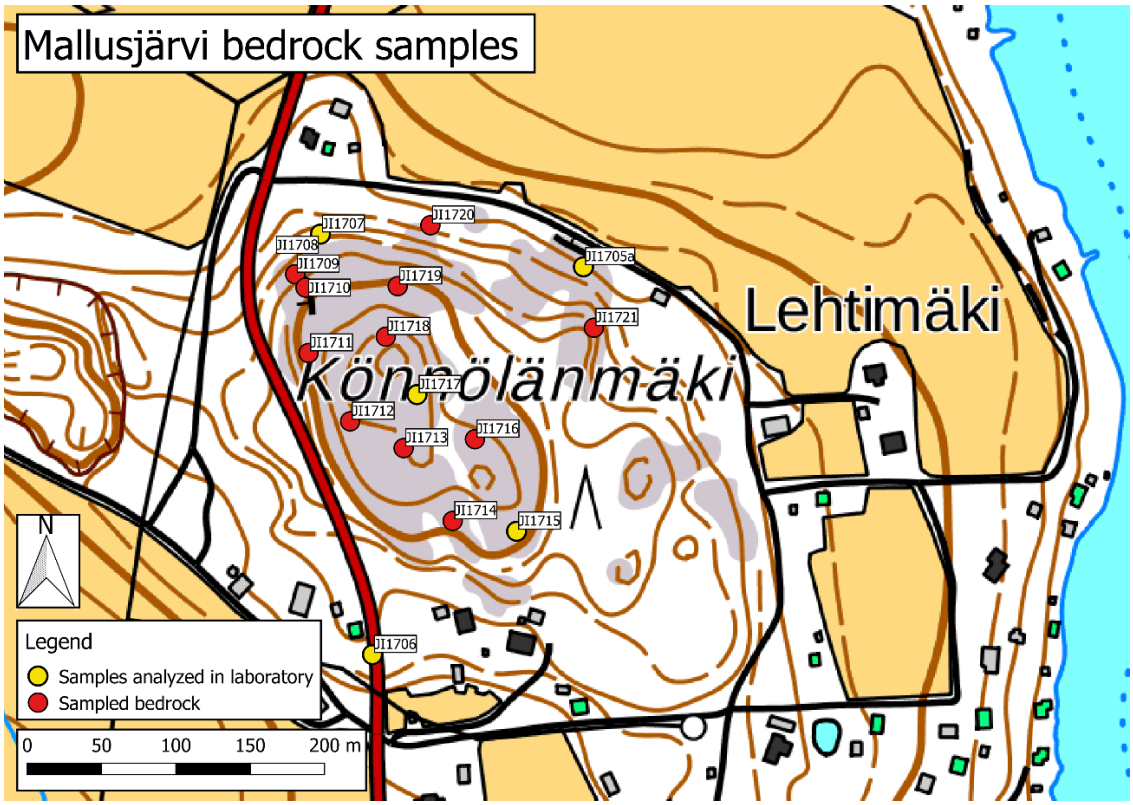

Figure 23: Location of bedrock samples collected from Mallusjärvi. Original map acquired from the open data file download service of the National Land Survey of Finland (basic map raster).

With a variation from 42.92% (43.64%) to 45.31% (46.01%) of SiO_2 and 15.33% (15.59%) to 20.51% (21.18%) of MgO, the Mallusjärvi samples are on the borderline of being mafic or ultramafic. With LOI normalized values, the amounts of these components are closer to the Tjusterby samples, but there is still a significant difference between the two units. For SiO_2, only the sample with the lowest concentration from Mallusjärvi has less of the element than the most silica rich sample from Tjusterby. For MgO, the highest value of the Mallusjärvi samples is far off the lowest value in the Tjusterby samples. If CaO is the only component to be extensively affected by being depleted in the serpentinization process (Mével 2003, Palandri & Reed 2004), it can be assumed that the protolith for the Tjusterby serpentinites was more ultramafic in its nature than the Mallusjärvi unit. On the other hand, the Al_2O_3 contents, with a range from 3.43% to 5.21 % (3.56% to 5.3%), are low in Mallusjärvi, and indicative rather an ultramafic than a mafic rock unit (De Wos & Tarvainen 2005). The Fe_2O_3(T) contents show some variations (10.94% to 16.93%, 11.28% to 17.21% with LOI excluded) but are generally high in the Mallusjärvi samples, with a roughly similar range as in Tjusterby. The biggest difference between the major elements in the Mallusjärvi and Tjusterby rocks is in the amounts of CaO, which with a range of 12.42% to 14.85% (12.83% to 14.85%) is roughly 200 times more abundant than in the Tjusterby serpentinites. As the Mallusjärvi samples are about twice as rich in CaO compared to the average of several mafic/ultramafic rock types (Best 2003), they can themselves be seen as being enriched in the component. But this

comparison between the amount of CaO for the two areas shows just how much Ca is leached from the rock unit in the serpentinization process.

Of the remaining oxide compounds the amounts of MnO and K_2O are quite similar between the Tjusterby serpentinites and Mallusjärvi, with roughly a two-fold difference in both cases, MnO being more abundant in Mallusjärvi and K_2O in Tjusterby. For Na_2O, there is a difference of roughly one magnitude, with a range from 0.45% (0.47%) to 0.68% (0.7%) in the Mallusjärvi samples. TiO_2 shows a larger variation in the Mallusjärvi samples compared to most other oxides, with a range from 0.39% (0.41%) to 1.15% (1.17%). This again is a distinctive difference from Tjusterby, where the amounts of TiO_2 were generally one order of magnitude lower. The component that makes the largest difference between Tjusterby and Mallusjärvi is LOI, which rises with the increasing water content through stronger fluid alteration. In the Mallusjärvi samples, LOI had a variation from 1.49% to 3.61%, which is quite normal for unserpentinized gabbros and ultramafic rocks (van Nostrand 2015).

The contents of most minor elements in the Mallusjärvi samples are clearly lower than what is observed in Tjusterby. Ni is quite stable, varying from 200 ppm to 280 ppm, which is roughly one order of magnitude lower than in Tjusterby. Cr is closer to the amounts seen in Tjusterby, with a variance from 740 ppm to 1630 ppm. For Zn, the highest values observed in Mallusjärvi (80 and 100 ppm) are higher than the lowest values in the Tjusterby serpentinites, but are far lower than the maximum values of 1740 and 2830 ppm seen in them. Cu, Pb and As are very low in Mallusjärvi, all samples being at or below the detection limit for each element. As mentioned earlier, Pb and As belong to the group of FME, which had large variations in the Tjusterby serpentinites. As fluids had a smaller role in Mallusjärvi, the contents of these elements are constantly much lower. V and Co have contents of the similar magnitude in both Mallusjärvi and in the Tjusterby serpentinites, with contents of V being constantly higher in Mallusjärvi, while the Co contents are higher in Tjusterby.

The REE contents of the Tjusterby and Mallusjärvi ultramafic rocks were shown in table 10, and chondrite-normalized spider diagrams were shown in figures 12 (Tjusterby) and 13 (Mallusjärvi). These data are somewhat incomplete in the sense that the element contents in some of the Tjusterby samples were below the detection limits, but this does not prevent a comparison between the two sample groups. When looking at the data, it does not appear to be dramatically different between the Tjusterby and Mallusjärvi rocks in the values seen in table 10, but in figures 12 and 13 the distribution is more uneven. The Tjusterby serpentinites are more scattered, compared to the Mallusjärvi samples, which form a relatively close population in figure 13. This can both be seen as an

indication of how geochemically homogeneous the Mallusjärvi body is, and how much more internal differences there are within the Tjusterby serpentinite bodies.

As serpentinization is dependent on the circulation of fluids in the rock unit affected by them, it is expected that there would be more variation in the elemental content in a serpentinized ultramafic body, compared to unserpentinized bodies. The clearest difference in an individual element between Tjusterby and Mallusjärvi is for Eu, since there is a clear negative anomaly for this element for the Tjusterby samples in figure 12, but not for the Mallusjärvi samples in figure 13. The amounts of Eu are often regarded to be connected with the distribution of plagioclase in igneous rocks (e.g. Duchesne 1982), with positive anomalies being connected with an enriched amount of the mineral. In this case, it is unclear if the differences in the Eu-contents are fully due to this explanation, as the difference in the amounts of plagioclase observed in thin sections in the Tjusterby and Mallusjärvi samples were not so significant.

4.3.3. Unserpentinized samples from Tjusterby and samples from Pukkila

The amphibolitic/gabbroic samples collected from outcrops in the Tjusterby area, roughly 500 m south of the eastern magnetic anomaly in figure 19, were mostly taken to prove the differences between the serpentinites and the amphibolites and gabbros seen in bedrock onshore. Similarly, several unserpentinitzed boulders were sampled in Tjusterby, in order to see a likelihood between them and the bedrock on the southern side of the magnetic anomalies. Sampling of unserpentinized boulders was focused on rocks interpreted in the field as gabbroic or amphibolitic, leaving out the granitic boulders that were the most common rock type in the area. In addition, a few samples were analyzed because of their abnormally high magnetic susceptibility (T1721 and T1741). No systematic mapping or sampling was done on the northern side of the magnetic anomaly for this thesis, but on a short visit to the island of Kalvholmen north of the Pernajanlahti bay, some gabbroic and amphibolitic outcrops were encountered, contradictory to the bedrock map published by GTK, according to which the area was purely granitic. Thus, boulders of this type found onshore in the Tjusterby sampling area are regarded to possibly be derived from outcrops on Kalvholmen. A simple comparison can be made between these boulders and the bedrock in Tjusterby by examining elemental contents in the samples. Differing from the previous sections with the Tjusterby serpentinites and the samples from Mallusjärvi, where one element or compound at a time was discussed**,** the descriptions below are based on comparisons between samples of differing rock types. These rock types have been determined based on geochemistry, mineralogy and field observations.

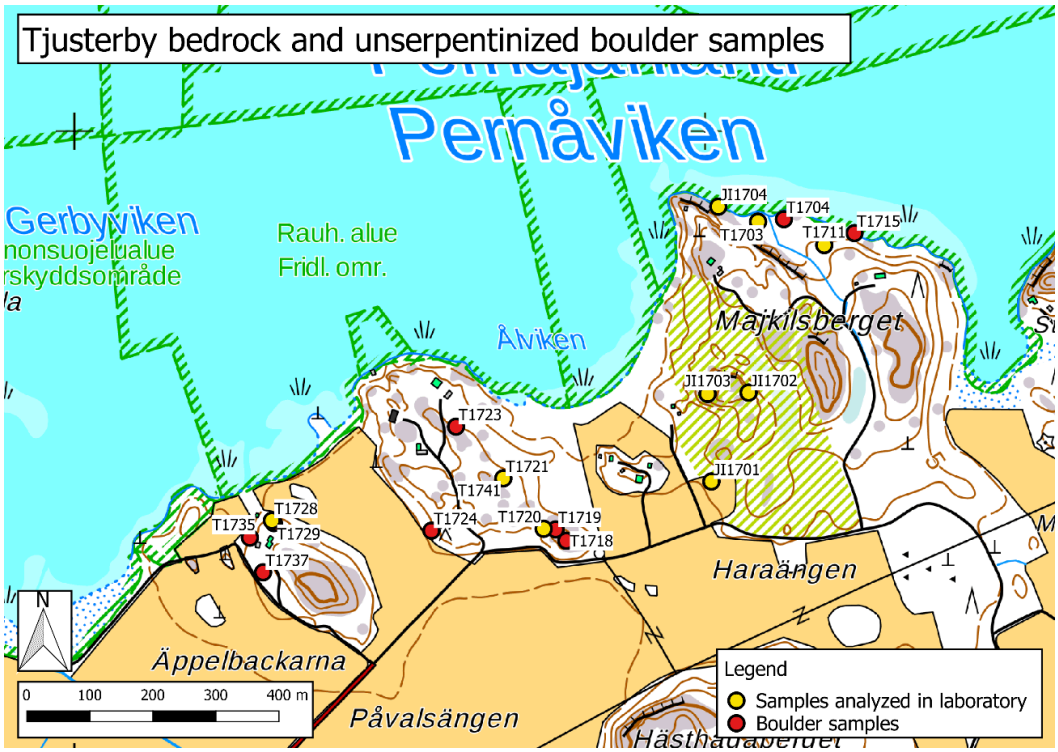

Figure 24: Locations of the unserpentinized samples collected from Tjusterby. Samples beginning with the letter T refer to boulders, samples beginning with JI are from outcrop. Original map acquired from the open data file download service of the National Land Survey of Finland (basic map raster).

As some of the samples collected in Pukkila also bear resemblance to the bedrock in Tjusterby, these two sample groups are in a similar manner briefly compared with each other. Sampling from outcrops in Pukkila produced somewhat unexpected results, since the bedrock seen in the area was different from the interpretation based on bedrock maps covering the area. As such, in a geochemical sense the samples vary from mafic to clearly felsic, the mafic rocks being amphibolites and the rocks with higher silica content being mica schists. As no comparative units to felsic schists were encountered in Tjusterby, these samples are only briefly discussed below. As a continuation from previous sections, the major element contents are again reported in such a way that numbers with LOI excluded are written in parentheses.

Of the laboratory-analyzed unserpentinized boulder samples from Tjusterby, only T1703 can be classified as an amphibolite, the rest being gabbros or unspecified, highly magnetic metamorphic rocks (T1721 and T1741). Of the bedrock in Tjusterby, samples JI1701 and JI1702 are, based on both geochemical and mineralogical interpretations, biotite-hornblende schists. Sample JI1703 is on similar bases classified as gabbro and JI1704 as amphibolite. Geochemically, there are some differences between the gabbros and amphibolites, but they are not characteristic enough to base a division into rock types on geochemistry alone. Or rather, the geochemistry between boulders and outcrop samples within the same rock type is too variable. For example, MgO is a component with quite clear differences between the gabbroic and amphibolitic boulders. In the

gabbros, the MgO content varies between 11.77% (11.91% with LOI excluded) and 18.16% (18.80%), whereas in the amphibolitic boulder sample MgO has a value of 6.17% (6.28%). But in the outcrop samples from Tjusterby all samples have much lower values, with the gabbroic sample having a MgO content of 2.78% (2.82%) and the others showing a variation from 1.19% (1.20%) to 4.28% (4.32%). A similar trend can be noted for CaO, for which the contents in the gabbroic boulders, with a variation from 9.80% (10.15%) to 16.20% (16.52%), is much higher than the amount in the amphibolitic sample (5.74%, 5.85% with LOI excluded). In the outcrop samples, CaO has a range from 4.25% (4.27%) to 9.83% (9.86%) in the mica schists and the amphibolite, whereas the gabbroic sample shows a value of 6.23% (6.32%).

Of the remaining major elements in the unserpentinized samples from Tjusterby, SiO_2 shows lower values in the gabbroic boulders (range from 41.14% to 50.36%, 41.61% to 51.36% with LOI excluded) than in both the amphibolitic boulder sample (52.61%, 53.59% without LOI) and all of the outcrop samples (amphibolite and the biotite-hornblende schists 50.75%-62.63% (50.88%-62.96%), gabbro 57.58% (58.40%)). Al_2O_3 is more variable, with a range from 4.74% (4.83%) to 11.61% (11.74%) in the gabbroic boulders and 14.87% (15.15%) in the amphibolitic boulder. In outcrop samples, the amphibolite and the biotite-hornblende schists have a range from 13.90% (13.97%) to 16.09% (16.25%) and the gabbroic sample has a value of 17.39% (17.64%). Fe_2O_3(T) is similar to Al_2O_3 in showing highly variable values for the samples. Noteworthy exceptions in the Fe-content are samples T1721 and T1741, which were sampled because of their strong magnetic properties. Fe_2O_3 is the dominant compound in these samples, with values of 41.59% (42.42%) for sample T1721 and 43.51% (44.52%) for sample T1741. In compensation with a high Fe-content, SiO2, MgO and CaO are clearly lower in these two samples compared with the rest of the unserpentinized rocks in Tjusterby.

Looking at the differences in the amounts of all these major compounds, it is hard to see clear connections between the boulder samples and the outcrop in Tjusterby. This is of course mostly because of the very limited sample amount, with only one amphibolitic boulder and one gabbroic outcrop sample, which inhibits any larger conclusions of comparing amphibolitic and gabbroic boulder samples with the same rock type from outcrop. When observing minor elements in the unserpentinized samples from Tjusterby, a more specific difference can be seen in the composition between the gabbroic boulders and the rest of the samples. Values for Ni and Cr are clearly enriched in the gabbroic boulders, with a variance from 200 ppm to 540 ppm Ni and 1420 ppm and 1600 ppm Cr, compared with a maximum of 50 ppm Ni and 80 ppm Cr in the other samples. Thus, the amouts of Ni and Cr in gabbroic boulders in Tjusterby are on a similar level as in the samples from Mallusjärvi, and Cr is almost at the level of the serpentinitic samples from Tjusterby. Co is also slightly enriched in the gabbroic boulders, but all other minor

elements show quite similar values with all unserpentinized boulder samples. Partly due to the influence of fluids, the Tjusterby serpentinites are highly enriched in many minor elements compared to the unserpentinized samples. The only notable exception is V, which often seems to be slightly depleted in the serpentinites compared to other samples from Tjusterby.

In Pukkila, samples JI1736 and JI1749 are now classified as mica schists, and since these hornblende-absent samples do not have representative counterparts in Tjusterby, they will not be discussed further. When sampling was planned in Pukkila the idea was to compare some outcrops with an assumed peridotitic assemblage thought to be found in the area with the serpentinites from Tjusterby. The idea to find some connections between the areas was based on relatively similar bedrock maps, with peridotites, gabbros and amphibolites being marked in the Pukkila area (DigiKP 200, digital map database). But as no peridotites or gabbros were encountered during the field work in the area, a shorter evaluation is now done between the amphibolites from Pukkila and with the outcrop samples from Tjusterby. The Pukkila samples are classified as amphibolites based on their high contents of hornblende seen in thin section, and also by visible foliation in some of the outcrops.

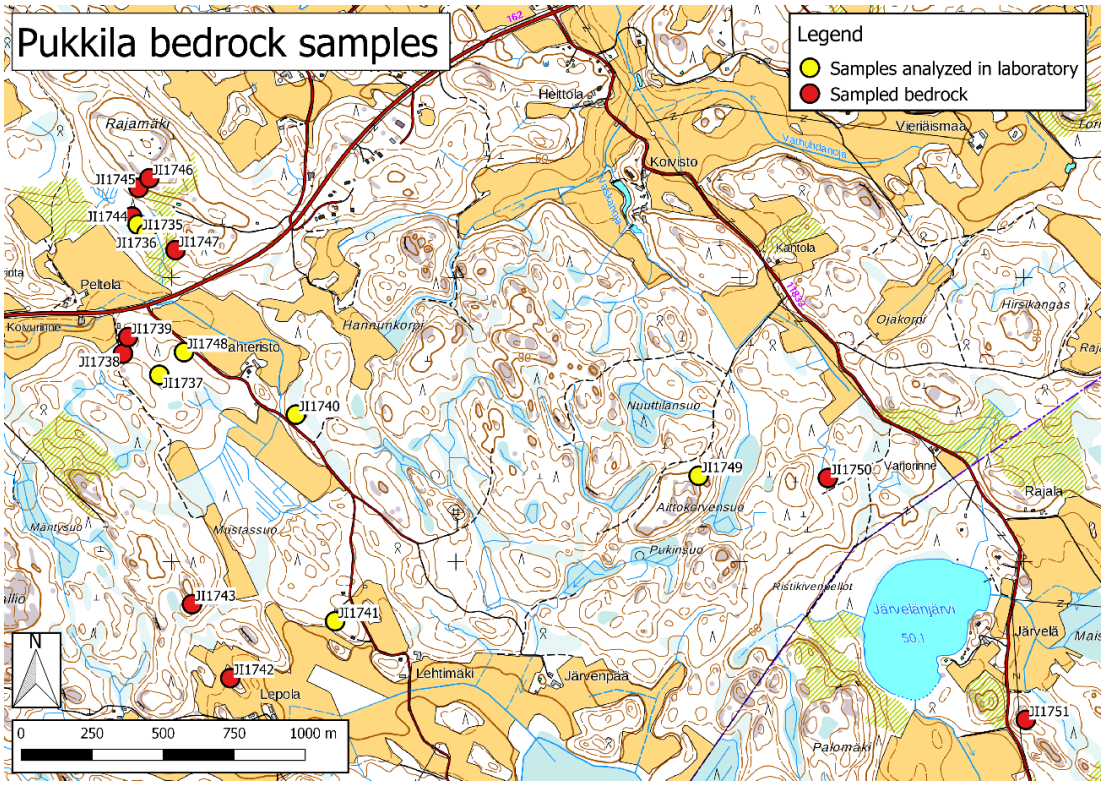

Figure 25: Location of the bedrock samples collected in Pukkila. Original map acquired from the open data file download service of the National Land Survey of Finland (basic map raster).

Altogether five amphibolitic samples from Pukkila were analyzed for geochemistry. These were located within a distance of about 1.5 km from each other, over which their composition changes slightly. When comparing them with the four outcrop samples from

Tjusterby, notable differences can be observed. SiO_2 varies from 48.78% (49.77% excluding LOI) to 53.51% (54.32%) in Pukkila, which is lower than what was recorded for Tjusterby. For Al_2O_3 the situation is quite similar, since the Pukkila samples have a variation from 10.05% (10.25%) to 16.72% (17.11%). Fe_2O_3 is less variable than in Tjusterby, with a range from 10.39% (11.10%) to 14.23% (14.56%). Perhaps the clearest differences between the two areas are seen in the amounts of MgO and CaO, which are clearly higher in the Pukkila samples. MgO in Pukkila varies from 6.17% (6.31%) to 12.43% (12.68%), which by average is about three times higher than what was seen in outcrop samples in Tjusterby. CaO in Pukkila has a range from 4.25% (4.27%) to 9.83% (9.86%), which by average is about 50% higher than in Tjusterby. Such significant differences in the amounts of several major elements between these two areas do not suggest any connection between them, at least in a geochemical sense. A similar conclusion can be drawn from the minor elements. Ni and Cr are very variable in Pukkila (Ni with a range from <20 ppm to 210 ppm, Cr varying from 20 ppm to 1140 ppm), clearly differing from the constantly low values in the Tjusterby outcrop. Zn, Cu and Pb are of relatively similar amounts in both areas, but larger differences are again seen in the amounts of As. All Pukkila samples have As values below the detection limit, which suggests that hydrothermal fluids have not had any role in the formation of these amphibolites (Breuer & Pichler 2013).

4.4. Petrography

As is the case for geochemistry, the petrographical differences can also be used as evidence for the origin of different lithological units. The petrographical investigations are in this thesis based on thin section observations, with this discussion mostly focusing on brief interpretations about the internal differences in the serpentinite sample group and with comparisons of other sampling areas with the Tjusterby material. Petrographical differences for the serpentinitic sample group are in general based on e.g. the geotectonic setting, the intensity of fluid alteration, conditions of pressure and temperature and the nature of the protolith (Mével 2003, Evans 2008, Schwartz et al. 2012, Lamadrid et al. 2017, Sonzogni et al. 2017).

4.4.1. Tjusterby serpentinites

Altogether 11 serpentinitic samples from Tjusterby were cut into thin sections for this study. As seen in the previous descriptions, all these samples are relatively similar to each other with only small variations in the ratio of serpentine to other minerals, and in the textural pattern of the serpentine minerals. The degree of serpentinization is high in every sample, since no identifiable olivine or pyroxene were observed in any of them, again with the exception of sample T1732. Excluding this sample, the only significant differences were in the amounts of other minerals than serpentine, i.e. phlogopite,

brucite, plagioclase and the opaque phases. The variation in the amount of phlogopite is the most significant of these, since it goes from absent in some samples (T1717, T1732, T1736 and T1742) 20% in sample T1709. As was mentioned in the geochemistry discussion, is a good correlation between the K contents with the amount of phlogopite in the rock. Compared with phlogopite, plagioclase and the opaque minerals are more evenly distributed. Plagioclase is present in every sample from 1% to 8%, while the opaque minerals have a range from 7% to 14%. Accessory minerals include brucite, chlorite and garnet. Brucite is often mentioned as a common by-product in the serpentinization process (e.g. Sonzogni et al. 2017), but in the Tjusterby samples, it was only identified in T1701 and T1707. Small amounts of chlorite alteration could be seen in several samples, but chlorite was clearly identified only in sample T1733. Like chlorite, garnet was also only observed in one thin section (T1733). In serpentinitic associations, the garnet is likely to be the Mg-rich end-member pyrope (Nesse 1991).

Although some differences in the texture of the serpentine minerals were seen in thin sections, it is not possible to identify the type of serpentine (antigorite, chrysotile, lizardite) based on optical properties alone (Groppo et al. 2006). A hint that chrysotile and lizardite might be more common than antigorite in Tjusterby can be seen in the geochemical data, where enrichments of Cl, B Sr, U, Sb, Rb and CS have been suggested to be associated with these minerals (Kodolányi et al. 2011). As the three serpentine sub-types have their own specific stability fields in terms of pressure and temperature, knowing the type of mineral would help in the determination of the conditions where the fluid alteration took place (Evans 2004). But while the serpentine group minerals are the most dominant phases in the thin sections, the presence of other minerals might be more informative. Brucite, a magnesium hydroxide, is regarded as a relatively common mineral in serpentinitic rocks (e.g. Moody 1976). It is, however, not always present and it's occurrence is at least partially dependent on the Mg-content of the protolith, which would mean that serpentinites with an olivine-dominant composition would be most likely to contain more brucite (Iyer 2007). Still, some contradiction exists about this, since brucite has been proven to be absent from serpentinites with both dunitic and harzburgitic protoliths, as reviewed from several sources by Sonzogni et al. (2017). This lack of brucite explained (Sonzogni et al. 2017) by possible serpentinization through a multi-stage reaction process, where brucite first is a reaction product, and then when the reaction proceeds, it is consumed to be formed into serpentine and/or magnetite. Another explanation for the lack of brucite by Sonzogni et al. (2017) is a late weathering of the mineral in a cold water environment. As noted above, brucite is only rarely present in the Tjusterby serpentinites. But as it is not completely lacking, there must have been enough Mg during the serpentinization process to produce both

serpentine minerals and brucite, which would imply that a pyroxenitic protolith is unlikely in the case of Tjusterby.

Similar to brucite, talc is a mineral that sometimes is regarded to be a reaction product in serpentinization (e.g. Mével 2003). Although it's presence cannot be accurately used as a direct indication of the protolith petrography, as talc can be absent from serpentinites of all varieties (Sonzogni et al 2017, according to several sources), it's absence might also be indicative of the same reason as the presence of brucite: the Mg-content of the protolith. Since talc is commonly associated with the alteration of orthopyroxene (Mével 2003), a talc-rich sample would be assumed to be derived from an orthopyroxene-rich source. As with brucite, the amount of talc in rocks can be affected after the initial formation of the mineral in later processes. But as the presence of brucite and the absence of talc in the Tjusterby samples both have a connection to the amount of the Mg-rich mineral olivine in the protolith, it points to the assumption that the protolith for the Tjusterby serpentinite had at least some amount of olivine in it. This would leave out both pyroxenites and harzburgites with substantial modal orthopyroxene, since in these, talc has been noted to take the place of brucite (Evans 2008). When present, talc can thus be used as an indication of some protolith properties for serpentinization, but it's presence or absence cannot be used as a tool for identifying the physical properties for serpentinization, since talc is stable over a wide range of temperatures (Mével 2003).

The amount of opaque minerals is quite even in the Tjusterby samples. But as there are several isotropic minerals constituting the opaque group, their accurate identification is not possible. Despite of this, it is fair to assume magnetite to be common, partly since the values for magnetic susceptibility data were constantly high in the Tjusterby serpentinites and partly because magnetite is known to be common in association with serpentinitic rocks (e.g. Moody 1976, Mével 2003). Although it is common, it is however not always present, since completely magnetite-free serpentinites are known both in nature and from laboratory experiments (Lafay et al. 2012). The factors controlling the presence of magnetite in serpentinites have been debated for some time, and in a relatively recent publication by Klein et al. (2014) they have been linked to the serpentinization temperature and to the Fe-content of brucite. According to that study, magnetite-poor serpentinites are preferentially formed in temperatures below 200°C and in association with Fe-rich brucite, while magnetite is more common in rocks serpentinized in higher temperatures, and together with Fe-poor brucite. The Fe-content of brucite was not possible to evaluate for this thesis, but the presence of magnetite suggests relatively high temperatures during serpentinization. This is supported by the identification of chlorite in one sample, since chlorite is known to be most stable in temperatures from 300°C to 500°C (Mével 2003).

As sample T1732 is the only half-serpentinized sample, and thus also contains unaltered olivine and pyroxene, it deserves a short separate discussion. This sample is mostly composed of ortho- (35%) and clinopyroxene (10%), serpentine (30%) and olivine (15%). The ratio of pyroxenes to olivine is thus quite high, but it is necessarily not fully representative of the ratios of these minerals in the rock prior to alteration, since olivine and pyroxenes might be subject to alteration at different stages of the serpentinization process. Still, if assumed that this sample from, one single boulder is representative of the other, fully serpentinized samples in Tjusterby, it can be speculated that their common protolith was abundant in both olivine and pyroxenes. Thus, it did not represent either of the end-members of the ultramafic spectrum, i.e. the olivine-poor pyroxenites or pyroxene-poor dunites. This deduction is coherent with the assumption made earlier in the discussion about brucite and talc. It also would mean that a harzburgitic origin is possible for the Tjusterby serpentinites, which also would support the careful assumptions about geochemistry in the previous comparison with the data of Deschamps et al. (2013). The thin section of sample T1732 also contained some phlogopite (2%), plagioclase (1%) and opaque minerals (7%). The amount of the opaque minerals and the value of magnetic susceptibility is lower in this sample than in most of the other serpentinites, which could imply a slightly lower magnetite content. But as magnetite can't be directly identified in thin section, this is not possible to prove.

4.4.2. Mallusjärvi

Three thin sections were made of the samples collected in the Mallusjärvi area. As mentioned in the discussion about geochemistry, there is not much internal variation within the Mallusjärvi sample group. This is also evident in the thin sections, since all of them are composed of pyroxene, olivine, iddingsite and opaque minerals, as well as plagioclase in samples JI1705a and JI1715. The textural resemblance between the samples is clear, with typically intergrown and irregularly shaped mineral grains being most common. Some alteration has taken place in the Mallusjärvi unit, since the loosely defined mineral referred to as iddingsite is relatively abundant. The composition of iddingste has been described as a mixture of clay minerals, chlorite and iron oxide, and is a common alteration form of olivine in hydrothermal and weathering conditions (Eggleton 1984). Another form of alteration observed in one sample (JI1707) is the rare occurrence of serpentine in association with olivine. In this case it is only seen on a minor fracture surface, and thus serpentinization as a process in Mallusjärvi is not comparable with Tjusterby. But it suggests that some form of water-related alteration has taken place, albeit on a small scale. Due to the heavy serpentinization in the Tjusterby samples, a detailed comparison of the mineral assemblages between Mallusjärvi and the assumed protolith for Tjusterby is difficult to make, but as a careful interpretation they seem to have some differences. If the half-serpentinized rock in sample T1732 is representative

for all Tjusterby serpentinites before complete serpentinization, it can be assumed that pyroxene minerals are more dominating in Mallusjärvi than in Tjusterby, and that olivine is less abundant in Mallusjärvi. Even when accounting for this ratio between pyroxenes and olivine to be affected by the alteration of the minerals into serpentine and iddingsite, pyroxene is still relatively more abundant in the thin sections made of the Mallusjärvi samples. This is comparable with the geochemical results, where the Mallusjärvi samples had higher SiO_2 and lower MgO than the Tjusterby serpentinites both before and after adjusting for LOI.

One significant petrographical feature in the Mallusjärvi samples is the highly variable amount of opaque minerals, which ranges from 4% to 25%. As all Mallusjärvi samples also showed high magnetic susceptibility values, magnetite is probably one of these opaque minerals. The ratio of magnetite to other opaque minerals in the Mallusjärvi samples is unclear, but it is likely to be lower in sample JI1705a compared to samples JI1707 and JI1715, as sample JI1705a had 25% isotropic minerals. Although this sample had a considerably high magnetic susceptibility and was more Fe-rich than the other two samples, the differences are probably not large enough to explain such a variation in the amount of isotropic minerals with the amount of magnetite alone. But as the geochemical data do not show any significant enrichment of any element for sample JI1705a, no further deductions about the nature of the opaque minerals can be made through these data either. As discussed above, magnetite formation is a common product in the serpentinization of mafic-ultramafic rocks. But as no real signs of serpentinization were seen in the Mallusjärvi samples, it is shown that magnetic properties in ultramafic rocks can be present without serpentine alteration as well.

4.4.3. Unserpentinized samples from Tjusterby and bedrock samples from Pukkila

Thin sections were made of three samples from unserpentinized boulders from Tjusterby, of four bedrock samples from Tjusterby and of five bedrock samples from Pukkila. They are here briefly discussed in a similar manner as for the geochemistry section above, i.e. by comparing the other samples to bedrock samples from Tjusterby. Less attention is now paid to the unserpentinized boulder samples from Tjusterby, as thin sections were only made of one amphibolitic boulder and of the magnetic samples T1721 and T1741, which do not have comparable units in sampled bedrock. The samples from Pukkila are mineralogically more consistent with each other, but bear only limited resemblance to the amphibolitic part of the Tjusterby bedrock.

When the bedrock samples were taken in Tjusterby they were thought to be amphibolitic and gabbroic, but a closer inspection of the mineral contents reveals that samples JI1701 and JI1702 have more quartz, (33% in JI1701, 40% in JI1702), and less hornblende (10% and 20%, respectively), that would be expected of amphibolites. As biotite also is

more common in both samples (27% in JI1701 and 25% in JI1702) than hornblende, biotite-hornblende schist is a more representative name for these samples. The term schist is applicable, since a preferred orientation of both biotite and hornblende was observed. No metamorphic texture was observed in the gabbroic sample JI1703, which is rich in plagioclase (49%) and biotite (21%), with quartz and plagioclase both constituting 15%. A noticeable feature was the low amount of opaque minerals (1%) in this sample. As the value for magnetic susceptibility for it was low, a lack of magnetite is one explanation for the low amount of opaque minerals. Sample JI1704 is the only true amphibolite collected in outcrop in Tjusterby. This sample contains mostly hornblende (60%), with associated quartz (25%) and plagioclase (10%). Opaque minerals make up 5% of it, but as the magnetic susceptibility value this sample was low, they are likely to constitute of other minerals than magnetite.

The amphibolitic boulder sample from Tjusterby (T1703) has a more variable mineralogical composition compared to the amphibolitic bedrock sample in Tjusterby (JI1704). Although the amounts of hornblende are roughly similar between these two samples, plagioclase is much more common in the boulder sample, constituting 25% of it. For quartz, the situation is the opposite, since thin section T1703 only has 3% of the mineral, while it was much more common in the bedrock. In addition, the boulder sample includes biotite and apatite, which are absent in the amphibolitic bedrock sample. Thus, if sample T1703 had been transported from an amphibolite unit on the island of Kalvholmen (immediately north of the serpentinite bodies in Tjusterby) it can be seen both based on mineralogy and geochemistry that the amphibolitic bedrock north and south of the Pernajanlahti bay would be quite different.

Boulder samples T1721 and T1741 were earlier shown to be heavily magnetic and to have high iron contents. Their magnetism can be explained by high contents of opaque minerals, which make up 25% of both thin sections. As with the serpentinitic boulders in Tjusterby, these opaque minerals are likely to be dominated by magnetite. These two samples were also rich in garnet, which is indicative of a medium metamorphic grade. But since no known outcrops in the area match the mineralogical, geochemical and geophysical properties of these two samples, their origin can’t be estimated.

Petrographic evaluations of the Pukkila samples revealed that the material consists of amphibolites and mica schists. As the very quartz-rich (56%) mica schist (sample JI1736) does not contain any hornblende, it is mineralogically quite different from the hornblende-biotite schists in the Tjusterby bedrock. It is also abnormal compared to the Pukkila amphibolites, indicating that the neighboring metamorphic rocks in Pukkila have less in common to each other than the hornblende-biotite schist and amphibolite have in Tjusterby. Also, the amphibolites in Pukkila are, despite being classified as the same

rock type, not similar to the Tjusterby amphibolite. Based on the thin section studies they are generally richer in hornblende and contain much less quartz than the Tjusterby amphibolite. They also contain biotite and in some cases chlorite and rare garnet, which are not seen in the Tjusterby samples. In the Pukkila samples, an internal petrographic difference in the amphibolite samples can be seen. The northernmost amphibolite sample (JI1735) is richest in hornblende (71%) and contains least biotite (3%) compared with the rest of the samples. Samples JI1737 and JI1748 are located relatively closely to each other and are not too different from sample JI1735. A bigger change can be seen when comparing these with sample JI1741, which is located about 1 km further south. Despite being classified as an amphibolite, this sample contains much less hornblende (30%) and much more biotite (30%) than the rest of the Pukkila amphibolites. If it wasn't for the low amount of quartz (10%), this sample could be compared with the hornblende-biotite schists in the Tjusterby bedrock.

4.5. The relation between Tjusterby and Svecofennian mafic lithologies

After an evaluation of the properties of the serpentinite bodies in Tjusterby and of their comparison to two geographically adjacent units marked as ultramafic on bedrock maps, a brief look on the relation of Tjusterby to mafic and ultramafic units on a broader perspective can be made. Mafic-ultramafic rock associations exist throughout the Fennoscandian shield and more locally in the Svecofennian domain in Southern and Central Finland. Granitoids are much more common within the plutonic lithologies in these areas (Simonen 1980), but despite their limited volume the mafic-ultramafic intrusions are important in providing information about the mantle sources at convergent plate margins and playing a part in the metamorphic evolution around the areas of their emplacement by generating heat upwards within the crust (Peltonen 2005). Most studies regarding mafic-ultramafic intrusions in the Svecofennian domain in Finland have been focused on the economically more interesting Kotalahti and Vammala Nickel Belts around the Central Finland Granitoid Complex (Makkonen 2005, Makkonen 2015). Since all the mafic-ultramafic plutonic rocks have been emplaced during a relatively short time period of 1.89-1.87 Ga in connection with the Svecofennian Orogeny, they have, rather by age data, been divided into groups by their geotectonic domains (Peltonen 2005). This division is based on three groups, of which the spatially closest to Tjusterby is the second group, the Synvolcanic intrusions of the Arc complex of Southern Finland. This group does not cover the Tjusterby area or the southernmost part of Finland, but by being the closest one it is in this case the most logical point of comparison for the Tjusterby serpentinites.

The intrusions in the second group of Peltonen (2005) make up part of the Häme Belt and are associated with metavolcanic rocks and were crystallized at low pressures. They

are thought to be derived from a relatively depleted mantle source and have generally low potential for magmatic sulphide deposits. An example of the Häme Belt, with the shortest distance to Tjusterby, is the Hyvinkää layered intrusion, 70 km to the NW from Tjusterby. It is a gabbro complex with constituents of layered peridotites, pyroxenites, olivine gabbros, gabbronorites and granophyre, with some unlayered gabbros. This complex intrusion shows how differing mafic-ultramafic units can be within a relatively small area, indicating the complexity of comparing a heavily altered serpentinite unit to unaltered intrusions occurring tens of kilometers away when trying to find common features to point out a similar origin. In bedrock maps covering the central and southern parts of Finland numerous but small mafic-ultramafic bodies can be seen scattered over large areas. This is mostly due to fragmentation caused by faulting and overthrusting during the Svecofennian Orogeny (Makkonen 2005). Since many units are small in size, they have not all individually been described in literature. All of them have likely not been identified, either, especially in areas where outcrops are sparse or absent, like in the submarine example in Tjusterby. Because of the fragmented nature of these intrusions, it is suggested that the protolith for the Tjusterby serpentinites also would be part of the second intrusion type described by Peltonen (2005).

Of the known serpentinites in Finland, most are located near greenstone belts in the northern and eastern parts of the country (Sotka 1983). In Southern Finland serpentinites seem to be rare and appear as minor zones of alteration in contact with local mafic-ultramafic units. The Tjusterby serpentinites are relatively isolated from known similar units, but looking at a broader picture their existence is not too peculiar. The bedrock in Southern and Central Finland in general is complicated, due to e.g. arc complex accretion and subduction during the Svecofennian Orogeny (Nironen 1997). This means that differing lithologies are found within relatively confined areas, and the role of subduction zones is a sign that altering fluids could get in contact with the bedrock. In the discussion about geochemistry it was seen that the geochemical data of the Tjusterby serpentinites had some resemblance serpentinites related to harzburgites in a subduction zone environment. As subduction has notably had a major role in the evolution of the geology of the Fennoscandian shield, it should not be too far-fetched to regard subduction related fluids to have a connection to the serpentinization of the units studied in Tjusterby.

5. Conclusions

This thesis concerns two previously unknown bodies of serpentinized ultramafic rocks at Tjusterby in the eastern Uusimaa region in southern Finland. The recognition of the study object was initially based on inspections of old aeromagnetic maps and till sample data from the area, and it was confirmed through more enhanced ground magnetometry surveys and boulder sampling. As the studied serpentinized ultramafic bodies are located under water and thus inaccessible in outcrop, the descriptions of the investigation methods can serve as an indication of the usability of them in situations where direct sampling of the object of interest is impossible. In addition to the main study object in Tjusterby, this work included two other areas, Mallusjärvi in the Päijät-Häme region and Pukkila in the Uusimaa region, both used as reference examples of assumed ultramafic lithologies.

The results received from geochemical and petrographical investigations of the serpentinite samples in Tjusterby were used as a base of evaluating the geotectonic conditions where serpentinization of the initially unaltered ultramafic unit took place, and of recognizing the rock type of the same unaltered protolith. Based on comparisons between the geochemical data of the Tjusterby serpentinites and literature data, it seems likely that the geotectonic environment in which the Tjusterby object was serpentinized, was in a subduction zone, rather than in other settings of abyssal and mantle wedge environments. Of different rock types, the data that was the base of comparison to the Tjusterby serpentinites included harzburgites and dunites, of which the geochemical data from harzburgites was generally slightly closer to the Tjusterby serpentinites. This is not a final conclusion, however, since possible protoliths to be affected by serpentinization include several more rock types than were presented in the referenced geochemical data. The petrographical investigations provided some supplementary information to the geochemical data. The mineral assemblage of the Tjusterby serpentinites was relatively homogeneous, as the samples contained mostly serpentine, phlogopite, opaque phases, plagioclase, and in some occasions brucite, chlorite and garnet. Petrographically, most information regarding the rock type of the unaltered protolith for the serpentinites was seen in the presence of brucite and the absence of talc in the thin sections, both referring to elevated Mg-contents in the rock. This indicates a protolith rich in olivine. The opaque minerals were relatively abundant in most thin sections. These have not been optically distinguished, but as the values for magnetic susceptibility were constantly high in the Tjusterby serpentinites, it is evident that magnetite is one of the most common opaque phases in them.

The serpentinite bodies presented in this study are relatively small in size. As they happen to be located completely under water and thus are not present in outcrop, they could only be detected through indirect investigation methods. As the bedrock in the

Svecofennian domain in Finland is largely fragmented into lithological units of variable sizes, for many of which outcrops are rare or completely lacking, it is likely that other similar small ultramafic and serpentinitic units exist within it. Since especially serpentinites often show strong magnetic properties and thus are likely to be distinguishable from surrounding bedrock on aeromagnetic maps, similar research as has been done in Tjusterby could be projected to recognize comparable serpentinite units in other areas within the Svecofennian domain as well.

6. Acknowledgements

I wish to thank my supervisor, professor Krister Sundblad, for providing me with the subject for this thesis, and for the encouraging support from the beginning of the field work to the end of the writing process. Regarding field work, I am also grateful to Sethi Thim from the Institute of Technology of Cambodia for helping me both with boulder tracing and for providing the magnetic susceptibility data used in this thesis. For the magnetometric data I am thankful to professor Jüri Plado from the University of Tartu for providing the instruments used for the measurements, and for processing the gathered data. Special thanks also go to students participating in the field courses in ore prospecting in 2015–2017 for collecting till and boulder samples and for helping in magnetometry surveys that provided data for this thesis. Finally, I am grateful to the K.H. Renlund Foundation for providing economic support to make it possible to complete this thesis.

7. References

Aeromagnetic Map. Map Sheet 302109 - Pernå. Geological Survey of Finland, 2001.

Best, M.G. 2003. *Igneous and Metamorphic Petrology*, Second Edition. Blackwell Science Ltd. Turin.

Boynton, W.V. 1984. Cosmochemistry of the Rare Earth elements; meteorite studies. *In:* Henderson, P. (Editor): *Rare Earth element geochemistry*. 63–114. Elsevier Sci. Publ. Co., Amsterdam.

Breuer, C., Pichler, T. 2013. Arsenic in marine hydrothermal fluids. *Chemical Geology* 348, 2–14.

Debret, B., Andreani, M., Godard, M., Nicollet, C., Schwartz, S., Lafay, R. 2013. Trace element behavior during serpentinization/de-serpentinization of an eclogitized oceanic lithosphere: A LA-ICPMS study of the Lanzo ultramafic massif (Western Alps). *Chemical Geology* 357, 117–133.

Deschamps, F., Godard, M., Guillot, S., Hattori, K. 2013. Geochemistry of subduction zone serpentinites: A review. *Lithos* 178 (2013) 96–127.

DigiKP 200 Bedrock of Finland – DigiKP 200. Geological Survey of Finland. Accessed 19.12.2018. http://gtkdata.gtk.fi/Kalliopera/index.html

Duchesne, J-C. 1982. The lanthanides as geochemical tracers of igneous processes: an introduction. *In:* Sinha, S.P. (ed.). *Systematics and the properties of the lanthanides. NATO ASI Series. Series C, Mathematical and physical sciences;* no. 109. 543–560. D. Reidel Publishing Cmpany, Dordrecht.

De Vos, W., Tarvainen, T. (Chief eds.) 2005. *Geochemical Atlas of Europe. Part 2. Interpretation of geochemical maps, additional tables, figures, maps, and related publications*. Geological Survey of Finland, Espoo.

Eggleton, R.A. 1984. Formation of iddingsite rims on olivine: A transmission electron microscope study. *Clays and Clay Minerals*, Vol. 32, No. 1. 1–11.

Evans, B.,W. 2004. The serpentinite multisystem revisited: Chrysotile is metastable. *International Geology Review*, 46:6, 479–506.

Evans, B.W. 2008. Control of the products of serpentinization by the $Fe^{2+}Mg_{-1}$ exchange potential of olivine and orthopyroxene. *Journal of Petrology,* Vol 49, No. 10, 1873–1887.

Glückert, G. 1974. Map of glacial striation of the Scandinavian ice sheet during the last (Weichsel) glaciation in northern Europe. *Bulletin of the Geological Society of Finland* 46, 1–8.

Groppo, C., Rinaudo, C., Cairo, S., Gastaldi, D., Compagnoni, R. 2006. Micro-raman spectroscopy for a quick and reliable identification of serpentine minerals from ultramafics. *European Journal of Mineralogy*, 18, 319–329.

Guillot, S, Hattori, K. 2013. Serpentinites: Essential roles in geodynamics, arc volcanism, sustainable development, and the origin of life. *Elements*, Vol 9, pp 95–98.

Hirth, G., Guillot, S. 2013. Rheology and tectonic significance of serpentinite. *Elements*, Vol. 9, 107–113.

Ingves, J. 2016.Till geochemistry in Garpgård and Tjusterby, Itä-Uusimaa, SE Finland. *BSc. thesis*, University of Turku. 56 pp.

Iyer, K. 2007. Mechanisms of serpentinization and some geochemical effects. *Series of dissertations submitted to the Faculty of Mathematics and Natural Sciences, University of Oslo*. No. 674.

Klein, F., Bach, W., Humphris, S., E., Kahl, W-A., Jöns, N., Moskowitz, B., Berquo, T. 2014. Magnetite in seafloor serpentinite – Some like it hot. *Geology*, 42, 135–138.

Kodolányi, J., Pettke, T., Spandler, C., Kamber, B.S., Gmélig, K. 2011. Geochemistry of ocean floor and fore-arc serpentinites: Constraints on the ultramafic input to subduction zones. *Journal of Petrology*, Volume 53, Issue 2, (2012) pp. 235–270.

Lafay, R., Montes-Hernandez, G., Janots, E., Chiriac, R., Findling, N., Toche, F. 2012. Mineral replacement rate of olivine by chrysotile and brucite under high alkaline conditons. *Journal of Chrystal Growth* 347, 62–72.

Laitala, M. 1964. Geological map of Finland. Pre-quaternary rocks. 1:100 000. Sheet – 3021 – Porvoo. Geological Survey of Finland.

Lamadrid, H.M., Rimstidt, J.D., Scwartzenbach, E.M., Klein, F., Ulrich, S., Dolocan, A., Bodnar, R.J. 2017. Effect of water activity on rates of serpentinization of olivine. *Nature Communications* 8, 16107.

Lanza, R., Meloni, A. 2006. *The Earth´s magnetism – An introduction for geologists*. Springer-Verlag Berlin Heidelberg.

Makkonen, H.V. 2005. Intrusion model for Svecofennian (1.9 Ga) mafic-ultramafic intrusions in Finland. *Geological Survey of Finland, Special Paper* 38, 11–14.

Makkonen, H.V. 2015. Nickel deposits of the 1.88 Ga Kotalahti and Vammala Belts. *In:* Maier, W.D., Lahtinen, R. and O'Brien, H. *Mineral Deposits of Finland*, 253–290. Elsevier, Amsterdam.

Makkonen, H.V., Halkoaho, T., Konnunaho, J., Rasilainen, K., Kontinen, A., Eilu, P. 2017. Ni-(Cu-PGE) deposits in Finland - Geology and exploration potential. *Ore Geology Reviews*, Vol. 90, 667–696.

Malpas, J. 1992. Serpentine and the geology of serpentinized rocks. *In*: Roberts, B., A. and Proctor, J. (eds), *The ecology of areas with serpentinized rocks. A world view*, 7–30. Kluwer Academic Publishers.

McClenaghan, M.B., Paulen, R.C. 2018. Application of till mineralogy and geochemistry to mineral exploration. *In*: Menzies, J., van der Meer, J. (Editors). *Past glacial environments*, 2nd ed. Elsevier Ltd, Amsterdam.

Menzies, M., A., Long, A., Ingram, G., Tatnell, M., Janecky, D. 1993. MORB peridotite-sea water interaction: experimental constraints on the behaviour of trace elements, $^{87}SR/^{86}SR$ and $^{143}Nd/^{144}Nd$ ratios. *Geological Society, London, Special Publications*, 76, 309–322.

Mével, C. 2003. Serpentinization of abyssal peridotites at mid-ocean ridges. *C.R. Geosciense* 335 (2003) 825–852.

Mielke, J.E. 1979. Composition of the Earth's crust and distribution of the elements. *In*: Siegel, F.R. (ed.) 1979. *Review of research on modern problems in geochemistry*. International Association for Geochemistry and Cosmochemistry. Unesco, Leuven.

Moody J.B. 1976. Serpentinization: a review. *Lithos*, vol. 9, Issue 2, 125–138.

National Land Survey of Finland. File service of open data. Material downloaded from site during October 2018. https://tiedostopalvelu.maanmittauslaitos.fi/tp/kartta?lang=en.

Nesse, W.D. 1991. *Introduction to optical mineralogy*, 2nd ed. Oxford University Press.

Nironen, M. 1997. The Svecofennian orogen: A tectonic model. *Precambrian Research* 86 (1997) 21–44.

NOAA (National Oceanic and Atmospheric Administration). 2014. *US/UK world magnetic model – epoch 2015.0 main field total intensity*. Map developed by NOAA/NGDC & CRIES

van Nostrand, T.S. 2015. Lithogeochemistry of ultramafic, gabbroic and tonalitic rocks from the Northeastern Archean Ashuanipi Complex, Western Labrador: Implications for petrogenesis and mineral potential. *Current Research, Newfoundland and Labrador Department of Natural Resources*, Geological Survey, Report 15–1, 191–213.

Palandri, J.L., Reed, H.M. 2004. Geochemical models of metasomatism in utramafic systems: Serpentinization, rodingitization, and sea floor carbonate chimney precipitation. *Geochimica et Cosmochimica Acta*, Vol 68, No. 5,1115 1133.

Peltonen, P. 2005. Svecofennian mafic-ultramafic intrusions. *In*: Lehtinen, M., Nurmi, P.A., Rämö, O.T. (Eds.), *Precambrian geology of Finland – Key to the evolution of the Fennoscandian Shield*. 407–442. Elsevier Science B.V., Amsterdam.

Reynard, B. 2012. Serpentine in active subduction zones. *Lithos* 178 (2013) 171–185.

Salminen, R., Hartikainen, A., 1985. Glacial transport of till and its influence on the interpretation of geochemical results in North Karelia, Finland. *Geological Survey of Finland, Bulletin 335.* Espoo.

Salonen, V.P. 1987. Glacial transport distance distributions of surface boulders in Finland. *Geological Survey of Finland, Bulletin 338*. Espoo.

Sarala, P, 2015. Surficial geochemical exploration methods. *In*: Maier, W.D., Lahtinen, R. and O'Brien, H. *Mineral deposits of Finland*, 781–792. Elsevier, Amsterdam.

Schmitt, D.R., Han, Z., Kravchinsky, V.A., Escartin, J. 2007. Seismic and magnetic anisotropy of serpentinized ophiolite: Implications for oceanic spreading rate dependent anisotropy. *Earth and planetary science letters* 261, 590–601.

Schwartz, S., Guillot, S., Reynard, B., Lafay, R., Debret, B., Nicollet, C., Lanari, P., Auzende, A.L. 2012. Pressure-temperature estimates of the lizardite-antigorite transition in high pressure serpentinites. *Lithos* 178 (2013), 197–210.

Simonen, A. 1980. The Precambrian in Finland. *Geological Survey of Finland, Bulletin 304*. Espoo.

Sonzogni Y., Treiman, A.H., Schwenzer, S.P. 2017. Serpentinite with and without brucite: A reaction pathway analysis of a natural serpentinite in the Josephine ophiolite, California. *Journal of Mineralogical and Petrological Sciences*, Vol. 112, 59–76.

Sotka, P. 1983. Serpentiniittien esiintymisalueet Suomessa. *Outokumpy Oy:n malminetsinnän raportit*.

White, W.M. 2013. *Geochemistry*. Wiley-Blackwell.

Appendix

Table 1: Complete geochemical data for all samples ananlyzed in laboratory.

Analyte Symbol	SiO2	Al2O3	Fe2O3(T)	MnO	MgO	CaO	Na2O	K2O	TiO2	P2O5	LOI	Total
Unit Symbol	%	%	%	%	%	%	%	%	%	%	%	%
Detection Limit	0,01	0,01	0,01	0,001	0,01	0,01	0,01	0,01	0,001	0,01		0,01
Analysis Method	FUS-ICP	FUS-ICP	FUS-ICP	FUS-ICP	FUS-ICP	FUS-ICP	FUS-ICP	FUS-ICP	FUS-ICP	FUS-ICP	FUS-ICP	FUS-ICP
T17 01	34,04	2,93	12,28	0,215	34,22	0,17	0,04	0,49	0,087	0,01	12,9	97,37
T17 03	52,61	14,87	11,3	0,172	6,17	5,74	3,67	2,68	1,372	0,16	1,83	100,6
T17 07	32,89	1,62	14,92	0,123	35,19	0,05	0,05	0,39	0,035	0,02	12,16	97,44
T17 09	31,9	3,71	14,27	0,101	32,49	0,04	0,07	0,67	0,093	< 0.01	11,69	95,03
T17 10	37,98	2,62	11,64	0,118	32,81	0,11	0,03	0,69	0,053	< 0.01	12,48	98,53
T17 11	50,36	4,74	7,9	0,154	16,93	16,2	0,65	0,23	0,585	0,06	1,94	99,76
T17 13	33,2	1,97	15,63	0,13	34,33	0,08	0,02	0,01	0,066	< 0.01	13,13	98,56
T17 14	32	2,49	13,08	0,114	35,63	0,06	0,04	0,02	0,095	< 0.01	13,42	96,95
T17 17	33,54	1,96	12,44	0,118	37,4	0,04	0,01	< 0.01	0,084	0,01	12,99	98,61
T17 20	41,14	11,61	14,96	0,234	11,77	15,02	1,15	0,88	2,335	0,24	1,14	100,5
T17 21	37,75	10,67	41,59	1,407	3,87	2,09	0,02	0,14	0,626	0,45	1,96	100,6
T17 22	34,55	1,71	12,36	0,11	36,16	0,06	0,05	0,59	0,075	< 0.01	12,09	97,75
T17 26	35,09	1,63	12,78	0,114	35,12	0,05	0,04	0,52	0,037	< 0.01	12,92	98,29
T17 27	35,34	1,2	8,22	0,118	38,67	0,06	0,05	0,28	0,042	< 0.01	13,84	97,81
T17 28	43,67	8,61	12,71	0,217	18,16	9,8	0,66	0,73	0,666	0,17	3,38	98,77
T17 30	34,95	3,67	13,86	0,138	33,2	0,71	0,14	0,26	0,107	0,01	12,35	99,4
T17 32	40,22	6,55	11,64	0,166	26,38	5,88	0,69	0,06	0,449	0,02	6,41	98,47
T17 33	34,96	2,44	10,77	0,138	34,92	0,04	0,04	0,79	0,063	0,01	13,61	97,79
T17 36	33,14	2,35	12,42	0,119	35,87	0,04	0,02	< 0.01	0,098	< 0.01	13,83	97,88
T17 39	33,87	1,82	10,94	0,14	36,69	0,03	0,04	0,02	0,053	< 0.01	14,51	98,12
T17 41	33,99	11,26	43,51	1,553	3,95	2,4	0,02	0,37	0,56	0,43	2,28	100,3
T17 42	34,68	2,34	12,52	0,109	36,04	0,06	0,05	0,03	0,084	0,02	13,15	99,08
JI17 01	54,66	16,09	10,64	0,156	4,28	7,11	3,31	1,71	1,275	0,19	1	100,4
JI17 02	62,63	13,9	10,22	0,144	1,19	4,25	2,94	1,98	1,02	0,29	0,52	99,08
JI17 03	57,58	17,39	7,29	0,115	2,78	6,23	3,59	2,3	0,878	0,24	1,4	99,78
JI17 04	50,75	14,21	16,37	0,281	4,12	9,83	2,27	0,52	1,838	0,25	0,26	100,7
JI17 05A	42,92	5,21	16,93	0,202	15,33	14,48	0,63	0,19	1,153	0,03	1,62	98,68
JI17 06	43,21	3,43	13,39	0,213	19,35	14,42	0,45	0,16	0,394	0,03	3,61	98,66
JI17 07	45,31	3,95	12,73	0,2	18,45	14,85	0,67	0,16	0,512	0,03	1,49	98,34
JI17 15	44,19	4,82	10,94	0,183	18,93	14,51	0,68	0,32	0,544	0,03	3	98,15
JI17 17	45,06	3,56	12,33	0,178	20,51	12,42	0,52	0,18	0,41	0,02	3,12	98,31
JI17 35	48,78	10,05	11,11	0,207	12,43	11,45	1,13	0,86	0,829	0,08	1,97	98,9
JI17 36	74,43	11,42	4,73	0,036	1,52	1,51	2,27	2,22	0,479	0,12	0,82	99,56
JI17 37	53,51	10,33	10,93	0,18	10,68	9,55	1	0,94	0,569	0,08	1,48	99,25
JI17 40	51,92	12,89	11,34	0,172	9,6	9,75	1	1,05	0,664	0,13	1,73	100,3
JI17 41	49,59	16,72	14,23	0,137	6,17	6,74	0,99	2,51	0,921	0,16	2,29	100,4
JI17 48	53,38	11,49	10,39	0,166	9,74	10,49	0,8	0,7	0,596	0,08	1,93	99,77
JI17 49	66,85	14,21	6,2	0,05	2,15	2,17	2,92	2,6	0,634	0,13	1,17	99,08

Analyte Symbol	Sc	Be	V	Ba	Sr	Y	Zr	Cr	Co	Ni	Cu	Zn
Unit Symbol	ppm	ppm	ppm	ppm	ppm	ppm	ppm	ppm	ppm	ppm	ppm	ppm
Detection Limit	1	1	5	2	2	1	2	20	1	20	10	30
Analysis Method	FUS-ICP	FUS-ICP	FUS-ICP	FUS-ICP	FUS-ICP	FUS-ICP	FUS-ICP	FUS-MS	FUS-MS	FUS-MS	FUS-MS	FUS-MS
T17 01	11	36	56	< 2	10	2	5	3810	191	2480	550	1340
T17 03	40	1	283	432	136	31	103	60	32	< 20	< 10	90
T17 07	6	3	66	< 2	4	2	2	6590	149	1790	190	210
T17 09	6	3	199	34	4	1	3	> 10000	185	4290	500	200
T17 10	7	8	79	14	5	2	10	2360	146	1710	110	750
T17 11	75	< 1	231	81	125	10	24	1570	50	200	40	50
T17 13	9	6	87	6	3	1	3	2900	146	2010	880	50
T17 14	11	3	56	5	< 2	< 1	4	4960	155	2330	350	490
T17 17	9	1	57	9	2	2	7	4720	138	1650	130	70
T17 20	40	8	337	227	438	19	164	1420	84	700	< 10	170
T17 21	13	2	137	12	78	27	140	80	48	40	220	170
T17 22	6	5	62	12	4	5	3	5700	126	2280	< 10	180
T17 26	6	3	41	5	6	7	3	4420	141	1960	280	2830
T17 27	7	5	50	5	4	13	4	4230	142	2190	110	970
T17 28	33	2	240	53	75	15	46	1600	67	540	< 10	220
T17 30	12	1	68	9	12	4	6	2680	132	1120	220	1300
T17 32	34	3	164	5	13	9	18	2050	101	720	220	50
T17 33	10	3	48	< 2	4	9	3	3360	117	1810	10	1350
T17 36	10	2	48	< 2	< 2	2	3	2250	131	1770	240	1740
T17 39	7	< 1	47	< 2	< 2	3	2	2880	141	1780	110	550
T17 41	16	2	141	58	107	35	151	80	55	50	330	160
T17 42	9	2	43	< 2	2	2	9	2810	144	1630	90	150
JI17 01	23	2	216	422	260	23	132	30	23	< 20	< 10	90
JI17 02	22	3	20	604	223	59	254	< 20	11	< 20	< 10	120
JI17 03	13	3	103	625	406	17	207	40	10	< 20	30	100
JI17 04	38	2	358	46	168	42	171	< 20	34	< 20	< 10	140
JI17 05A	61	< 1	609	20	129	12	25	740	77	200	< 10	100
JI17 06	60	< 1	197	30	103	6	11	1370	84	270	10	70
JI17 07	61	< 1	236	18	97	9	20	1480	78	240	10	80
JI17 15	57	< 1	207	42	136	9	16	1540	72	260	10	60
JI17 17	56	< 1	192	22	73	7	15	1630	74	280	< 10	60
JI17 35	59	7	327	159	108	18	43	1140	55	210	60	180
JI17 36	11	2	56	334	149	21	241	100	8	30	30	50
JI17 37	56	1	261	192	97	15	63	140	49	60	80	70
JI17 40	42	2	271	172	257	14	43	500	42	60	40	80
JI17 41	23	1	606	400	162	4	49	20	46	< 20	60	100
JI17 48	46	< 1	239	115	121	16	58	700	43	130	20	80
JI17 49	16	1	90	525	218	23	237	110	12	30	20	70

Analyte Symbol	Ga	Ge	As	Rb	Nb	Mo	Ag	In	Sn	Sb	Cs	La
Unit Symbol	ppm	ppm	ppm	ppm	ppm	ppm	ppm	ppm	ppm	ppm	ppm	ppm
Detection Limit	1	1	5	2	1	2	0,5	0,2	1	0,5	0,5	0,1
Analysis Method	FUS-MS	FUS-MS	FUS-MS	FUS-MS	FUS-MS	FUS-MS	FUS-MS	FUS-MS	FUS-MS	FUS-MS	FUS-MS	FUS-MS
T17 01	5	3	813	287	< 1	18	< 0.5	< 0.2	10	1,9	107	0,9
T17 03	16	1	6	96	4	< 2	< 0.5	< 0.2	2	< 0.5	2,8	11,7
T17 07	4	2	189	142	< 1	< 2	< 0.5	< 0.2	< 1	< 0.5	13,8	0,6
T17 09	8	2	46	302	< 1	< 2	< 0.5	< 0.2	2	< 0.5	41,7	1,2
T17 10	4	1	138	265	2	< 2	< 0.5	< 0.2	8	< 0.5	57,5	0,8
T17 11	7	< 1	6	4	3	< 2	< 0.5	< 0.2	5	< 0.5	< 0.5	4,3
T17 13	3	2	47	3	< 1	< 2	< 0.5	< 0.2	10	< 0.5	0,6	0,5
T17 14	3	1	12	< 2	< 1	< 2	< 0.5	< 0.2	15	< 0.5	0,9	1,6
T17 17	2	2	55	< 2	< 1	< 2	< 0.5	< 0.2	4	< 0.5	< 0.5	1,6
T17 20	16	2	8	27	36	< 2	0,5	< 0.2	139	< 0.5	< 0.5	23,9
T17 21	23	4	< 5	11	12	2	0,6	< 0.2	4	< 0.5	0,9	46
T17 22	3	2	934	155	< 1	< 2	< 0.5	< 0.2	3	3,1	41,2	0,9
T17 26	3	2	17	131	< 1	< 2	< 0.5	< 0.2	< 1	< 0.5	50,3	1,7
T17 27	2	2	14	48	< 1	< 2	< 0.5	< 0.2	2	< 0.5	20,2	2,6
T17 28	13	3	40	46	3	< 2	< 0.5	< 0.2	4	< 0.5	4,9	8,5
T17 30	5	1	< 5	63	< 1	< 2	< 0.5	< 0.2	13	< 0.5	34,8	3,6
T17 32	5	1	< 5	< 2	< 1	< 2	< 0.5	< 0.2	38	< 0.5	0,9	1,3
T17 33	3	2	284	155	< 1	< 2	< 0.5	< 0.2	3	1	20,1	1,8
T17 36	3	1	43	< 2	< 1	< 2	< 0.5	< 0.2	21	0,7	< 0.5	1,7
T17 39	3	2	8	< 2	< 1	< 2	< 0.5	< 0.2	4	< 0.5	0,6	2,2
T17 41	23	4	< 5	27	11	< 2	0,6	< 0.2	4	< 0.5	1,1	44,7
T17 42	3	2	284	< 2	< 1	< 2	< 0.5	< 0.2	5	0,7	< 0.5	2,5
JI17 01	20	1	< 5	80	8	< 2	< 0.5	< 0.2	3	< 0.5	18	21,4
JI17 02	22	2	14	114	8	< 2	0,6	< 0.2	7	< 0.5	14,2	39,5
JI17 03	22	2	39	122	13	< 2	0,7	< 0.2	6	< 0.5	18	31,7
JI17 04	24	2	26	10	8	< 2	< 0.5	< 0.2	8	< 0.5	1,4	67,9
JI17 05A	11	2	< 5	< 2	1	< 2	< 0.5	< 0.2	< 1	< 0.5	< 0.5	3,8
JI17 06	5	1	< 5	3	< 1	< 2	< 0.5	< 0.2	< 1	< 0.5	0,7	2,6
JI17 07	7	2	< 5	< 2	< 1	< 2	< 0.5	< 0.2	< 1	< 0.5	0,8	3,7
JI17 15	7	1	< 5	8	< 1	< 2	< 0.5	< 0.2	< 1	< 0.5	1,1	3,7
JI17 17	5	2	< 5	3	< 1	< 2	< 0.5	< 0.2	< 1	< 0.5	< 0.5	2,8
JI17 35	13	3	< 5	39	8	< 2	< 0.5	< 0.2	8	< 0.5	3,1	7,8
JI17 36	13	< 1	< 5	112	8	< 2	0,7	< 0.2	5	< 0.5	10	36,7
JI17 37	12	< 1	< 5	36	5	< 2	< 0.5	< 0.2	3	< 0.5	3,4	8,1
JI17 40	14	2	< 5	46	4	< 2	< 0.5	< 0.2	1	< 0.5	6,5	8,7
JI17 41	17	1	< 5	127	4	< 2	< 0.5	< 0.2	2	< 0.5	6,3	11
JI17 48	12	2	< 5	37	3	< 2	< 0.5	< 0.2	1	< 0.5	3,1	10
JI17 49	18	< 1	< 5	126	11	< 2	0,7	< 0.2	4	< 0.5	12,6	42,6

Analyte Symbol	Ce	Pr	Nd	Sm	Eu	Gd	Tb	Dy	Ho	Er	Tm	Yb
Unit Symbol	ppm	ppm	ppm	ppm	ppm	ppm	ppm	ppm	ppm	ppm	ppm	ppm
Detection Limit	0,1	0,05	0,1	0,1	0,05	0,1	0,1	0,1	0,1	0,1	0,05	0,1
Analysis Method	FUS-MS	FUS-MS	FUS-MS	FUS-MS	FUS-MS	FUS-MS	FUS-MS	FUS-MS	FUS-MS	FUS-MS	FUS-MS	FUS-MS
T17 01	2,4	0,28	1,1	0,3	0,09	0,4	< 0.1	0,3	< 0.1	0,2	< 0.05	0,2
T17 03	26,5	3,58	15,7	4,6	1,24	5,1	0,9	5,6	1,2	3,4	0,5	3,3
T17 07	1,9	0,24	0,8	0,2	< 0.05	0,2	< 0.1	0,2	< 0.1	< 0.1	0,06	< 0.1
T17 09	2,8	0,4	1,4	0,5	0,06	0,5	< 0.1	0,3	< 0.1	0,2	< 0.05	0,2
T17 10	2,7	0,39	1,7	0,5	0,08	0,4	< 0.1	0,3	< 0.1	0,2	< 0.05	0,2
T17 11	9,6	1,38	6,3	2	0,68	2,1	0,3	2	0,4	1	0,15	0,9
T17 13	1,2	0,13	0,5	0,2	< 0.05	0,2	< 0.1	0,2	< 0.1	0,1	< 0.05	0,1
T17 14	2,7	0,23	0,8	0,1	0,1	0,2	< 0.1	0,2	< 0.1	0,1	< 0.05	0,1
T17 17	2,4	0,24	1	0,3	0,07	0,3	< 0.1	0,4	< 0.1	0,2	< 0.05	0,2
T17 20	52	6,19	25,5	5,7	2,12	5,3	0,8	4,4	0,8	2	0,28	1,7
T17 21	102	9,98	37	6,9	1,26	6	0,9	5,2	1	3,1	0,46	2,9
T17 22	3,6	0,52	2,3	0,7	0,08	0,8	0,1	0,9	0,2	0,5	0,06	0,3
T17 26	4,9	0,65	2,7	0,9	0,08	1,1	< 0.1	0,4	< 0.1	0,1	< 0.05	0,1
T17 27	7,5	0,9	3,4	1,3	0,06	1,7	0,3	1,7	0,3	0,8	0,09	0,5
T17 28	21,5	2,97	13,2	3	1,01	3,2	0,5	2,8	0,5	1,5	0,22	1,5
T17 30	9,2	1,06	3,9	0,7	0,19	0,8	0,1	0,6	0,1	0,4	0,05	0,4
T17 32	3,4	0,56	2,8	1,1	0,28	1,5	0,3	1,7	0,4	1,1	0,15	0,9
T17 33	6,1	0,89	3,9	1,3	0,1	1,7	0,2	1,1	0,2	0,4	< 0.05	0,2
T17 36	3,8	0,4	1,5	0,3	0,07	0,4	< 0.1	0,3	< 0.1	0,1	< 0.05	0,2
T17 39	7,4	0,9	3,7	0,8	0,11	0,8	< 0.1	0,3	< 0.1	0,1	< 0.05	< 0.1
T17 41	111	9,74	35,8	7,2	1,19	6,1	1	6,2	1,3	3,7	0,54	3,6
T17 42	4,1	0,4	1,8	0,3	0,09	0,4	< 0.1	0,5	< 0.1	0,3	< 0.05	0,3
JI17 01	43,9	5,4	21,5	5,1	1,28	5,1	0,7	4,2	0,8	2,4	0,34	2,2
JI17 02	82,9	9,98	41,5	9,7	2,31	10,5	1,7	10,3	2,1	6	0,88	5,8
JI17 03	62,4	7,22	27,3	5	1,55	4,2	0,6	3,1	0,6	1,8	0,27	1,8
JI17 04	105	10,3	37,4	7,3	2,15	7,7	1,2	7,7	1,6	4,6	0,68	4,4
JI17 05A	10,2	1,56	8	2,4	0,7	2,8	0,4	2,5	0,5	1,3	0,17	1,1
JI17 06	6,4	0,94	4,5	1,3	0,39	1,6	0,2	1,4	0,2	0,7	0,09	0,6
JI17 07	9,2	1,35	6,9	2	0,58	2,2	0,3	2	0,4	1	0,14	0,8
JI17 15	9,1	1,35	6,4	2	0,59	2,1	0,3	1,8	0,3	0,9	0,12	0,8
JI17 17	6,7	1,02	4,9	1,4	0,45	1,7	0,3	1,5	0,3	0,8	0,1	0,6
JI17 35	18,1	2,55	11,8	3,1	0,95	3,4	0,5	3,2	0,7	2	0,3	1,8
JI17 36	70,8	8,06	29,4	5,6	1,11	4,7	0,7	4,1	0,8	2,3	0,33	2,2
JI17 37	19,8	2,64	10,6	2,8	0,72	3,2	0,5	3,2	0,6	1,8	0,29	2
JI17 40	18,7	2,46	10,6	2,6	0,78	2,7	0,4	2,5	0,5	1,4	0,22	1,4
JI17 41	21,5	2,23	8	1,2	0,73	1	0,1	0,8	0,2	0,5	0,09	0,6
JI17 48	20,6	2,59	10,8	2,8	0,77	2,8	0,5	2,9	0,6	1,7	0,25	1,6
JI17 49	83,1	9,42	34,2	6,7	1,39	5,3	0,8	4,5	0,8	2,4	0,35	2,3

Analyte Symbol	Lu	Hf	Ta	W	Tl	Pb	Bi	Th	U	Total S
Unit Symbol	ppm	ppm	ppm	ppm	ppm	ppm	ppm	ppm	ppm	%
Detection Limit	0,01	0,2	0,1	1	0,1	5	0,4	0,1	0,1	0,01
Analysis Method	FUS-MS	FUS-MS	FUS-MS	FUS-MS	FUS-MS	FUS-MS	FUS-MS	FUS-MS	FUS-MS	CS
T17 01	< 0.01	< 0.2	< 0.1	25	3,8	834	0,9	< 0.1	< 0.1	0,44
T17 03	0,51	2,9	0,4	2	0,9	< 5	< 0.4	3,5	1,4	< 0.01
T17 07	< 0.01	< 0.2	< 0.1	25	1,8	10	0,6	0,2	2,2	0,11
T17 09	< 0.01	< 0.2	< 0.1	12	7,1	26	2,1	0,3	0,1	0,38
T17 10	< 0.01	< 0.2	0,1	61	1,8	308	0,7	0,4	0,1	0,13
T17 11	0,14	0,5	0,2	10	0,2	5	< 0.4	0,3	0,1	< 0.01
T17 13	< 0.01	< 0.2	< 0.1	33	0,2	30	1,9	< 0.1	0,2	0,14
T17 14	< 0.01	< 0.2	< 0.1	46	1,2	104	0,5	< 0.1	< 0.1	0,15
T17 17	< 0.01	< 0.2	< 0.1	10	0,3	7	< 0.4	0,1	1,3	0,02
T17 20	0,25	4,5	2,3	1	0,2	8	1,1	3,5	1	< 0.01
T17 21	0,45	4,3	1	< 1	< 0.1	7	< 0.4	14,5	4,6	0,53
T17 22	< 0.01	< 0.2	< 0.1	24	2,3	8	1,1	< 0.1	< 0.1	0,02
T17 26	< 0.01	< 0.2	< 0.1	9	5,9	749	0,7	0,4	0,3	0,21
T17 27	0,06	< 0.2	< 0.1	4	2,7	56	0,9	< 0.1	8,2	0,14
T17 28	0,22	1,7	0,2	3	0,7	< 5	0,9	0,9	0,8	< 0.01
T17 30	0,06	< 0.2	< 0.1	7	2	836	< 0.4	0,2	0,1	0,35
T17 32	0,13	0,8	< 0.1	2	0,5	< 5	< 0.4	0,2	0,2	0,32
T17 33	< 0.01	< 0.2	< 0.1	16	2,5	15	0,6	< 0.1	< 0.1	0,29
T17 36	< 0.01	< 0.2	< 0.1	30	2,3	1460	< 0.4	< 0.1	0,5	0,2
T17 39	< 0.01	< 0.2	< 0.1	12	1,4	31	0,4	< 0.1	2,3	0,1
T17 41	0,53	4,6	0,9	< 1	0,3	9	0,4	15,9	4	0,96
T17 42	< 0.01	< 0.2	< 0.1	12	0,2	5	0,5	< 0.1	1,6	< 0.01
JI17 01	0,35	3,5	0,6	1	0,4	7	< 0.4	5,8	1,9	
JI17 02	0,89	6,1	0,8	< 1	0,6	12	< 0.4	10,2	2,5	
JI17 03	0,27	5,6	1,1	< 1	0,7	19	< 0.4	14	6,4	
JI17 04	0,68	4,9	0,5	< 1	< 0.1	7	< 0.4	5,6	2,1	0,05
JI17 05A	0,16	1,3	< 0.1	4	< 0.1	< 5	< 0.4	0,5	0,2	
JI17 06	0,09	0,4	< 0.1	< 1	< 0.1	< 5	< 0.4	0,5	0,2	
JI17 07	0,12	0,5	< 0.1	< 1	< 0.1	< 5	< 0.4	0,6	0,2	
JI17 15	0,13	0,5	< 0.1	< 1	< 0.1	< 5	< 0.4	0,5	0,2	
JI17 17	0,1	0,6	< 0.1	< 1	< 0.1	< 5	< 0.4	0,4	0,2	
JI17 35	0,31	2,2	3,7	< 1	< 0.1	< 5	3,7	2,2	1,2	< 0.01
JI17 36	0,34	4,9	0,7	< 1	0,5	14	< 0.4	10,7	3,1	
JI17 37	0,33	1,7	0,5	1	< 0.1	< 5	< 0.4	0,6	1,1	
JI17 40	0,21	1,3	0,4	4	< 0.1	7	0,5	2,7	0,9	
JI17 41	0,09	1,5	0,3	< 1	0,3	6	< 0.4	3,9	1,3	
JI17 48	0,26	2	0,3	< 1	< 0.1	8	< 0.4	3	1	
JI17 49	0,35	5,5	0,8	3	0,4	15	< 0.4	13,3	3,1	

Analyte Symbol	Pd	Pt	Au	Cr	C-Organic(calc)
Unit Symbol	ppb	ppb	ppb	%	%
Detection Limit	1	1	2	0,01	0,5
Analysis Method	FA-MS	FA-MS	FA-MS	FUS-XRF	IR
T17 01	< 1	< 1	5		
T17 07	14	12	2		
T17 09	2	14	2	2,09	
T17 13	1	1	4		
T17 14	1	< 1	2		< 0.5
T17 22	13	16	4		
T17 27	3	6	< 2		< 0.5
T17 39					< 0.5